CONTROLLABLE SELF-ASSEMBLY BASED ON INTERACTION OF BORONIC ACIDS AND DIOLS

CONTROLLABLE SELF-ASSEMBLY BASED ON INTERACTION OF BORONIC ACIDS AND DIOLS

By

Dan Zhang, B. ENG., M. Sc

A Thesis

Submitted to the School of Graduate Studies

in Partial Fulfillment of the Requirements

for the Degree

Doctor of Philosophy

McMaster University

DOCTOR OF PHILOSOPHY (2011) McMaster University

(Department of Chemical Engineering) Hamilton, Ontario

TITLE: Controllable Self-assembly Based on Interaction of Boronic Acids and Diols

AUTHOR: Dan Zhang

M.Sc. (Tianjin University)

SUPERVISORS: Professor Robert Pelton

NUMBER OF PAGES: vi, 79

American Chemical Society's Policy on Theses and Dissertations

If your university requires a signed copy of this letter see contact information below.

Thank you for your request for permission to include **your** paper(s) or portions of text from **your** paper(s) in your thesis. Permission is now automatically granted; please pay special attention to the implications paragraph below. The Copyright Subcommittee of the Joint Board/Council Committees on Publications approved the following:

> Copyright permission for published and submitted material from theses and dissertations
> ACS extends blanket permission to students to include in their theses and dissertations their own articles, or portions thereof, that have been published in ACS journals or submitted to ACS journals for publication, provided that the ACS copyright credit line is noted on the appropriate page(s).
>
> Publishing implications of electronic publication of theses and dissertation material
> Students and their mentors should be aware that posting of theses and dissertation material on the Web prior to submission of material from that thesis or dissertation to an ACS journal may affect publication in that journal. Whether Web posting is considered prior publication may be evaluated on a case-by-case basis by the journal's editor. If an ACS journal editor considers Web posting to be "prior publication", the paper will not be accepted for publication in that journal. If you intend to submit your unpublished paper to ACS for publication, check with the appropriate editor prior to posting your manuscript electronically.

If your paper has **not** yet been published by ACS, we have no objection to your including the text or portions of the text in your thesis/dissertation in **print and microfilm formats**; please note, however, that electronic distribution or Web posting of the unpublished paper as part of your thesis in electronic formats might jeopardize publication of your paper by ACS. Please print the following credit line on the first page of your article: "Reproduced (or 'Reproduced in part') with permission from [JOURNAL NAME], in press (or 'submitted for publication'). Unpublished work copyright [CURRENT YEAR] American Chemical Society." Include appropriate information.

If your paper has already been published by ACS and you want to include the text or portions of the text in your thesis/dissertation in **print or microfilm formats**, please print the ACS copyright credit line on the first page of your article: "Reproduced (or 'Reproduced in part') with permission from [FULL REFERENCE CITATION.] Copyright [YEAR] American Chemical Society." Include appropriate information.

Submission to a Dissertation Distributor: If you plan to submit your thesis to UMI or to another dissertation distributor, you should not include the unpublished ACS paper in your thesis if the thesis will be disseminated electronically, until ACS has published your paper. After publication of the paper by ACS, you may release the entire thesis (**not the individual ACS article by itself**) for electronic dissemination through the distributor; ACS's copyright credit line should be printed on the first page of the ACS paper.

Use on an Intranet: The inclusion of your ACS unpublished or published manuscript is permitted in your thesis in print and microfilm formats. If ACS has published your paper you may include the manuscript in your thesis on an intranet that is not publicly available. Your ACS article cannot be posted electronically on a publicly available medium (i.e. one that is not password protected), such as but not limited to, electronic archives, Internet, library server, etc. The only material from your paper that can be posted on a public electronic medium is the article abstract, figures, and tables, and you may link to the article's DOI or post the article's author-directed URL link provided by ACS. This paragraph does not pertain to the dissertation distributor paragraph above.

Questions? Call +1 202/872-4368/4367. Send e-mail to copyright@acs.org or fax to +1 202-776-8112. 10/10/03, 01/15/04, 06/07/06

Abstract

The interaction of boronic acid with diols is reversible and pH-dependent. Boronate groups are able to form complex with 1,2- diol or 1,3-diols at pH values above 9. Therefore, the unique property of boronic esters was employed to exploit controllable self-assembly by three independent mechanisms, each of which is independent of the other two. The three interaction mechanisms are 1) electrostatic attraction between positive polymers and negative surfaces. 2) Polyethylene glycol (PEG)—phenolic polymer complex formation, which is one type of hydrogen bonding. 3) Phenylboronate (PBA) binding to polyols.

To exploit these interactions, families of water-soluble and bifunctional copolymers containing pairs of non-interacting groups were prepared and characterized. Characterization includes structure, molecular weight, composition, etc. These bifunctional polymers can specifically interact with two other types of polymers/surfaces. Therefore, it provides a possibility to prepare complex assemblies by using multiple polymer/polymer interactions in one step.

The utility of multiple, independent interactions was demonstrated by formation of self-assembled multilayer thin films on both silicon wafers and polystyrene latex particles. Moreover, the formation of well-defined nanoparticle aggregates with three different sizes of polystyrene latex particles was studied to extend the application of controllable self-assembly by multiple interactions. The assembly structures of multilayers and latex aggregates were controllable by adjusting the pH and addition of competitive small molecules.

In addition to the study of multilayer self-assembly, a new approach for controllable deposition of latex nanoparticles on surfaces was also exploited. Regenerated cellulose films were chemically modified to fabricate the cellulose films bearing surface phenylboronic acid groups (cellulose-PBA). The poly(glycerol monomethacrylate)- stabilized polystyrene (PGMA-PS) latex particles were used to have reversible, pH-dependent adsorption onto the cellulose-PBA by the interaction of boronic acids and diols. Specific adsorption of PGMA-PS onto cellulose-PBA was observed at pH 10.5, whereas the latex particles were removed at pH 4.

Acknowledgements

First of all, I am deeply thankful to my supervisor, Dr. Robert Pelton, for his supervision during my study, instructing me the knowledge of colloid and polymer science and teaching me skills of presentation and paper writing. Also, I would like to thank my supervisory committee members, Dr. Shiping Zhu and Dr. Gianluigi Botton for their valuable suggestions and generous help on my research work.

I wish to thank Natural Sciences and Engineering Research Council of Canada (NSERC) for their financial support of my research work. Especially, I am grateful to Dr. Steven P. Armes, Dr. Hiroo Tanaka and Dr. Laura Harrington for their advice and close collaboration on my papers.

I would like to thank Dr. Shiping Zhu and Dr. Harald Stöver for usage of their instruments, to Dr. H. Sheardown and Ms. Lina Liu for my ellipsometry measurements; to Ms. Marcia Reid for the help of TEM and SEM measurements; to Ms. Marnie Timleck for the help of confocal microscope measurements; to Dr. Steve Kornic for his help and support in NMR, FT-IR and elemental analysis measurements.

I am also grateful to all the current and previous group members in McMaster Interfacial Technologies Group for their help and encouragement, especially our lab manager Mr. Doug Keller and lab secretaries Ms. Francis Lima and Ms. Sally Watson their assistance during my study. I acknowledge Dr. Chengming Li, Dr. Hiroo Tanaka, Dr. Chen Lu and and Dr. Xiaonong Chen for their support and helpful suggestions on polymer science and characterization technologies, and Dr. Xianhua Feng, Dr. Wei Chen and Dr. Yuguo Cui for their useful discussions on my research project.

I also wish to give my special thanks to the staffs in Department of Chemical Engineering, Ms. Kathy Goodram, Ms. Lynn Falkiner, Ms. Nanci Cole, and Ms. Andrea Vickers for their administrative assistance, and Mr. James Lei, Mr. Paul Gatt, Ms. Justyna Derkach and Mr. Dan Wright for their technical support.

Finally, I would like to thank my parents and my wife, Lei Zheng for their love and support.

TABLE OF CONTENTS

Abbreviations

AIBN	2,2'-azobisisobutyronitrile
APBA	3-acrylamide phenylboronic acid
ARS	Alizarin Red S
BTM	benzyl trimethyl ammonium chloride
CLSM	confocal laser scanning microscopy
DADMAC	diallyldimethyl ammonium chloride
DLS	dynamic light scattering
DMA	2-dimethylaminoethylmethacrylate
DMF	dimethylformamide
DMSO	dimethyl sulfoxide
EDC	N-(3-dimethylaminopropyl)-N'-ethylcarbodiimide hydrochloride
GPC	gel permeation chromatography
LB	Langmuir-Blodgett
LBL	layer by layer
NMR	nuclear magnetic resonance
PAA	polyacrylic acid
PBA	phenylboronic acid
PEG	polyethylene glycol
PEO	polyethylene oxide

PGMA	poly(glycerol monomethacrylate)
PS	polystyrene
PSS	polystyrene sulfonate
PVA	polyvinyl alcohol
PVAm	polyvinylamine
QCM	quartz crystal microbalance
SAM	self-assembled monolayer
SAXD	small angle X-Ray diffraction
SEM	scanning electron microscope
TEM	transmission electron microscopy
TEMPO	2,2,6,6-tetramethylpiperidine-1-oxyl

Chapter 1 Introduction and Background Review

1.1 Introduction

Surface treatment with water-soluble polymers has been exploited in many industrial fields for decades to influence the ultimate properties of commercial products. A typical example is the dramatic improvement of paper strength by adsorbing polymer coatings onto the surfaces of cellulose fibers before papermaking. However, one of the limitations of this approach is that polymers can only form a monolayer and they do not adsorb onto themselves[1]. Ideally, it is desirable to have multilayer property in many technological situations including rising biotechnology and some traditional industries.

This thesis describes new ways to assemble nanoscale structures on both macroscopic surfaces and on colloidal particles. Initially, organic films were prepared using Langmuir-Blodgett (LB) film techniques in the early 20th century[2]. The LB films are formed at the water/air interface and are composed of amphiphilic molecules with both a hydrophilic end and a hydrophobic end. The thickness of thin films can be precisely controlled because they are vertically assembled on surfaces and each monolayer thickness is known. LB technique provides an approach to prepare both a monolayer and multilayer organic thin films at the molecular level. However, the application of LB films is limited by the high demand for equipment and operational complexity. An alternative method to fabricate multilayer thin films on surfaces is self-assembly technique. At first, self-assembled monolayers (SAM) method was introduced. A well-organized monolayer film can be formed by the chemical reactions between the substrate and some specific molecules in solutions. A major disadvantage of this method is that the assembly is restricted by some specific types of chemical reactions and substrates. In order to solve the issues addressed above, a self assembly technique by physical adsorption was introduced to prepare multilayer thin films. The approach to obtaining multilayer thin films by physical adsorption was proposed by Decher[3], which is called Layer-by-layer formation (LBL). In this method, a surface is consecutively treated with anionic and cationic polymer solutions. As a result, multiple polymeric layers are formed by electrostatic attraction between the two types of polymers.

However, the simulation and preparation of controllable complex structures usually requires multiple and independent interaction mechanisms. For example, there are

multiple types of interactions in the tertiary structure of proteins, such as hydrogen bonding, salt bridges and hydrophobic interactions. All these interactions operate together both within the protein itself and between different proteins to achieve some particular functions. Therefore, a single interaction is not enough in the study of biochemistry/biomaterials and the diversity of driving forces is the cornerstone of more complex self-assembled structures.

To achieve the goal of applying multiple interactions in one system, I exploited three polymer-polymer or polymer-surface interaction mechanisms, each of which is independent of the other two. The three interaction mechanisms to be exploited are:
1) Polycation/polyanion interaction (polyelectrolyte complex). It is well understood due to its strong and long-range interaction.
2) Polyethylene glycol (PEG)—phenolic polymer complex formation, which is one type of hydrogen bonding. A hydrogen bond is usually stronger than the van der Waals force, but weaker than a covalent bond. The hydrogen bonding shows properties of the covalent bonding: It involves a finite number of interaction partners and is directional. Moreover, it is insensitive to electrostatics and ionic strength.
3) Phenyl boronate-cis diol complex formation, which is one type of covalent bonds. One important feature of boronate ester bonds is that boronic acids react with diol bearing compounds in alkaline condition and can be manipulated by pH values. The other property of boronate ester bonds is that the bond strength is weak. For example, the equilibrium constant of boronic acid for bonding to glucose is 26 L/mol which corresponds to a free energy of -7.9 kJ/mol[4]. By contrast, the bond energy of a hydrogen bond is usually from 5 to 30 kJ/mol.

The complex formation between boric acid and diols was recognized over 100 years ago. In 1842, it was first reported that the acidity of boric acid solutions was increased by sugars[5]. Since then, the study of the interaction between boronic acids and diols has attracted an extensive attention. So far, a large number of articles on the interaction between boronic acid and diols have been published[6-7]. Among these works, two research fields are developed; mainly boronic acid based self assembly and saccharide responsive sensors. Fujita et al. summarized the current development of boronic acids in molecular self assembly[8], while Fang et al. reviewed the progress on boronic acid based fluorescent glucose sensors, utilizing boronic acid moiety as responsive site[9].

A typical example of the trilayer assembly is illustrated in Figure 1[10], which shows an

assembly of three polymer layers with three independent interactions on solid surfaces.

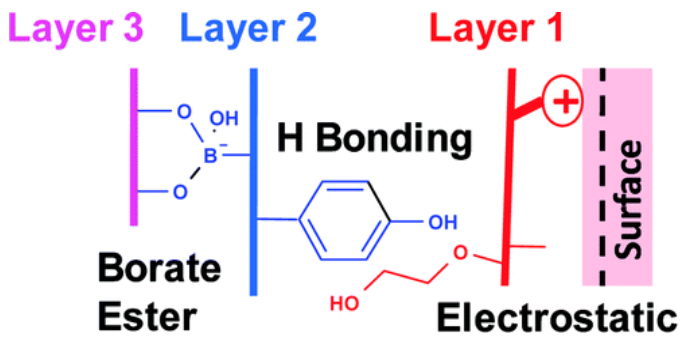

Figure 1 An example of trilayer polymer assembly

In general, the surfaces of natural substances such as fibers, tissues, etc. are negatively charged. Thus, cationic groups from the first layer of polymer interact electrostatically with the negatively charged substrate. The PEG groups from the Layer 1 polymers are subsequently bound to the phenolic groups from the second layer copolymers. Similarly, boronic acid containing polymers (Layer 2 copolymers) bind with polyols (Layer 3 polymers). To my knowledge, no one has been able to generate such structure before. From a scientific perspective, my work is the first demonstration of the independent exploitation of three types of polymer-polymer interactions (electrostatic complexation, PEO-phenolic complexation and boronate-polyol complexation) to develop controllable complex structures.

In addition to the exploitation of boronic acid-based trilayer self-assembly, I also exploited a new approach for controllable deposition of nanoparticles on surfaces. This method is based on pH-dependent condensation of borate ions with polyols. Cellulose films were chemically modified to give phenylboronic acid groups. Two poly(glycerol monomethacrylate), (PGMA)-coated polymer colloids prepared in Dr. Armes' lab were used as diol containing nanoparticles. Hence, a pH-dependent deposition of PGMA-stabilized PS latexes onto cellulose surfaces bearing phenylboronic acid groups (cellulose-PBA) was also demonstrated in my thesis.

1.2 Background Review

1.2.1 Interaction Mechanism between Boronic Acids and Diols.

Boric acid is a typical Lewis acid composed of an electron deficient boron atom and three hydroxyl groups. It is soluble in cold water but has much better solubility in warm water. When dissolved in water, boric acid (pka=9.0)[11] becomes weak electrolyte $B(OH)_3 \cdot H_2O$, which generates a small amount of $B(OH)_4^-$ and H^+, showing a very weak acidity.

The condensation of borate ions and 1,2-diols or 1,3-diols occurs in alkaline condition, producing five or six membered rings spontaneously. In general, the complex formation is more favorable in solution at high pH, because of the release of angle strain which is a result from trigonal planar sp^2 hybridization of boron atoms at low pH to tetrahedral sp^3 at high pH[12]. Interestingly, this process is reversible and pH can be used as a switch to turn on or off the interaction between boronate ions and cis-diols. Therefore, the properties of borate ester offer the possibility of considerable applications, such as affinity chromatography[13-14], drug delivery[15-17], receptor and sensor for carbohydrates[18-20], protecting groups for diols and diamines[21-26], bioconjugation[27-28] and labeling of proteins and cells[29-31].

In 1959, the first quantitative study of the interaction between phenylboronic acid and diols was reported by Lorand[12]. The method used in the experiments is called the pH-depression method, which is based on the fact that the pka of boron bearing groups can be lowered after binding with diols[4, 12]. However, the binding constants measured by spectroscopic methods are much lower than those by the pH-depression method. For instance, the binding constant of fructose and phenylboronic acid is 160 M^{-1}, as determined by fluorescent method[32]. On the other hand, the binding constant is 4370 M^{-1} when pH-depression method is used[9]. Thus, Wang and his coworkers reported a series of studies to propose the reasons of this phenomenon[4].

Scheme 1 shows the binding mechanism of a boronic acid and a diol[9]. A phenylboronic acid in a trigonal form (1) can transform to an anionic tetrahedral form (2) in water. Similarly, boronate ester (3) also has two different forms in water. Therefore, there are three binding constants in total. The first binding contant ($K_{eq\text{-}trig}$) refers to the conversion from trigonal boronic acid (1) to the trigonal boronate ester (3). The second binding constant ($K_{eq\text{-}tet}$) refers to the conversion from tetrahedral boronate (2) to tetrahedral

boronate ester (4). Obviously, both $K_{eq\text{-}trig}$ and $K_{eq\text{-}tet}$ cannot represent the overall binding ability of boronic acid and diols. Consequently, the third binding constant (K_{eq}), defined as the overall binding constant, was introduced in the study.

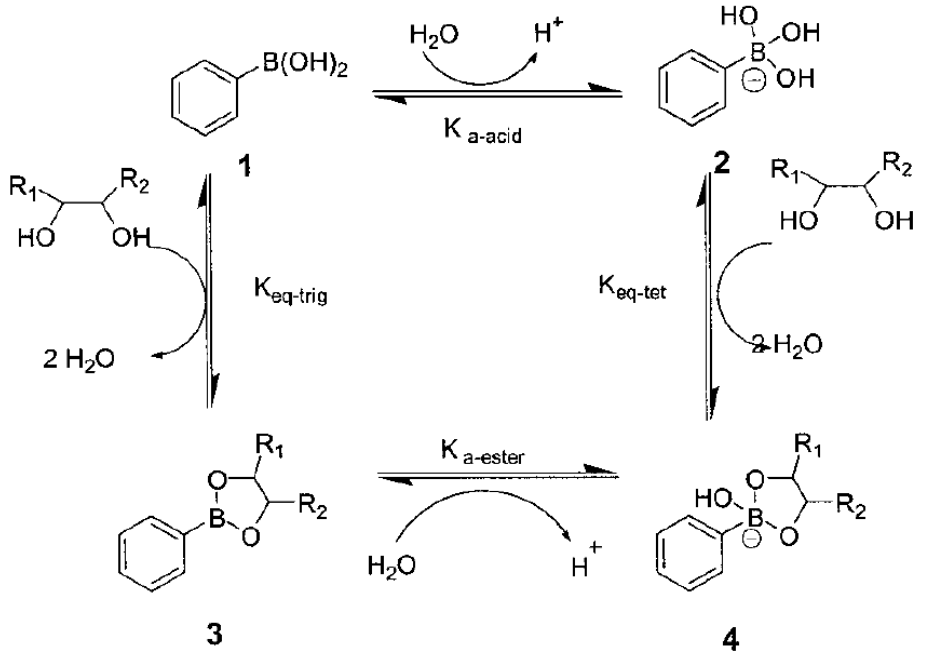

Scheme 1 The interaction of phenylboronic acid and diols (Fang et al. 2004)[9]

Scheme 2 shows the overall binding process of a boronic acid and a diol. Springsteen and Wang found that the binding constant measured by the pH depression method was the $K_{eq\text{-}tet}$, whereas the measurements using the spectroscopic method would obtain the K_{eq}[4, 33].

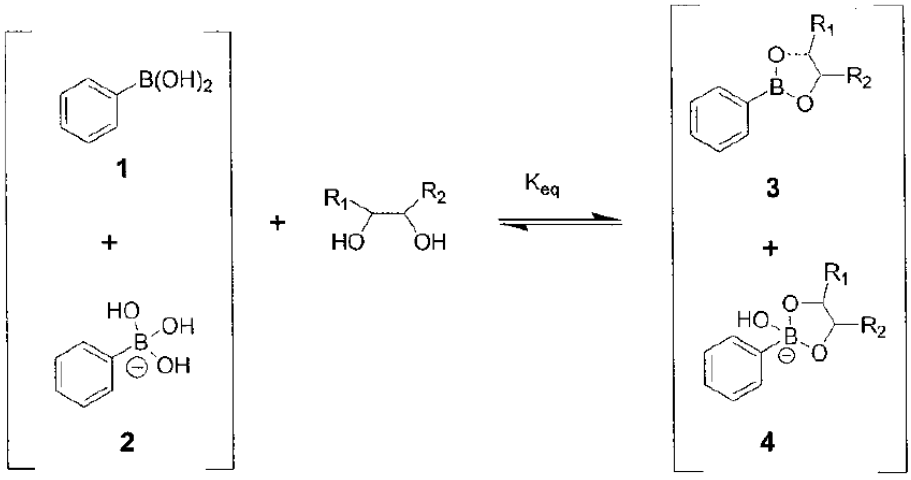

Scheme 2 Overall binding between phenylboronic acids and diols. (Fang et al. 2004)[9]

Springsteen and Wang also investigated the relationship among Ktet, K_{trig} and K_{eq} (Equations (1)-(6))[4], which offers a convenient way to compare different binding constants measured by various methods.

$$K_{eq} = (([BD^-][H^+] / K_{a\text{-}ester}) + [BD^-]) / (([B^-][H^+] / K_{a\text{-}acid}) + [B^-])([D] + [D^-])) \quad (1)$$

$$K_{eq\text{-}tet} = [BD^-] / [H^+]([D^-]/[D]+[D^-])[B^-][Diol] \quad (2)$$

$$K_{eq\text{-}trig} = [BD] / [H^+]([D^-]/[D]+[D^-])[B][Diol] \quad (3)$$

$$K_{eq\text{-}tet} = \frac{1+\frac{[H^+]}{K_{a\text{-}acid}}}{1+\frac{[H^+]}{K_{a\text{-}ester}}} \times K_{eq} \quad (4)$$

$$K_{eq\text{-}trig} = \frac{1+\frac{[H^+]}{K_{a\text{-}acid}}}{1+\frac{[H^+]}{K_{a\text{-}ester}}} \times K_{eq}\frac{K_{a\text{-}acid}}{K_{a\text{-}ester}} \quad (5)$$

$$K_{eq} = \%acid \times K_{eq-trig} + \%ester \times K_{eq-tet} \quad (6)$$

B = Trigonal Boronic Acid, BD = Complex of Trigonal Boronic Aicd and Diol

B^- = Tetrahedral Boronic Acid, BD^- = Complex of Tetrahedral Boronic Acid and Diol

It is generally accepted that boronate ester formation usually occurs at pH values above 8, whereas there are some reports on borate-diol bond formation at lower pH values[1]. Dr. James and other scientists have studied the forms of the compound N-methyl-o-(phenylboronic acid)-N-benzylamine (A) at both high and low pH[2-3]. As the scheme 3 shows, (A) and (C) illustrate that there is no nitrogen-boron bond, but (D) and (E) indicate that there is a nitrogen-boron bond, which creates a cyclic form. The species (B) is protonated at low pH, thereby the nitrogen cation makes the formation of nitrogen-boron bond impossible.

The coordinative nitrogen to boron bonds (N-B or N→B) have been investigated for

decades. The bond energy of a N-B bond depends highly on the substituents on both nitrogen atom and boron atom; the Lewis acidity of boron can be increased by electron withdrawing groups, and the Lewis alkalinity of nitrogen can also be increased by electron donating groups[8].

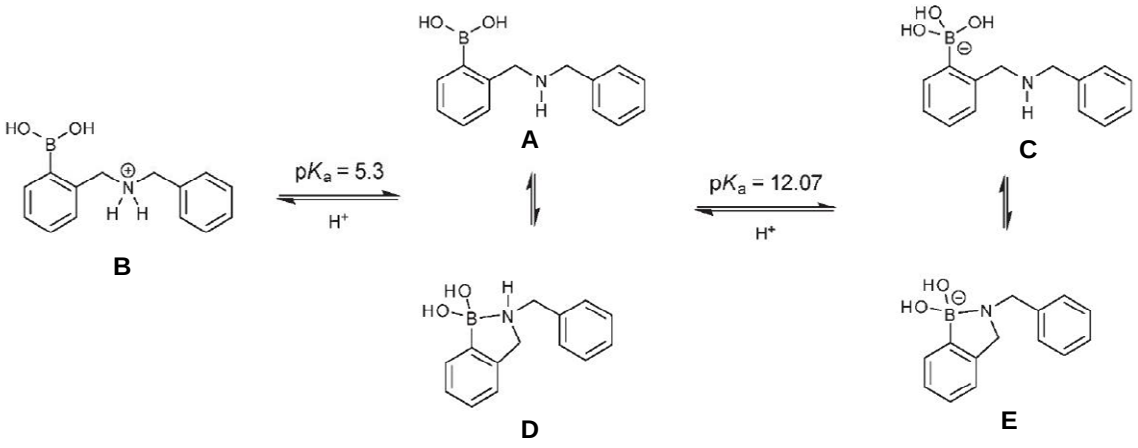

Scheme 3 The interaction between nitrogen and boron at various pH and their cyclic and acyclic forms. (Fujita et al. 2008)[8]

1.2.2 Molecular Self Assembly

Langmuir-Blodgett (LB) film technology is a well known technique and is widely employed to prepare organic thin films. Traditionally, the basic approach is to spread amphiphilic molecules with one hydrophobic and one hydrophilic end to form a monolayer at air/water interface, and then immerse a substrate into (or from) the liquid. Sequentially, a monolayer thin film is transferred onto the substrate by compressing the movable barrier of Langmuir–Blodgett trough at a constant pressure and moving the substrate vertically. Multilayer thin films can be fabricated by repeatedly moving the substrate through the air-water interface. The classic examples of the molecules comprising LB films are long-chain fatty acid or alcohol, studied firstly by Langmuir and his student Blodgett[2]. LB film technique provides a convenient route to obtain uniform organic thin films onto a solid support such as glass, silicon, or quartz[2]. However, Langmuir-Blodgett films are metastable structure, and the interaction between molecules/molecules or molecules/substrate is weak. As a result, the application of LB film technology is limited

to a certain extent. In order to overcome this drawback, recent efforts have focused on other self assembly techniques.

Self assembly refers to a technology that a disordered system of basic structural units forms an organized structure or pattern driven among the units themselves, without external guidance. Molecular self-assembly is a ubiquitous phenomenon in living systems and it is also the basis of formation of various biological structures (proteins, nucleic acids, membrane, liposomes, etc.) in life science. Recently, the molecular self-assembly technique has received a lot of interest in preparation of electrochromic devices[37], microcapsules for controllable release of active chemicals[38-39], biomedical applications[40] and so on.

Self-assembled monolayer (SAM) is an organized layer of molecules formed spontaneously on a substrate. For a self-assembled system prepared by a chemical method, a variety of molecules can be applied to the formation of self assembly films. Traditionally, a substrate is cleaned, dipped into the solution and then the active head groups of molecules spontaneously react with the substrate. Consequently, molecular chains are fixed tightly onto the solid support and a monolayer is formed.

Due to the stability and diversity of self assembly monolayers, great attention has been devoted to exploit various self assembly films by chemical method and related works have also been extensively reported[41-48]: (1) Thiol or bisulfide assembled on the surfaces of copper, silver and gold. They are able to form monolayers by Metal-sulfur bonds. (2) Organosilane assembled on thesurfaces of silica, glass, aluminum oxide and quartz. They can form monolayers by Si-O-Si bonds. (3) Some alcohols and carboxylic acids assembled on the surfaces of aluminum and aluminium oxide. (4) Alcohols and amines assembled on the surface of platinum.

In 1997, a popular method of multilayer fabrication by physical absorption was reported by Decher[3]. As shown in Figure 2, the multilayer thin films were fabricated by alternately dipping a substrate into the polyanion and polycation solutions. Due to the electrostatic attraction, the negative charge containing polymers was absorbed spontaneously onto the positive charged surface and then polycations was absorbed onto the polyanion layer. In the recent decades, there are a large number of papers and patents describing fundamentals and applications of polyelectrolyte multilayer films. For example, Wågberg and his coworkers reported that the multilayer formation using consecutive adsorption of

cationic and anionic polymers gives extremely strong fiber-fiber adhesion in paper[49].

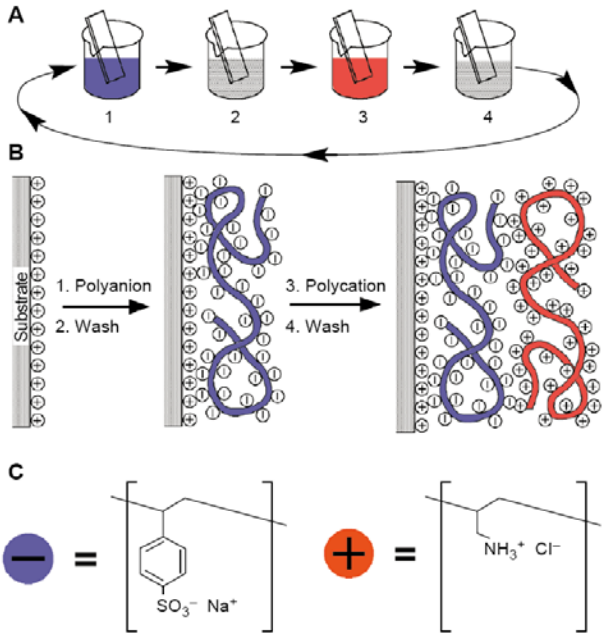

Figure 2 Schematic process of the bilayer deposition. Two typical polyions are poly(allylamine hydrochloride) and sodium salt of poly(styrene sulfonate). (Decher et al. 1997)[3]

Presently, such simple and powerful method has been widely applied in preparation of various layer-by-layer (LBL) films. In comparison to chemical absorption, the classic approach is much easier to obtain a thin polyelectrolyte multilayer on various substrates. Scheme 4 shows that a wide range of materials can be selected in LBL deposition[50]: polyelectrolytes, such as polyvinylamine (PVAm) and polystyrene sulfonate (PSS); some biomacromolecules, such as enzymes and antibodies, and small molecules, such as titanium dioxide and calcium carbonate.

In the early stage of development, a large body of literature focused on electrostatically driven layer-by-layer assembly[3, 51-57]. Many other interactions were subsequently employed as the driving forces of the polymer assembly, including hydrogen bonding[58-61],

coordinate bonding[62], covalent bonding[63-64], etc. At least one of the interactions is necessary as the driving force for multilayer build-up.

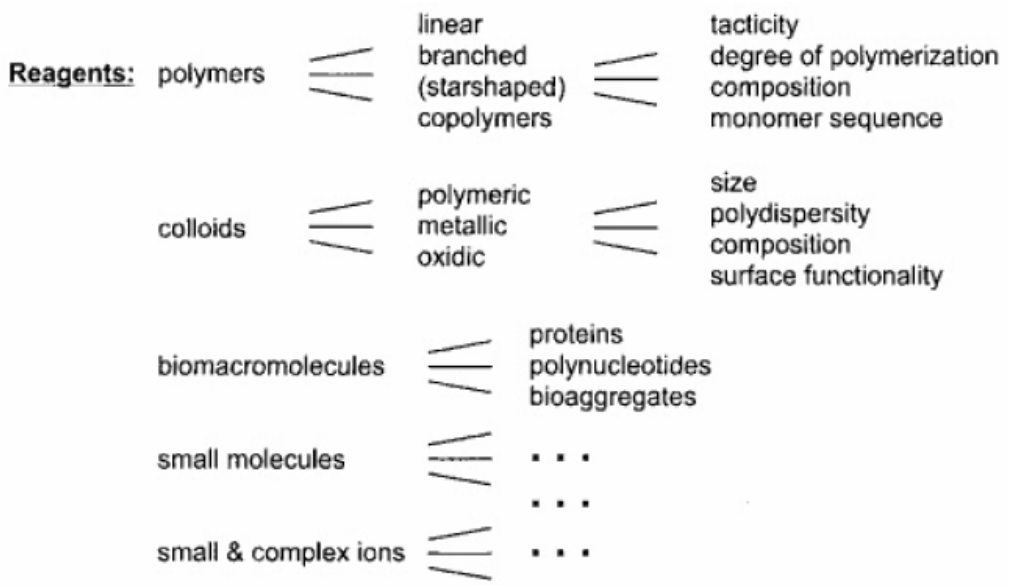

Scheme 4 Various reagents for LbL deposition (Decher et al. 2006)[50]

Among all the driving forces above, boronate ester formation with polyols is unique and it plays a critical role in self-assembly thin films[10]. The main reasons are summarized as follows: (a) the boronate- diol complex formation is reversible. Boronate groups are able to form complex with 1,2- diol or 1,3-diols at pH values above 9. Moreover, the pH window can be lowered by locating amine groups near the boronic acid group; (b) diols are ubiquitous in nature as a moiety of saccharides. Therefore, the interaction between boronic acids and polyols has a tremendous application in biochemistry and biotechnology, offering a possibility of large-scale, low cost and directed assembly in aqueous solutions; (c) boronate ester interaction is a covalent bonding. The interaction between boronic acids and diols is directional, which is different from the non-covalent interaction. This thesis will demonstrate that borate-diol interactions can be used to control self-assembly.

1.3 Objectives

The overall objective of my work in this thesis is to develop novel and controllable methods for self assembly. The specific objectives of the thesis are:

1. *Bifunctional Copolymer Synthesis and Characterization* The goal was to prepare and characterize families of bifunctional copolymers. Characterization includes structure, molecular weight, composition and aqueous solution properties.

2. *Trilayer Film Self Assembly and Characterization* The goal was to develop an approach to trilayer thin film self assembly on solid substrates while minimizing undesired solution complex formation. The pH and other factors were employed as switches to achieve this objective. Ellipsometry and dynamic light scattering (DLS) were used to probe the structure of trilayer thin films.

3. *Formation of* Controllable *Latex Aggregates* The goal was to design controllable latex aggregates with multiple and independent interactions. The pH was used to manipulate the interaction of polymers, containing boronic acid moieties, with polyols.

4. *Reversible Particle Deposition on Films* The goal was to deposit particles bearing diol groups onto a regenerated cellulose film, bearing phenylboronic acid groups (cellulose-PBA). Deposition was driven by the boronate ester formation with polyol latex surface coating. It will offer a new approach for a specific, pH-dependent nanoparticle deposition on surfaces.

1.4 Thesis Outline

Chapter 1 This chapter presents the research background of this thesis, including the interaction of boronic acid and diols, and the application of the interaction in self-assembly thin films. The specific objectives and an outline of the thesis are also introduced in this chapter.

Chapter 2 In this chapter, three independent polymer/polymer complexing mechanisms are used to assemble polymer trilayers onto anionic surfaces in water.

Polymer-surface and polymer-polymer attraction were driven by (1) electrostatic attraction between positively charged polymers bearing benzyl trimethyl ammonium chloride (BTM) groups and negatively charged surfaces; (2) polyethylene glycol (PEG) binding to phenolic (Ph) groups; and (3) phenylboronate (PBA) binding to polyols. The approach was to prepare copolymers with the following pairs of compatible interacting groups: BTM/Ph, BTM/PEG, PBA/PEG, and PBA/Ph.

Chapter 3 This chapter describes the assembly of multilayer thin films on both a silicon wafer and a polystyrene latex particle. The formation of well-defined nanoparticle aggregates with three different sizes of polystyrene latex particles is also introduced. The self-assembly was based on three driving forces: 1) electrostatic interaction of oppositely charged surfaces and polymers; 2) hydrogen bonding between phenolic donor and a PEG acceptor; and, 3) condensation of phenylboronic acid containing polymers with polyols. Thickness and polymer coverage of absorbed multilayer polymers are described as a function of pH. With adjustments of the pH and addition of competitive small molecules, the assembly structures of multilayers and nanoparticle aggregates were controllable.

Chapter 4 Described in this chapter is the boronate mediated deposition of latex particles on cellulose films. Poly(glycerol monomethacrylate)-stabilized polystyrene latex (PS-PGMA) displayed specific, pH-dependent deposition onto regenerated cellulose film, bearing phenylboronic acid groups (cellulose-PBA). Deposition was driven by the boronate ester formation with polyol latex surface coating. Deposition occurred at pH 10 whereas deposition did not occur and deposited particles desorbed at pH 4. The distribution of boronate groups in the cellulose films was determined by exposure to Alizarin Red S (ARS), which formed a fluorescent complex with phenylboronic acid. Confocal microscopy was used to quantify boronate distribution though the film. The interaction gives a new tool for controlling nanoparticle deposition on surfaces.

Chapter 5 This chapter summarizes the main conclusions and contributions of this project.

1.5 References

1. Fleer, G. J.; Cohen Stuart, M. A.; Scheutjens, J. M. H.; Cosgrove, T.; Vincent, B., Polymers at interfaces. *Chapman & Hall: London* 1993.

2. Talham, D. R.; Yamamoto, T.; Meisel, M. W., Langmuir-blodgett films of molecular organic materials. *Journal of Physics-Condensed Matter* 2008, *20* (18).

3. Decher, G., Fuzzy nanoassemblies: Toward layered polymeric multicomposites. *Science* 1997, *277* (5330), 1232-1237.

4. Springsteen, G.; Wang, B. H., A detailed examination of boronic acid-diol complexation. *Tetrahedron* 2002, *58* (26), 5291-5300.

5. Deutsch, A.; Osoling, S., Conductometric and potentiometric studies of the stoichiometry and equilibria of the boric acid-mannitol complexes. *Journal of the American Chemical Society* 1949, *71*, 1637-1640.

6. De Geest, B. G.; Jonas, A. M.; Demeester, J.; De Smedt, S. C., Glucose-responsive polyelectrolyte capsules. *Langmuir* 2006, *22* (11), 5070-5074.

7. Islam, T. M. B.; Yoshino, K.; Sasane, A., B-11 nmr study of p-carboxybenzeneboronic acid ions for complex formation with some monosaccharides. *Analytical Sciences* 2003, *19* (3), 455-460.

8. Fujita, N.; Shinkai, S.; James, T. D., Boronic acids in molecular self-assembly. *Chemistry-an Asian Journal* 2008, *3* (7), 1076-1091.

9. Fang, H.; Kaur, G.; Wang, B. H., Progress in boronic acid-based fluorescent glucose sensors. *Journal of Fluorescence* 2004, *14* (5), 481-489.

10. Zhang, D.; Tanaka, H.; Pelton, R., Polymer assembly exploiting three independent interactions. *Langmuir* 2007, *23* (17), 8806-8809.

11. Babcock, L.; Pizer, R., Dynamics of boron acid complexation reactions - formation of 1-1 boron acid ligand complexes. *Inorganic Chemistry* 1980, *19* (1), 56-61.

12. Lorand, J. P., Edwards J.O., Polyol complexes and structure of the benzeneboronate ion. *Journal of Organic Chemistry* 1959, *24*, 769-774.

13. Gildengorn, V. D., Reversed-phase affinity chromatography of ecdysteroids with boronic acid-containing eluents. *Journal of Chromatography A* 1996, *730* (1-2), 147-152.

14. Liu, X. C.; Scouten, W. H., Studies on oriented and reversible immobilization of glycoprotein using novel boronate affinity gel. *Journal of Molecular Recognition* 1996, *9* (5-6), 462-467.

15. Kitaoka, T.; Isogai, A.; Onabe, F., Chemical modification of pulp fibers by tempo-mediated oxidation. *Nordic Pulp & Paper Research Journal* 1999, *14* (4), 279-284.

16. Liu, F.; Song, S. C.; Mix, D.; Baudys, M.; Kim, S. W., Glucose-induced release of glycosylpoly(ethylene glycol) insulin bound to a soluble conjugate of concanavalin a. *Bioconjugate Chemistry* 1997, *8* (5), 664-672.

17. Zhang, S. R.; Trokowski, R.; Sherry, A. D., A paramagnetic cest agent for imaging glucose by mri. *Journal of the American Chemical Society* 2003, *125* (50), 15288-15289.

18. Gray, C. W.; Houston, T. A., Boronic acid receptors for alpha-hydroxycarboxylates: High affinity of shinkai's glucose receptor for tartrate. *Journal of Organic Chemistry* 2002, *67* (15), 5426-5428.

19. Lavigne, J. J.; Anslyn, E. V., Teaching old indicators new tricks: A colorimetric chemosensing ensemble for tartrate/malate in beverages. *Angewandte Chemie-International Edition* 1999, *38* (24), 3666-3669.

20. Zhao, J. Z.; Fyles, T. M.; James, T. D., Chiral binol-bisboronic acid as fluorescence sensor for sugar acids. *Angewandte Chemie-International Edition* 2004, *43* (26), 3461-3464.

21. Evans, D. A.; Polniaszek, R. P.; Devries, K. M.; Guinn, D. E.; Mathre, D. J., Synthetic studies in the lysocellin family of polyether antibiotics - the total synthesis of ferensimycin-b. *Journal of the American Chemical Society* 1991, *113* (20), 7613-7630.

22. Floresparra, A.; Paredestepox, C.; Josephnathan, P.; Contreras, R., Preparation of new quinic acid boron esters in aprotic media. *Tetrahedron* 1990, *46* (12), 4137-4148.

23. Gypser, A.; Michel, D.; Nirschl, D. S.; Sharpless, K. B., Dihydroxylation of polyenes using narasaka's modification of the upjohn procedure. *Journal of Organic Chemistry* 1998, *63* (21), 7322-7327.

24. Liljebris, C.; Nilsson, B. M.; Resul, B.; Hacksell, U., Regio- and stereoselective reactions of 17-phenyl-18,19,20-trinorprostaglandin f-2 alpha isopropyl ester. *Journal of Organic Chemistry* 1996, *61* (12), 4028-4034.

25. McMurry, J. E.; Erion, M. D., Stereoselective total synthesis of the complement inhibitor k-76. *Journal of the American Chemical Society* 1985, *107* (9), 2712-2720.

26. Oshima, K.; Kitazono, E.; Aoyama, Y., Complexation-induced activation of sugar oh groups. Regioselective alkylation of methyl fucopyranoside via cyclic phenylboronate in the presence of amine. *Tetrahedron Letters* 1997, *38* (28), 5001-5004.

27. Frantzen, F.; Grimsrud, K.; Heggli, D. E.; Sundrehagen, E., Protein-boronic acid conjugates and their binding to low-molecular-mass cis-diols and glycated hemoglobin. *Journal of Chromatography B-Biomedical Applications* 1995, *670* (1), 37-45.

28. Wiley, J. P.; Hughes, K. A.; Kaiser, R. J.; Kesicki, E. A.; Lund, K. P.; Stolowitz, M. L., Phenylboronic acid-salicylhydroxamic acid bioconjugates. 2. Polyvalent immobilization of protein ligands for affinity chromatography. *Bioconjugate Chemistry* 2001, *12* (2), 240-250.

29. Chang, M. C. Y.; Pralle, A.; Isacoff, E. Y.; Chang, C. J., A selective, cell-permeable optical probe for hydrogen peroxide in living cells. *Journal of the American Chemical Society* 2004, *126* (47), 15392-15393.

30. Vandenburg, Y. R.; Zhang, Z. Y.; Fishkind, D. J.; Smith, B. D., Enhanced cell binding using liposomes containing an artificial carbohydrate-binding receptor. *Chemical Communications* 2000, (2), 149-150.

31. Yang, W. Q.; Fan, H. Y.; Gao, X. M.; Gao, S. H.; Karnati, V. V. R.; Ni, W. J.; Hooks, W. B.; Carson, J.; Weston, B.; Wang, B. H., The first fluorescent diboronic acid sensor specific for hepatocellular carcinoma cells expressing sialyl lewis x. *Chemistry & Biology* 2004, *11* (4), 439-448.

32. Yoon, J.; Czarnik, A. W., Fluorescent chemosensors of carbohydrates - a means of chemically communicating the binding of polyols in water based on chelation-enhanced quenching. *Journal of the American Chemical Society* 1992, *114* (14), 5874-5875.

33. Springsteen, G.; Wang, B. H., Alizarin red s. As a general optical reporter for studying the binding of boronic acids with carbohydrates. *Chemical Communications* 2001, (17), 1608-1609.

34. Niwa, M.; Sawada, T.; Higashi, N., Surface monolayers of polymeric amphiphiles carrying a copolymer segment composed of phenylboronic acid and amine. Interaction with saccharides at the air-water interface. *Langmuir* 1998, *14* (14), 3916-3920.

35. Bosch, L. I.; Fyles, T. M.; James, T. D., Binary and ternary phenylboronic acid complexes with saccharides and lewis bases. *Tetrahedron* 2004, *60* (49), 11175-11190.

36. Bosch, L. I.; Mahon, M. F.; James, T. D., The b-n bond controls the balance between locally excited (le) and twisted internal charge transfer (tict) states observed for aniline based fluorescent saccharide sensors. *Tetrahedron Letters* 2004, *45* (13), 2859-2862.

37. Hammond, P. T., Form and function in multilayer assembly: New applications at the nanoscale. *Advanced Materials* 2004, *16* (15), 1271-1293.

38. Donath, E.; Sukhorukov, G. B.; Caruso, F.; Davis, S. A.; Mohwald, H., Novel hollow polymer shells by colloid-templated assembly of polyelectrolytes. *Angewandte Chemie-International Edition* 1998, *37* (16), 2202-2205.

39. Caruso, F.; Caruso, R. A.; Mohwald, H., Production of hollow microspheres from nanostructured composite particles. *Chemistry of Materials* 1999, *11* (11), 3309-3314.

40. Schneider, A.; Vodouhe, C.; Richert, L.; Francius, G.; Le Guen, E.; Schaaf, P.; Voegel, J. C.; Frisch, B.; Picart, C., Multifunctional polyelectrolyte multilayer films: Combining mechanical resistance, biodegradability, and bioactivity. *Biomacromolecules* 2007, *8* (1), 139-145.

41. Troughton, E. B.; Bain, C. D.; Whitesides, G. M.; Nuzzo, R. G.; Allara, D. L.; Porter, M. D., Monolayer films prepared by the spontaneous self-assembly of symmetrical and unsymmetrical dialkyl sulfides from solution onto gold substrates - structure, properties, and reactivity of constituent functional-groups. *Langmuir* 1988, *4* (2), 365-385.

42. Ihs, A.; Uvdal, K.; Liedberg, B., Infrared and photoelectron spectroscopic studies of ethyl and octyl xanthate ions adsorbed on metallic and sulfidized gold surfaces. *Langmuir* 1993, *9* (3), 733-739.

43. Sabatani, E.; Cohenboulakia, J.; Bruening, M.; Rubinstein, I., Thioaromatic monolayers on gold - a new family of self-assembling monolayers. *Langmuir* 1993, *9* (11), 2974-2981.

44. Li, T. T. T.; Liu, H. Y.; Weaver, M. J., Intramolecular electron-transfer at metal-surfaces .3. Influence of bond conjugation on reduction kinetics of cobalt(iii) anchored to electrodes via thiophenecarboxylate ligands. *Journal of the American Chemical Society* 1984, *106* (5), 1233-1239.

45. Maoz, R.; Sagiv, J., Penetration-controlled reactions in organized monolayer assemblies .2. Aqueous permanganate interaction with self-assembling monolayers of long-chain surfactants. *Langmuir* 1987, *3* (6), 1045-1051.

46. Demoz, A.; Harrison, D. J., Characterization of extremely low defect density hexadecanethiol monolayers on hg surfaces. *Langmuir* 1993, *9* (4), 1046-1050.

47. Tillman, N.; Ulman, A.; Schildkraut, J. S.; Penner, T. L., Incorporation of phenoxy groups in self-assembled monolayers of trichlorosilane derivatives - effects on film thickness, wettability, and molecular-orientation. *Journal of the American Chemical Society* 1988, *110* (18), 6136-6144.

48. Whitesides, G. M.; Laibinis, P. E., Wet chemical approaches to the characterization of organic-surfaces - self-assembled monolayers, wetting, and the physical organic-chemistry of the solid liquid interface. *Langmuir* 1990, *6* (1), 87-96.

49. Wagberg, L.; Forsberg, S.; Johansson, A.; Juntti, P., Engineering of fibre surface properties by application of the polyelectrolyte multilayer concept. Part i: Modification of paper strength. *Journal of Pulp and Paper Science* 2002, *28* (7), 222-228.

50. Decher, G. S. J. B., Wiley-vch. *Multilayer thin films* 2006.

51. Ariga, K.; Lvov, Y.; Kunitake, T., Assembling alternate dye-polyion molecular films by electrostatic layer-by-layer adsorption. *Journal of the American Chemical Society* 1997, *119* (9), 2224-2231.

52. Caruso, F.; Furlong, D. N.; Ariga, K.; Ichinose, I.; Kunitake, T., Characterization of polyelectrolyte-protein multilayer films by atomic force microscopy, scanning electron microscopy, and fourier transform infrared reflection-absorption spectroscopy. *Langmuir* 1998, *14* (16), 4559-4565.

53. Lvov, Y.; Ariga, K.; Ichinose, I.; Kunitake, T., Assembly of multicomponent protein films by means of electrostatic layer-by-layer adsorption. *Journal of the American Chemical Society* 1995, *117* (22), 6117-6123.

54. Schmitt, J.; Decher, G.; Dressick, W. J.; Brandow, S. L.; Geer, R. E.; Shashidhar, R.; Calvert, J. M., Metal nanoparticle/polymer superlattice films: Fabrication and control of layer structure. *Advanced Materials* 1997, *9* (1), 61-65.

55. Sun, Y. P.; Hao, E.; Zhang, X.; Yang, B.; Shen, J. C.; Chi, L. F.; Fuchs, H., Buildup of composite films containing tio2/pbs nanoparticles and polyelectrolytes based on electrostatic interaction. *Langmuir* 1997, *13* (19), 5168-5174.

56. Van Cott, K. E.; Guzy, M.; Neyman, P.; Brands, C.; Heflin, J. R.; Gibson, H. W.; Davis, R. M., Layer-by-layer deposition and ordering of low-molecular-weight dye molecules for second-order nonlinear optics (vol 41, pg 3236, 2002). *Angewandte Chemie-International Edition* 2002, *41* (19), 3719-3722.

57. Zhang, X.; Shen, J. C., Self-assembled ultrathin films: From layered nanoarchitectures to functional assemblies. *Advanced Materials* 1999, *11* (13), 1139-1143.

58. Kharlampieva, E.; Kozlovskaya, V.; Tyutina, J.; Sukhishvili, S. A., Hydrogen-bonded multilayers of thermoresponsive polymers. *Macromolecules* 2005, *38* (25), 10523-10531.

59. Zhang, H. Y.; Wang, Z. Q.; Zhang, Y. Q.; Zhang, X., Hydrogen-bonding-directed layer-by-layer assembly of poly(4-vinylpyridine) and poly(4-vinylphenol): Effect of solvent composition on multilayer buildup. *Langmuir* 2004, *20* (21), 9366-9370.

60. Lu, C.; Pelton, R., Peo flocculation of polystyrene-core poly(vinylphenol)-shell latex: An example of ideal bridging. *Langmuir* 2001, *17* (25), 7770-7776.

61. Lu, C.; Pelton, R., Factors influencing the size of peo complexes with a tyrosine-rich polypeptide. *Langmuir* 2004, *20* (10), 3962-3968.

62. Yang, H. C.; Aoki, K.; Hong, H. G.; Sackett, D. D.; Arendt, M. F.; Yau, S. L.; Bell, C. M.; Mallouk, T. E., Growth and characterization of metal(ii) alkanebisphosphonate multilayer thin-films on gold surfaces. *Journal of the American Chemical Society* 1993, *115* (25), 11855-11862.

63. Chan, E. W. L.; Lee, D. C.; Ng, M. K.; Wu, G. H.; Lee, K. Y. C.; Yu, L. P., A novel layer-by-layer approach to immobilization of polymers and nanoclusters. *Journal of the American Chemical Society* 2002, *124* (41), 12238-12243.

64. Zhang, F.; Jia, Z.; Srinivasan, M. P., Application of direct covalent molecular assembly in the fabrication of polyimide ultrathin films. *Langmuir* 2005, *21* (8), 3389-3395.

Chapter 2 Polymer Assembly Exploiting Three Independent Interactions

In Chapter 2, the synthesis and characterization of copolymers VAm-PBA-Ph and BTM-PEG were conducted by myself. Ellipsometry was used by me to study the trilayer self assembly on a silicon wafer. Professor Tanaka prepared and characterized the copolymers DMA-PBA-PEG and BTM-Ph. Gelation test and QCM were employed by him to investigate the self assembly and interactions of three polymers. Dr. Pelton did the calculation of the ellipsometry data with Harland's program in MathCAD. I wrote the first drafts and Dr. Pelton rewrote sections for the final version.

Polymer Assembly Exploiting Three Independent Interactions

Dan Zhang, Hiroo Tanaka, and Robert Pelton*

Department of Chemical Engineering, JHE-136, McMaster University, Hamilton, Ontario, Canada L8S 4L7

Received March 11, 2007. In Final Form: May 13, 2007

Three independent polymer/polymer complexing mechanisms were used to assemble polymer trilayers onto anionic surfaces in water. Polymer−surface and polymer−polymer attraction were driven by (1) electrostatic attraction between positive polymers bearing benzyl trimethyl ammonium chloride (BTM) groups and negative surfaces; (2) polyethylene glycol (PEG) binding to phenolic (Ph) groups; and (3) phenylboronate (PBA) binding to polyols. The approach was to prepare copolymers with the following pairs of compatible interacting groups: BTM/Ph, BTM/PEG, PBA/PEG, and PBA/Ph. The supporting surfaces were either silicon or anionic self-assembled on gold. The ultimate goal is to employ independent polymer/polymer interactions to prepare complex assemblies in a few steps.

Introduction

The assembly of 3D microscale objects from nanoscale particles and soluble polymers requires species−species interactions that are specific and, ideally, can be switched on or off. Furthermore, for complex structures, multiple and independent interaction mechanisms are required. For example, the biochemistry/biotechnology literature routinely uses streptavidin/biotin binding to assemble objects that bear antibodies, enzyme binding domains, or oligonucleotides, which can undergo a subsequent specific assembly or recognition step.[1] Most biologically based coupling reagents, although effective, are expensive and fragile and thus are practical only in high-value-added applications. In this contribution, we demonstrate three macromolecular interaction mechanisms between water-soluble polymers. None of these are new phenomena; however, we believe that this is the first time that all three have been exploited simultaneously. These approaches offer the possibility of large-scale, low cost, directed assembly in water.

The three interaction types are the following:

(1) Polyanion/polycation (polyelectrolyte complexes). These are strong long-range interactions that are well understood. Polyanion/polycation interactions are the basis of most layer-by-layer assembly.[2]

(2) Polyethylene glycol(PEG)−phenolic copolymer complex formation. We have characterized this complex formation both in solution[3−7] and on surfaces.[5] This type of complex formation is insensitive to electrostatics and to ionic strength.

(3) Phenyl boronate−cis diol complex formation. Boronate groups are known to complex with cis diols at pH values above 9. The pH window can be lowered by locating amine groups near the boronic acid group.[8]

Each of the above interactions involves the binary combination of specific groups (e.g., PEG/phenol, borate/diol, and anion/cation). To exploit these interactions, we have prepared copolymers containing pairs of noninteracting groups, thus giving bifunctional polymers that can specifically interact with two other types of polymers. Examples are shown in Figure 1, which shows two assemblies of three polymer layers on solid surfaces. For both assemblies, the surface/layer 1 interaction is electrostatic complexation, the layer 1/layer 2 interaction is PEG/phenolic complexation, and the layer 2/layer 3 interaction is boronate/cis diol complexation. In this article, we describe the preparation and characterization of the assemblies illustrated in Figure 1.

Experimental Section

Materials. 4-Acetoxystyrene, *p*-vinylbenzyl trimethyl ammonium chloride, 2-dimethylaminoethyl methacrylate (DMA), and poly(ethylene glycol) methacrylate (PEG, Mw 360 Da) were obtained from Aldrich. Poly(vinyl alcohol) (PVA, 1600 degrees of polymerization and 97.5−99.5% degree of hydrolysis) was purchased from Fluka. The DMA and PEG macromonomers were purified with an Aldrich inhibitor removal column. Other monomers and chemicals were reagent grade and used without further purification. Polyvinylamine (Mw 150 kDa) was supplied by BASF and was completely hydrolyzed in sodium hydroxide and purified by exhaustive dialysis.[9]

To prepare the monomer, 3-acrylamide phenylboronic acid (APBA), 3-aminophenylboronic acid monohydrate (3.10 g, 0.020 mol), and trimethylamine (1.53 g, 0.015 mol) were dissolved in tetrahydrofuran (30 mL). Acryloyl chloride (3.0 mL = 3.34 g, 0.033 mol) was dropped into this solution with ice cooling, and the mixture was stirred at room temperature for 2 h. The precipitate was removed by filtration. After evaporation to dryness, the residue was recrystallized twice from water, giving pale-yellow needlelike crystals: yield 2.37 g, 62%; boron content 5.6% (98.9%); UV maximum (EtOH) 272 nm. ^{1}H NMR: 5.76 (vinyl H), 6.37 (vinyl H_2), 7.33, 7.47,7.67, 7.84 (ArH).

Three copolymers were prepared by radical copolymerization. The total monomer concentration for the DMA-PBA-PEG polymerization was 0.15 mol/L 55 °C (5 h of reaction time), and the reaction was initiated with 2,2′-azobis(2-methylpropionamidine)·2HCl (4×10^{-4} mol/L). The BTM-Ph copolymers were prepared from a 0.8 mol/L monomers (4-acetoxystyrene and *p*-vinylbenzyltrimethyl ammonium chloride (BTM), 50:50 mol %) mixture in DMSO using a 0.4 mmol/L 2,2′-azobis(2-methylpropionamidine)·2HCl initiator at 65 °C for 25 h. The product was hydrolyzed in 0.6 N aqueous sodium hydroxide at 55 °C for 30 h. The strong infrared adsorption at 1750 cm^{-1} for the carbonyl group in the copolymer completely disappeared after hydrolysis. The molecular weights of

* Corresponding author. E-mail: peltonrh@mcmaster.ca. Tel: (905) 529 7070 ext. 27045. Fax: (905) 528 5114.

(1) Hermanson, G. T. *Bioconjugate Techniques*; Academic Press: San Diego, CA, 1996.
(2) Decher, G. *Science (Washington, D.C.)* **1997**, *277*, 1232−1237.
(3) Lu, C.; Pelton, R. *Langmuir* **2004**, *20*, 3962−3968.
(4) Lu, C.; Pelton, R. *Langmuir* **2001**, *17*, 7770−7776.
(5) Lu, C.; Richardson, R.; Pelton, R.; Cosgrove, T.; Dalnoki-Veress, K. *Macromolecules* **2004**, *37*, 494−500.
(6) Cong, R. J.; Pelton, R. *J. Colloid Interface Sci.* **2003**, *261*, 65−73.
(7) Cong, R. J.; Pelton, R.; Russo, P.; Doucet, G. *Macromolecules* **2003**, *36*, 204−209.
(8) Niwa, M.; Sawada, T.; Higashi, N. *Langmuir* **1998**, *14*, 3916−3920.
(9) Gu, L.; Zhu, S.; Hrymak, A. N. *J. Appl. Polym. Sci.* **2002**, *86*, 3412−3419.

10.1021/la700711a CCC: $37.00
Published on Web 07/13/2007

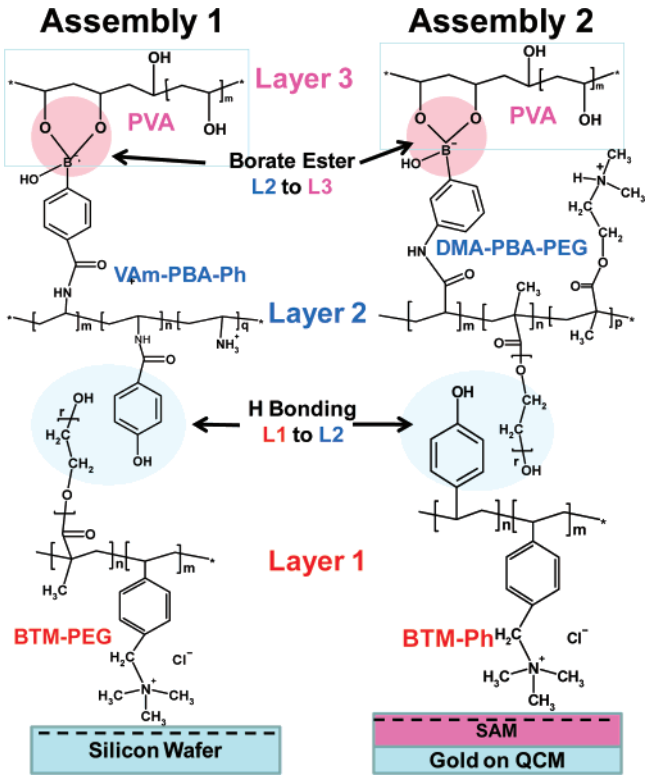

Figure 1. Two examples of trilayer polymer assembly based on electrostatics (surface to L1), hydrogen bonding (L1 to L2), and boronate ester formation (L2 to L3).

the three copolymers were measured by light scattering and were about 500 kDa. A detailed description of the polymerization and characterization will be provided in a future publication. The contents of cationic and anionic groups in the copolymers were measured by colloid (polyelectrolyte) titration[10,11] at pH 2 to 3 and pH 11 to 12, respectively. The copolymer compositions, expressed as mol percentages, were BTM(53%)-PEG(47%), BTM(52%)-Ph(48%), and DMA(28%)-PBA(27%)-PEG(32%)

Polyvinylamine was derivatized with 3-carboxyphenylboronic acid using *N*-(3-dimethylaminopropyl)-*N*′-ethylcarbodiimide hydrochloride coupling to give PBA substitution.[12] After purification, the product was coupled with 4-hydroxybenzoic acid to give VAm-PBA(13 mol %)-Ph(28 mol %).

Methods. The mutual interactions between pairs of copolymers in water were evaluated by observing gelation, which is defined as no flow when inverting test tubes 20 min after polymer mixing.

The quartz crystal microbalance (QCM) measurements were carried out using an AFFINIX Q (Inicium Co., Tokyo) instrument. A gold-coated quartz crystal electrode was treated with 2 mM sodium 3-mercapto-1-propanesulfonate for 8 h to give negative charges. After washing, the electrode attached to the QCM was immersed in the glass cuvette containing 9 mL of Milli-Q water at pH 2.9 or 6.2 and equilibrated under stirring at 28 °C. The appropriate amount (3−10 μL) of 0.1% BTM-Ph was added, and the self-assembly process was monitored by measuring the QCM frequency shift. The excess BTM-Ph was washed, and the electrode was immersed into 9 mL of the same pH medium as above, followed by adding 5 μL of 0.1% DMA-PEG and recording the frequency shift. After equilibrium was reached, 10 μL of 0.1% PVA was sequentially added to the same cuvette, and the frequency shift was monitored.

Dried film thickness values were determined by ellipsometric measurements (Exacta 2000 self-nulling ellipsometer, Waterloo, Ontario). Silicon wafers were first rinsed with 50 mL of methanol and toluene. They were then rinsed with sufficient water and treated with a buffered 1 wt % HF aqueous solution (7:1 NH_4F/HF) for 3 min. The HF treatment removed the surface oxidation layer. Finally, they were rinsed with Milli-Q water several times.

The tri-layer absorbed thin films were prepared as follows. Silicon wafers were immersed in the layer 1 polymer solution (0.40% PEG-BTM, pH 7.00) overnight (14 h) followed by gentle rinsing in Milli-Q water to remove weakly adsorbed polymer. Layer 2 (0.35% VAm-PBA-Ph, pH 6.85) and layer 3 (0.33% PVA, pH 7.00) were added the same way. For ellipsometric measurements, the wafer-supported films were dried at room temperature under a nitrogen atmosphere.

An ellipsometric measurement gives two parameters Δ and Ψ from which a corresponding film thickness and refractive index can be calculated from a uniform film model.[13] However, when the thickness of an organic film on a silicon wafer in air is less than 30 nm, ellipsometric parameters Ψ and Δ are rather insensitive to the refractive index of the film.[13] Therefore, we measured the refractive indices of the three copolymers separately by spin coating (3000 rpm with a P-6000 spin coater from Specialty Coating System, Inc.) thick films on wafers that were annealed under vacuum at 115 °C for 3 h. The refractive index values were calculated from Δ and Ψ, and the results for pure copolymer refractive indices are PEG-BTM (n_{L1}) 1.567, VAm-PBA-Ph (n_{L2}) 1.619, and PVA (n_{L3}) 1.557.

The dry film thicknesses for one-, two-, and three-layer films were calculated from the measured Δ and Ψ values assuming a uniform film model in which the refractive indices of the wafer (3.87−0.02i) and of the polymer films were entered into the model. The results from the modeling Exacta 2000 software were checked with Harland's[13] program, which we encoded in MathCAD. The refractive index values that were input were n_{L1} for a one-layer film, $0.5n_{L1} + 0.5n_{L2}$ for the two-layer films, and $^1/_3n_{L1} + {}^1/_3n_{L2} + {}^1/_3n_{L3}$ for the three-layer films. However, as explained above, the film thickness values are remarkably independent of the refractive index for the very thin organic films in air.

Results and Discussion

Four copolymers were prepared and characterized, and their structures are shown as layer 1 and layer 2 copolymers in Figure 1. Three of the four were prepared by conventional free radical copolymerization whereas the fourth, VAm-PBA-Ph, was prepared by consecutive derivatization of polyvinylamine.

Complex formation between complementary polymers was confirmed by gel formation in water. For example, DMA-PBA-PEG formed gels when mixed with PVA, which complexed via boronate ester formation. DMA-PBA-PEG also formed gels when mixed with BTM-Ph, reflecting complex formation between the polyether groups on DMA-PBA-PEG and the phenolic groups on BTM-Ph. The gel-formation boundaries for these two combinations are shown in Figure 2 as functions of pH. Both combinations formed gels over the entire pH range; this was unexpected for the boronate diol gel because boronate ester formation usually occurs at pH values above 8[14] whereas there is some evidence of borate−diol bond formation at lower pH values.[15,16]

PVA (4 wt %) was mixed with equal volumes of the two layer 1 polymers, BTM-Ph (4 wt %) and BTM-PEG (4 wt %), and there was no evidence of gel formation or precipitation, which suggests no interaction between layer 3 and layer 1 polymers in solution. Ellipsometric results, presented below, suggest that PEG-BTM and PVA also do not interact when layer 1 copolymer PEG-BTM is adsorbed on a wafer.

(10) Terayama, H. *J. Polym. Sci.* **1952**, *8*, 243−253.
(11) Tanaka, H.; Sakamoto, Y. *J. Polym. Sci., Part A: Polym. Chem.* **1993**, *31*, 2687−2691.
(12) Chen, W.; Lu, C.; Pelton, R. *Biomacromolecules* **2006**, *7*, 701−702.
(13) Tompkins, H. G. *A User's Guide to Ellipsometry*; Dover: New York, 1993.
(14) Shiino, D.; Kubo, A.; Murata, Y.; Koyama, Y.; Kataoka, K.; Kikuchi, A.; Sakurai, Y.; Okano, T. *J. Biomater. Sci., Polym. Ed.* **1996**, *7*, 697−705.
(15) Springsteen, G.; Wang, B. H. *Tetrahedron* **2002**, *58*, 5291−5300.
(16) Yan, J.; Springsteen, G.; Deeter, S.; Wang, B. H. *Tetrahedron* **2004**, *60*, 11205−11209.

Table 1. Summary of Ellipsometric Characterization of Assembly 1 (Figure 1)[a]

wafer coating	Ψ (deg)	Δ (deg)	film refractive index	film thickness (nm)
PEG-BTM	10.416	169.29	1.567	3.15
PEG-BTM + VAm-PBA-Ph	10.261	161.88	1.593	5.48
PEG-BTM + VAm-PBA-Ph + PVA	10.206	150.19	1.581	9.52
Control Experiment 1				
PEG-BTM	10.408	168.59	1.567	3.39
PEG-BTM + PVA	10.316	168.15	1.567	3.53
Control Experiment 2				
PEG-BTM + VAm-PBA-Ph	10.318	161.48	1.593	5.63
PEG-BTM + VAm-PBA-Ph + VAm-PBA-Ph	10.548	161.62	1.593	5.60

[a] The laser wavelength was 632.8 nm, and the incident angle was 70°. All film extinction coefficients were 0. The measurements were made under ambient laboratory conditions, and the results are the average of five measurements.

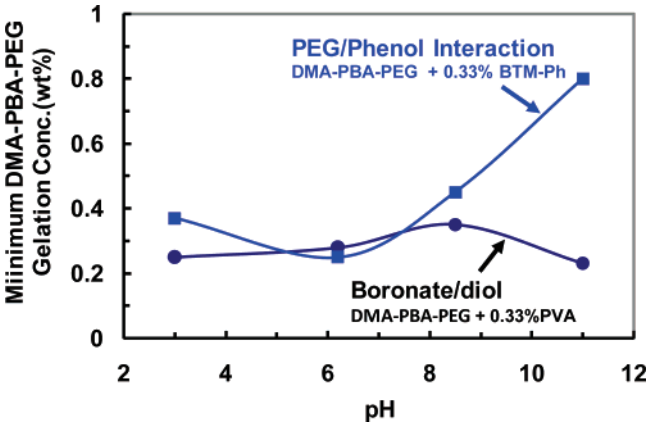

Figure 2. Minimum gelation concentrations for binary combinations of copolymers.

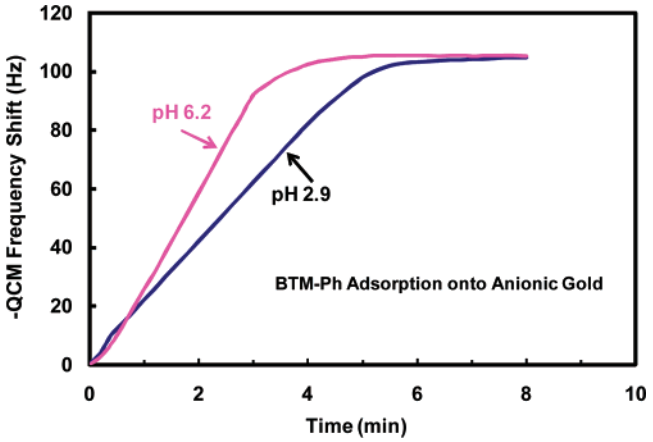

Figure 3. QCM frequency shift versus time for cationic copolymer BTM-Ph adsorption onto gold bearing anionic 3-mercapto-1-propanesulfonate groups.

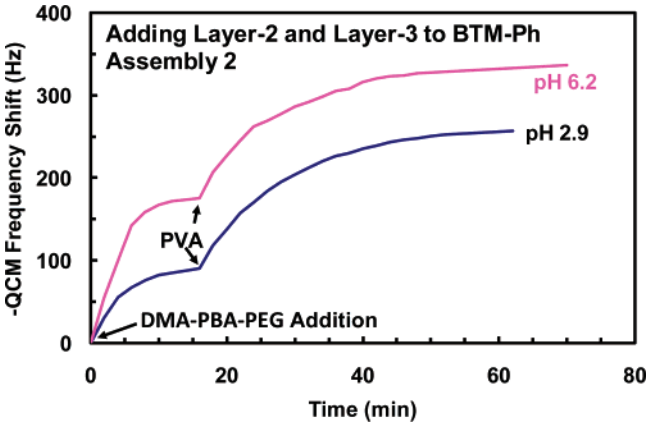

Figure 4. Following layer 2 and layer 3 buildup on a quartz crystal microbalance for assembly 2. (See Figure 1.)

The only potential cross talk in our current systems originates from both layer 1 and layer 2 being cationic. Thus, layer 2 copolymers are trifunctional and could have undergone electrostatic interactions with anionic surfaces and polymers if the surface was not saturated with layer 1 polymer. Future efforts will include the preparation of nonionic layer 2 polymers.

The two assemblies illustrated schematically in Figure 1 were prepared by layer-by-layer assembly. Assembly 1 was characterized at each step by ellipsometric analysis of the dried films, and the results are summarized in Table 1. The dry film thickness increased about 3 nm for each subsequent adsorbed layer. These dimensions seem to be consistent with published descriptions of consecutively adsorbed monolayers.[17−19]

Table 1 also shows the results for two control experiments. In the first experiment, a wafer coated with layer 1 polymer was exposed to layer 3 polymer (i.e., no layer 2). The film thickness did not increase, suggesting that layer 3 (PVA) did not adsorb onto layer 1 (PEG-BTM). In the second control experiment, the layer 1 + layer 2 assembly was dried and then exposed for a second time to the layer 2 polymer solution. There was no increase in the dry film thickness, suggesting no addition adsorption.

Finally, the control experiments summarized in Table 1 were done weeks after the assembly 1 measurements in the first part of Table 1 were made. The duplicated PEG-BTM films and the PEG-BTM + VAm-PBA-Ph films gave reproducible film thickness values to within 0.1 nm.

The building of assembly 2 (Figure 1) was followed by quartz crystal microbalance (QCM) measurements. Figure 3 shows the frequency shift due to the adsorption of layer 1 copolymer (BTM-Ph) at two pH values. The frequency shift corresponding to complete coverage was about 105 Hz. This corresponds to a polymer coverage of about 0.63 mg/m^2, assuming that each hertz corresponds to a mass change of 0.006 mg/m^2.[20,21]

Figure 4 shows the frequency shift as layer 2 (DMA-PBA-PEG) and layer 3 (PVA) were consecutively adsorbed onto BTM-

(17) Kharlampieva, E.; Sukhishvili, S. A. *Polym. Rev.* **2006**, *46*, 377−395.
(18) Kharlampieva, E.; Kozlovskaya, V.; Tyutina, J.; Sukhishvili, S. A. *Macromolecules* **2005**, *38*, 10523−10531.
(19) Zhang, H. Y.; Wang, Z. Q.; Zhang, Y. Q.; Zhang, X. *Langmuir* **2004**, *20*, 9366−9370.
(20) Okahata, Y.; Kawase, M.; Niikura, K.; Ohtake, F.; Furusawa, H.; Ebara, Y. *Anal. Chem.* **1998**, *70*, 1288−1296.
(21) Okahata, Y.; Niikura, K.; Sugiura, Y.; Sawada, M.; Morii, T. *Biochemistry* **1998**, *37*, 5666−5672.

Ph. The frequency shift for both polymers was greater at pH 6.2 than at pH 2.9, suggesting pH sensitivity in the bound polymer configurations.

The present work falls within a large body of literature describing electrostatically driven layer-by-layer assembly,[2] much less on hydrogen bonding-driven assembly,[17] and one example of mixed electrostatic plus boronate ester-driven assembly.[22] We believe our work may be the first example of three independent mechanisms simultaneously driving assembly. Future work will probe the sensitivity of film structure and properties to the details of copolymer structure and will explore routes to one-step multilayer assembly.

Acknowledgment. We acknowledge the Canadian government (NSERC) for funding. We thank Professor T. Kitaoka and Ph.D student S. Yokota (Kyushu University, Japan) for providing access to their QCM and for skillful technical support.

LA700711A

(22) Recksiedler, C. L.; Deore, B. A.; Freund, M. S. *Langmuir* **2006**, *22*, 2811−2815.

Chapter 3 Controlling Polymer and Nanoparticle Assembly by Three Independent Interactions

All the experiments involved in Chapter 3 were completed by myself, including the copolymer synthesis and characterization, the self-assembly of multilayers and nanoparticle aggregates, etc. I wrote the draft and Dr Pelton revised it. Also, Dr. Pelton contributed many helpful suggestions on my experiments and paper writing.

Chapter 3 Controlling polymer and nanoparticle assembly by three independent interactions

Abstract

The assembly of multilayer thin films on a silicon wafer or a polystyrene latex particle and the formation of well defined nanoparticle aggregates with three different sizes of polystyrene latex particles were based on three driving forces: 1) electrostatic attraction between oppositely charged surfaces and polymers; 2) hydrogen bonding between phenolic donors and PEG acceptors; and, 3) condensation of phenylboronic acid containing polymers with polyols. Thickness and polymer coverage of absorbed multilayer polymers are described as a function of pH. With adjustments of the pH and addition of competitive small molecules, the assembly structures of multilayers and nanoparticle aggregates are controllable.

3.1 Introduction

The assembly of polymers at the molecular level is desirable and vital to control the performance of surfaces and interfaces, particularly for polymeric and bioactive materials. One approach to prepare multilayers is Layer-by-layer assembly driven by electrostatic attraction[1-8]. Generally, one specific interaction is employed as the driving force of the assembly process. It can be electrostatic attraction[1], hydrogen bonding[9-10], coordinate bonding[11], covalent bonding[12-13], etc. However, there is no doubt that polymer and nanoparticle assembly based on multiple independent interactions can provide more flexibility in controlling surface composition and properties of multilayer thin films and complex composite particles.

Consequently, we demonstrate the self-assembly of multilayer thin films on solid supports and nanoparticle aggregates based on three independent interactions. Scheme 1 illustrates a typical example of multilayer assembly on an anionic surface. The three interactions involved are:

(1) Polyelectrolyte complexes (electrostatic attraction). These are strong long-range interactions. In 1997, Decher first reported the layer by layer (LBL) method to treat surfaces consecutively with anionic and cationic polymer to give multilayer structures[1]. Recently, there are a lot of papers describing fundamentals and applications of polyelectrolyte multilayer thin films.

(2) Polyethylene glycol (PEG)-phenolic copolymer complex formation. Our group has done much work on this interaction both in solution[9-10, 14-17] and on surfaces[15]. This type of complex formation is insensitive to electrostatics and to ionic strength.

(3) Phenyl boronate-diol complex formation. Boronate groups are known to complex with polyols at alkaline pH values. Recently some references report that this complex can be driven to form at lower values by having amine groups near the boronic acid groups[18].

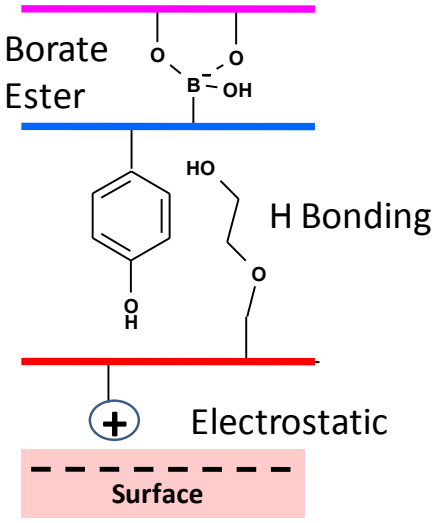

Scheme 1 An example of trilayer polymer assembly by three independent interactions

To exploit these interactions, a trilayer films (Assembly 1 in Figure 1) assembled onto anionic surfaces with three independent interaction mechanisms was introduced in our previous paper[19]. Two copolymers BTM-PEG and VAm-PBA-Ph were prepared and assembled by LBL method on a silicon wafer. The first layer copolymers (BTM-PEG) were prepared by conventional free radical copolymerization of poly-(ethylene glycol) methacrylate (PEG) and (4-acetoxystyrene and p-vinylbenzyltrimethyl ammonium chloride (BTM). The second layer copolymers (VAm-PBA-Ph) were prepared by consecutive derivatization of polyvinylamine with 3-carboxyphenylboronic acid (PBA) and 4-hydroxybenzoic acid (Ph). The third layer polymers, polyvinyl alcohol (PVA), purchased from Fluka. All the three polymers constitute the trilayer assembly by three independent interactions- see Assembly 1 in Figure 1. Ellipsometry was employed to characterize the thickness of the dried films assembled on a solid support. However, the original work was flawed because the layer 2 copolymer (VAm-PBA-Ph) was cationic and might compete with layer 1 for adsorption sites on the support surface.

Described in this chapter is the preparation and application of the second generation layer 1 and layer 2 copolymers, which were designed to prevent the interaction of layer 2 polymer with the supporting surface – see Assembly 2 in Figure 1. Specifically, we prepared bifunctional copolymers based on 3-acrylamide phenylboronic acid plus poly(ethylene glycol) methacrylate (APBA-PEG) and based on vinylphenol and

diallyldimethyl ammonium chloride (Ph-DADMAC) – see structures in Figure 1. These two bifunctional polymers can specifically interact with two other types of polymers/surface and provide a possibility to prepare complex assemblies in one step. Assembly 2 in Figure 1 shows the layer-by-layer self assembly of the three polymers. Firstly, the first layer polymer (Ph-DADMAC) interacted electrostatically with negatively charged surfaces. On the other hand, the phenolic groups from Ph-DADMAC formed hydrogen bonding with polyethylene glycol groups from APBA-PEG. Thus, Ph-DADMAC underwent independent electrostatic and hydrogen bonding interactions. Similarly, APBA-PEG, the second layer polymer, formed both hydrogen bonding with Ph-DADMAC and boronic acid-polyols condensation with the third layer polymer (PVA). The thicknesses of each polymer layer on a silicon wafer or a polystyrene particle were measured as a function of pH.

In this chapter, two new copolymers containing pairs of noninteracting groups were prepared to replace the old copolymers. Figure 1 shows two trilayer assemblies prepared by old and new approach. For Assembly 2 in Figure 1, the two water-soluble and bifunctional copolymers eliminated the potential crosstalk in the old trilayer assembly (Assembly 1), which provides a route to one-step multilayer assembly by three independent interactions. Moreover, the utility of multiple and independent interactions was also demonstrated by formation of complex latex aggregates. Specifically, copolymers Ph-DADMAC, APBA-PEG and polyvinylalcohol (PVA) were adsorbed on monodispersed polystyrene latexes with diameters 1 μm/500 nm/200 nm or 100 μm/10 μm/1μm in aqueous solutions. The particles self assembled to form hierarchical structures. Furthermore, pH could be used to turn on or off the interaction of phenyl boronate polymers with polyvinylalcohol.

3.2 Experimental

Materials

Diallyldimethyl ammonium chloride (DADMAC), 4-acetoxystyrene, poly-(ethylene glycol) methacrylate (PEG, Mw 360 Da) and monodispersed polystyrene latex suspensions with the diameters 200 nm, 500 nm, 1 μm, 10 μm (red) and 100 μm (blue) were all obtained from Aldrich. Poly(vinyl alcohol) (PVA, Mw. 72k and 97.5-99.5%

degree of hydrolysis) was purchased from Fluka. The PEG macromonomers were purified with an Aldrich inhibitor removal column (Product No. 306312) before use. Other chemicals were used without further purification. Details about the preparation and purification of monomer 3-acrylamide phenylboronic acid (APBA) have been described previously[19].

Methods

Copolymers Ph-DADMAC containing 4-acetoxystyrene (Ph) and diallyldimethyl ammonium chloride (DADMAC) and copolymers APBA-PEG containing 3-acrylamide phenylboronic acid (APBA) and poly(ethylene glycol) methacrylate (PEG) were prepared by free radical polymerization. The APBA-PEG copolymers were prepared from a 0.10 mol/L monomers (APBA and PEG, 20:80 mol %) mixture in 100 ml water using a 0.4 mmol/L potassium persulfate initiator at 65 ℃ for 8 hours. To prepare the copolymer, Ph-DADMAC, 0.1 mol monomer 4-acetoxystyrene was added drop by drop into 0.10 mol/L monomer DADMAC dissolved in 100 ml methanol/water (60:40 volume %) mixture in a three-neck glass flask reactor. The mixture was heated with an oil bath and purged with nitrogen under stirring with a stirring bar. The reaction was conducted at 65 ℃ for 10 hours using 0.4 mmol/L 2,2'-azobis(2-methylpropionamidine)·2HCl as an initiator. The polymer was hydrolyzed in 0.6 mol/L aqueous sodium hydroxide at 55 ℃ for 30 h to remove the acetate protecting group. The products were dialyzed against water for two weeks and were subsequently freeze-dried. The polymer compositions were determined by proton NMR to be Ph-DADMAC (63: 37 mol%) and APBA-PEG (13: 87 mol%).

The refractive index increments (dn/dc) of the copolymers Ph-DADMAC and APBA-PEG dissolved in deionized water were determined with a Bausch & Lomb Abbe-3L refractometer. The dn/dc for Ph-DADMAC is 0.144 mL/g and the dn/dc for APBA-PEG is 0.167 mL/g. The molecular weights were examined by static light scattering (Brookhaven BI-ISTW equipped with a 5 mW Ne-He laser). Copolymers were dissolved in deionized water and filtered through a syringe filter (Millex, pore size 5 μm, filter diameter 25 mm, Product No. Z227439) to remove dust particles. The data analysis was performed with a Brookhaven's Zimm plot analysis software and the molecular weights are $6.6\pm1.9\times10^5$ g/mol (Ph-DADMAC) and $8.3\pm0.86\times10^5$ g/mol (APBA-PEG).

The thickness of the dried polymer films on a silicon wafer were measured using Waterloo Digital Electronics Extra 2000 Faraday-Modulated Self-Nulling Ellipsometer. Silicon wafers were purchased from El-Cat Inc. (Waldwick, NJ). They were first rinsed with 50 ml methanol and toluene, and then treated with a buffered 1% HF aqueous solution (7:1 NH_4F/HF) to remove the oxidation layer before use. Hydrofluoric (HF) acid is extremely corrosive and toxic. All work associated with its use should be carefully conducted in a fume hood. Face protection and gloves are required when handling it. The disposal of HF should follow the procedures provided by the supplier. Multilayer polymer layers were assembled on a silicon wafer by layer-by-layer method (LbL). The silicon wafers were immersed in 0.1 wt% Ph-DADMAC solution with 2 mM NaCl first for three hours and rinsed gently by dipping 5 times into 2 mM NaCl solution to remove weakly adsorbed polymers. The pH of the solutions was adjusted with 0.1 M NaOH or HCl. The same procedures were sequentially carried out with 0.1 wt% APBA-PEG and with 0.1 wt% PVA. The multilayer thin films on silicon wafer were then dried at room temperature under a nitrogen atmosphere.

Ellipsometry measured two parameters Δ (phase difference) and Ψ (tan(Ψ) is the amplitude ratio upon reflection), from which film thickness and refractive index of dry films can be calculated. For a specific thin film, both the thickness and the refractive index can be calculated from a single test. Nevertheless, the measurement of refractive index is insensitive when the thickness of a dry film is less than 30 nm. Therefore, the refractive indices of the three copolymers were separately measured from their thick films, which were obtained by spin coating at 3000 rpm with acceleration for 100 rpm (P-6000 spin coater from Specialty Coating System, Inc.). Silicon wafers were cleaned before use with the same procedure described above. Three 1.0 g/L polymer solutions were prepared for spin coating. Thick polymer films on wafers were annealed under vacuum at 115℃ for 3 h. The results show that the copolymer refractive indices are Ph-DADMAC (nL1) 1.566, APBA-PEG (nL2) 1.516, and PVA (nL3) 1.557. The refractive indices of multilayer thin films are the arithmetic mean values of the refractive index of every polymer layer. Therefore, the refractive index values were nL1 for a one-layer film, 0.5nL1 + 0.5nL2 for the two-layer films, and 1/3nL1 + 1/3nL2 + 1/3nL3 for the three-layer films.

The densities of Ph-DADMAC polymer and APBA-PEG polymer were calculated from the following expression: ρ＝m/V (m is the mass of coated polymers on a wafer, V is the

volume of coated polymers). Thick polymer films were coated on a silicon wafer with 20 cm^2 area. The mass of the polymer layers was determined gravimetrically. A plasma beam was employed to cut the polymer film from top to bottom to facilitate measuring the film thickness by SEM. The polymer densities of Ph-DADMAC and APBA-PEG are 1.09 g/cm^3 and 1.17 g/cm^3, respectively. The density of PVA is 1.27 g/cm^3, which was obtained from Sigma. The details of the calculations are in the appendices.

Trilayer films were also assembled on the surfaces of a 500 nm diameter polystyrene latex suspension. Concentrated latex was added into 0.1 wt% Ph-DADMAC solution with 2 mM NaCl to give a latex concentration of 0. 1 g/L at certain pH. After three hours, the polystyrene particles were centrifuged at 6000 rpm which corresponds to a centrifugal force of 4000g for 40 minutes using a Beckman Allegra™ 25R bench centrifuge, and then redispersed in a 2 mM NaCl solution at certain pH by shaking the centrifuge tube. Two more centrifugations were conducted to remove weakly adsorbed polymers on the surface of the particles. Subsequently, the adsorption of the second layer polymers (0.1 wt% APBA-PEG) and the third one (0.1 wt% PVA) were used to prepare the bilayer assembly (layer 1 + layer 2) and then the third layer polymers PVA to fabricate the trilayer structures by the same procedure. The same pH values were kept during every preparation step of the trilayer structures at certain pH and the pH of the solutions was controlled with 0.1 M NaOH or HCl.

To study the nanoparticle assembly, three different polymers separately were adsorbed onto three latex particles with different sizes. For example, the preparation of 1 μm latex particles adsorbed with Ph-DADMAC polymers is the following: the polystyrene latex with 1 μm diameter was added into 0.1 wt% Ph-DADMAC solution with 2 mM NaCl to give a latex concentration of 0. 1 g/L. Afterwards, the latex particles were centrifuged at 6000 rpm for 30 minutes and redispersed in a 2 mM NaCl solution. Any loosely adsorbed polymer was removed by two more centrifugations. Similarly, 500 nm latex particles adsorbed with APBA-PEG polymers and 200 nm latex particles adsorbed with PVA polymers were prepared. Hereafter, three 0.05g/L latex suspensions with 2 mM NaCl were mixed with slow stirring at room temperature for 3 hours. The pH of the solutions was controlled with 0.1 M NaOH or HCl. Subsequently, a 20 μL mixed latex suspension was dried on a copper grid coated with Formvar at room temperature for TEM characterization. TEM images were acquired using a JEOL JEM-1200EX transmission electron microscope.

Optical micrographs of nanoparticle assembly in aqueous environment were taken from a drop of mixed latex suspension on a glass slide using an Olympus BX51 optical microscope with a Q-Imaging Retiga EXi digital camera (ImagePro software).

Dynamic light scattering (DLS) was employed to measure the sizes of latex particles. The concentration of polystyrene latex particles is 0.002 wt%, which is high enough to obtain reasonable scattering signals and also advantageous to prevent from latex aggregation. All the measurements were carried out at 25 °C with a Brookhaven 256 channel BI-9000 AT digital correlator and a Lexel 35 mW He−Ne laser (633 nm wavelength) at a scattering angle of 90°. The data were analyzed via the program CONTIN to give the particle sizes. The reported particle diameters are an average of three measurements.

Electrophoretic mobility measurements were performed with a Brookhaven ZetaPlus zeta potential analyzer using phase analysis light scattering (PALS) mode with BIC Pals Zeta Potential Analyzer software (version 2.5). All data were averaged over ten cycles with 15 scans for each.

3.3 Results

Two water-soluble and bifunctional polymers, Ph-DADMAC and APBA-PEG were prepared and characterized. The polymer compositions were determined by proton NMR and were Ph (63 mol %)-DADMAC (37 mol%) and APBA(13 mol%)-PEG (87 mol%). The molecular weights were Ph-DADMAC ($6.6\pm1.9\times10^5$ g/mol) and APBA-PEG ($8.3\pm0.86\times10^5$ g/mol), which were determined by static light scattering. Polyvinylalcohol (PVA) with molecular weight 72 kDa was used as layer 3 polymer to assemble trilayer films. Layer-by-layer method (LbL) was employed to assemble multilayer polymer layers on a silicon wafer. A clean silicon wafer was soaked in 0.1 wt% Ph-DADMAC solution with 2 mM NaCl for three hours and rinsed gently by dipping 5 times into 2 mM NaCl solution to remove non-adsorbed polymers. The pH values of the copolymer solution and NaCl solution were consistent by adjusting with 0.1 M NaOH or HCl. As a result, Ph-DADMAC copolymers containing the quaternary ammonium moieties were adsorbed onto the anionic silicon wafer. Similarly, 0.1 wt% APBA-PEG and 0.1 wt% PVA solutions were consecutively used to form the second and the third layers. The copolymer structure is shown in Figure 1.

The formation of multilayer polymer complex on a silicon wafer was monitored by an ellipsometric characterization of the dried films. The thicknesses of dried films are given as a function of pH in Figure 2 (A) and these values were used to estimate the coverage (mass/area) of adsorbed polymer. For Ph-DADMAC and APBA-PEG, the thickness of each layer is approximately 3 nm during entire pH range and it is consistent with the results of other consecutively adsorbed monolayers[19-21]. By contrast, the formation of phenyl boronate-polyol complex by APBA-PEG and PVA showed pH dependent behavior. The film thickness after exposure to layer 3 polymer did not increase at low pH, suggesting that PVA did not adsorb onto layer 2 polymer. However, the thickness of adsorbed PVA was 3 nm at high pH.

Based on the ellipsometry data and polymer densities, we calculated the coverage of the three adsorbed layers. The coverage of layer 1 and layer 2 polymers was approximately 3 mg/m^2 over the entire pH range, while there is almost no adsorption of layer 3 polymer at low pH. At pH 10.0, the coverage of layer 3 was 3 mg/m^2.

The trilayer polymer assemblies were also formed on 500 nm polystyrene latex particles by LBL adsorption. Microelectrophoresis was used to probe the surface charge of multilayer thin films adsorbed onto polystyrene particles and the results are summarized in Figure 3. Electrophoretic mobility of trilayer polymers as a function of pH was illustrated.

The electrophoretic mobility of the polystyrene particles adsorbed with layer 1 copolymers Ph-DADMAC decreased with the increase of pH, reflecting the presence of phenolic groups[22]. Similar trends were observed for the polystyrene particles adsorbed with layer 2 copolymers APBA-PEG. The decreasing pH values with the increase of pH illustrated the presence of the charged phenyl borate moieties. Layer 3 polymers PVA adsorbed on polystyrene particles showed zero electrophoretic mobility over the whole pH range, because the latex particles were covered with nonionic polymers. The electrophoretic mobility of trilayers (layer 1+2+3) on polystyrene particles showed similar mobility values with that of layer 2 polymers on polystyrene particles at low pH, whereas the trilayer curve dropped at high pH. Interestingly, the trilayer curve was between the layer 2 and layer 3 curves when pH is higher than 8.5. Figure 4 shows the schematic trilayer adsorption on polystyrene particles. The adsorption is controllable and

dependent on pH.

The adsorbed layer thicknesses for the various layers on polystyrene latex were estimated from the change in average diameter, measured by dynamic light scattering. Figure 5 shows the results for two experiments. In Figure 5 (A), dynamic light scattering shows the thicknesses of trilayer polymers adsorbed on monodispersed polystyrene particles in aqueous solutions. In water, the water-soluble polymer chains are outstretched. For layer 1 and layer 2 polymers, the thicknesses are approximately 20 nm over the entire pH range, whereas the thickness of layer 3 polymers polyvinyl alcohol is greatly dependent on pH.

I propose that hydrogen bonding was the driving force between layer 1 copolymers Ph-DADMAC and layer 2 copolymers APBA-PEG in multilayer assembly. The interaction between phenolic groups from Ph-DADMAC and PEG groups from APBA-PEG held the two copolymers together and then formed stable bilayer thin films. Undoubtedly, an easy way to disassemble the multilayer structures by disrupting this interaction is favorable in controllable self-assembly study. Therefore, another group of experiments shown in Figure 5 (B) were done weeks after the first group of experiments shown in Figure 5 (A). The duplicated film thickness of Ph-DADMAC copolymers and the film thickness of Ph-DADMAC + APBA-PEG gave larger error than before. In the experiments, some polyethylene glycol small molecules (PEG, Mw 600 Da) were added into the suspension of bilayer assembly on polystyrene particles. The dosage of PEG was 10 times (mol %) more than the PEG moiety of APBA-PEG polymers. The DLS measurements conducted one hour after mixing showed that the thickness has a distinct decrease from about 36 nm to 19 nm, indicating that small molecules PEG displaced layer 2.

To exploit the nanoparticle assembly by multiple independent interactions, the three types of polymers were used to direct the assembly of three different sized latex particles. Three polymers were separately adsorbed onto the surfaces of three different sized latex particles. Thus, the nanoparticle assembly formed after mixing by the interactions between polymers.

Electron micrographs and optical micrographs, displayed in Figure 6, show the formation of latex aggregates in both aqueous atmosphere and after they were dried between phenolic donor and a PEG acceptor. In TEM tests (A and B), layer 1 (Ph-DADMAC) and

layer 2 (APBA-PEG) polymers were adsorbed onto two monodispersed polystyrene particles with 1000 nm and 500 nm diameters. In optical microscopy tests (C and D), layer 1 and layer 2 polymers were supported by another two polystyrene particles with 100 μm and 10 μm diameters. Subsequently, two 0.05g/L latex suspensions with 2 mM NaCl were mixed with slow stirring at room temperature for 3 hours. The pH value of the mixed suspension was adjusted at 7. At neutral pH, two different sized latex particles formed satellite structures. Bigger nanoparticles were surrounded by smaller ones. The well-defined structure in Figure 6 illustrates the interaction between layer 1 and layer 2 copolymers in the nanoparticle assemblies.

Similarly, latex aggregates driven by boronate-polyols complex formation were shown in Figure 7. Layer 2 copolymers were adsorbed onto 500 nm polystyrene particles and layer 3 polymers (PVA) were adsorbed onto 200 nm polystyrene particles. The two suspensions were mixed at pH 10 with slow stirring for 3 hours. SEM (A) and TEM (B) showed the nanoparticle self-assembly when the mixed suspension was dried at room temperature. Also, layer 2 copolymers and layer 3 polymers were adsorbed onto 10 μm and 1 μm polystyrene particles for optical microscopy tests. The pH of the mixed suspension was adjusted to 4 and 10. From C and D in Figure 7, we conclude that layer 2 polymer supported by polystyrene particles formed boronate ester with layer 3 polymer adsorbed on another polystyrene particle at high pH. However, the self-assembly structure disassembled at low pH. Interestingly, the self-assembly process is reversible and can be easily controlled by pH.

Figure 8 shows TEM and optical microscopy images of reversible assembly of polystyrene particles adsorbed with different polymers. Ph-DADMAC, APBA-PEG and PVA were adsorbed on polystyrene latexes with diameters 1 μm/500 nm/200 nm (A-C) or 100 μm/10 μm/1μm in aqueous solutions (D). Picture A illustrated the self assembly of layer 1 particles and layer 2 particles at pH 4. However, there is no evidence that layer 2 particles interacted with layer 3 particles at low pH. In Pictures B-D, both hydrogen bonding and covalent bonding were used to achieve the self-assembly of the three types of nanoparticles. The nanoparticle assembly structures further confirmed the polyethylene glycol (PEG) - phenolic copolymer complex and phenyl boronate-polyols complex formation among the three polymers. The formation of latex aggregates shows a good example of utility of multiple, independent interactions. Furthermore, the aggregate structures can be easily controlled by adjusting pH. Optical microscope tests showed the

interactions among these three polymers in water. Compared with TEM pictures, the self-assembly of the nanoparticles in water excluded the possibility of the surface tension used as a driving force when the samples were dried. Picture E showed three polystyrene latexes with diameters 1000 nm/500 nm/200 nm, illustrating that there is no interaction among these three latex particles without polymer coatings.

3.4 Discussion

The major challenges in the design of copolymers involve their water solubility, pH sensitivity, composition and dual functionality. For example, commercial boronic acid containing monomers have terrible water solubility. Thus, I prepared the monomer 3-acrylamide phenylboronic acid (APBA) to give the copolymer better solubility in water. The hydrogen bonding comes from the interaction between phenol groups from layer 1 copolymers and PEG groups from layer 2 copolymers. However, I found that the layer 2 polymer become insoluble at low pH, if PEG moieties and phenol moieties were exchanged. Moreover, the composition is also important to the solubility of the copolymer. The feed ratio of each monomers and the solvent should be carefully controlled.

Thus, the selection of monomers and optimization of reaction conditions become particularly important. For example, layer 2 copolymers (VAm-PBA-Ph) in Assembly 1 have two functional groups (boronic acids and phenols). Boronic acid groups have interactions with layer 3 polymer PVA and phenol groups interact with PEG groups from layer 1 copolymer BTM-PEG. VAm-PBA-Ph was prepared by consecutive derivatization of polyvinylamine with 3-carboxyphenylboronic acid and 4-hydroxybenzoic acid. Polyvinylamine as the main chain has good solubility in water and much amine groups provide an ideal platform for grafting of small molecules. However, VAm-PBA-Ph is positively charged at high pH, due to the ionization of amine groups. Thus, layer 2 copolymer VAm-PBA-Ph may become trifunctional and have electrostatic attractions with anionic surfaces. To avoid the crosstalk, a new layer 2 copolymer APBA-PEG was prepared by traditional free radical copolymerization of monomers 3-acrylamide phenylboronic acid and poly(ethylene glycol) methacrylate.

The thickness of dry polymer films in the assembly system was measured by ellipsometry; thereby the polymer coverage of each polymer as a function of pH was calculated. The polymer coverage of layer 1 and layer 2 polymers is approximately 3 mg/m^2 for each over the entire pH range. In addition, the thickness of polymer films in aqueous solution was also measured, shown in Figure 5 (A), the thicknesses of layer 1 and layer 2 polymers are

approximately 16 nm in water over the entire pH range. The typical adsorbed layer thickness for polyelectrolytes on oppositely charged substrate is usually within dozens of nanometers. However, the film thickness is dependent on the molecular weight of the polymers, the nature and density of charged groups, pH values of polymer solutions, salt concentrations, surface roughness, etc[23].

The pH is not a decisive parameter of film thickness for layer 1 and layer 2 copolymers. Figure 2 (B) shows that the polymer coverage of layer 1 polymer reached its maximum at pH 10 and then decreased to average amount. One explanation is that the phenol moiety of layer 1 polymer was negatively charged with increasing pH, and the negative charges make the polymer configuration more compact on silicon surface by interacting with its DADMAC groups. However, the charge change of layer 1 polymer was screened by increasing ionic strength resulting from NaOH adding. It is unexpected that the change of the thickness of layer 2 polymers is not obvious with the change of pH, because hydrogen bonding, the interaction between PEG groups of layer 1 polymers and phenol groups of layer 2 polymers, is usually variable with pH[14, 24]. It is explained by the decreasing hydrogen bonding with PEG groups when the phenol groups are dissociated at high pH. In this work, A possible explanation for the consistent film thickness of layer 2 coplymers is that the complex of layer 1 and layer 2 exists by ion-dipole interaction[25] between PEG groups and the ionized phenol groups at high pH. However, more direct evidence is required to support this statement.

Salt concentration is another crucial factor in multilayer assemblies. It is found that it is possible to reverse the polyelectrolyte association, when the salt concentration is higher than critical salt concentration. Dubas reported the thickness of PAA/PDADMA multilayer film as a function of salt concentration[26]. The multilayer was stable to NaCl concentration up to around 0.4 mol/L, after which point the multilayer film decomposed. In my experiments, the salt concentrations were controlled at 2 mM. The low salt concentration has little influence on the formation of trilayer assembly.

In spite of the ever increasing understanding of interaction between PEG and phenolic polymers, the detailed structure of PEG/phenolic copolymers is still elusive. In current work, both of the layer 1 copolymers Ph-DADMAC and layer 2 copolymers APBA-PEG was random copolymers, leading to a more complicated situation. Pelton's group reported the possible structure of PEO chains hydrogen bonded to poly(vinyl phenol). They believe that no more than 1/4 of the polyether oxygens participate in the complex formation with poly(vinyl phenol), owing to the steric restriction[14, 27].

The PVA thickness curves shown in Figure 2 and Figure 5 (A) indicates that layer 3 polymers did not adsorb onto layer 2 polymer at low pH, but PVA with 3 nm thickness adsorbed onto APBA-PEG at high pH. This result is consistent with our study before[19], since boronate ester formation usually occurs at pH values above 8. Thus, pH could be used to turn on or off the interaction of layer 2 polymers and layer 3 polymers in this trilayer polymer system. In addition, interaction of layer 1 polymers and layer 2 polymers can also be controlled by adding some small molecules PEG, shown in Figure 5 (B). Low molecular weight PEG have a competition with the PEG moiety of APBA-PEG polymers, thereby PEG moiety of APBA-PEG polymers bound with phenol groups of layer 1 polymers was substituted by plentiful small molecules PEG. As a result, the initial bilayer structure was broken and the thickness of the polymer films had a great decrease.

In this chapter, a new self-assembly trilayer were prepared to replace the old one. The new copolymers eliminated the potential crosstalk in the old trilayer assembly. I also demonstrated the formation of controllable nanoparticle aggregates by multiple and independent interactions. Three independent polymer-polymer or polymer-surface interaction mechanisms were employed to prepare complex assemblies. These approaches offer the possibility of large-scale and low-cost self-assembly in one step. In future work, we will address other issues, such as kinetics of interaction, film properties to the details of copolymer composition, strength of complexes, etc.

3.5 Conclusions

1. Three independent polymer-polymer interactions, based on 1) electrostatic attraction, 2) hydrogen bonding, and 3) boronate ester formation were used to form layer-by-layer adsorbed polymers and to control the self-assembly of three types of nanoparticles.

2. Each of the three types of polymer-polymer interactions can be “turned off” independently: boronate esters are hydrolyzed by lowering pH; PEG-copolymer phenol H bonding is disrupted by low molecular weight PEG addition; and, electrostatic adsorption on the substrate is reversed by electrolyte addition.

3. Key design characteristics of the bi-functional copolymers are water solubility and the absence of interactions between layer-three and layer-one polymer. Moreover, layer 2 polymers and layer 3 polymer eliminates the feasibility of their electrostatic attractions with anionic surfaces.

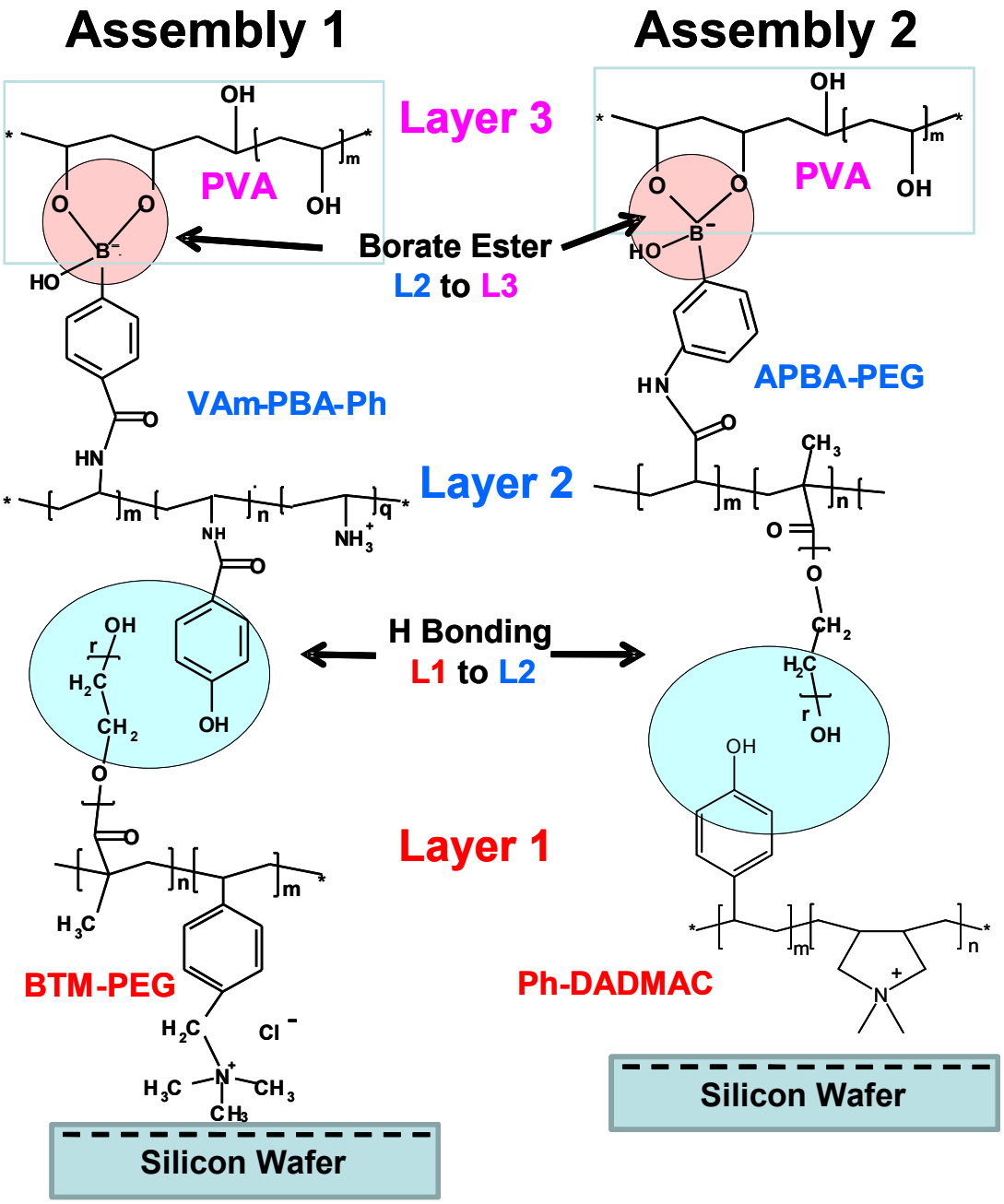

Figure 1 Two examples of trilayer polymer assembly based on electrostatics (surface to layer 1), hydrogen bonding (layer 1 to layer 2), and boronate/polyols complexation (layer 2 to layer 3)

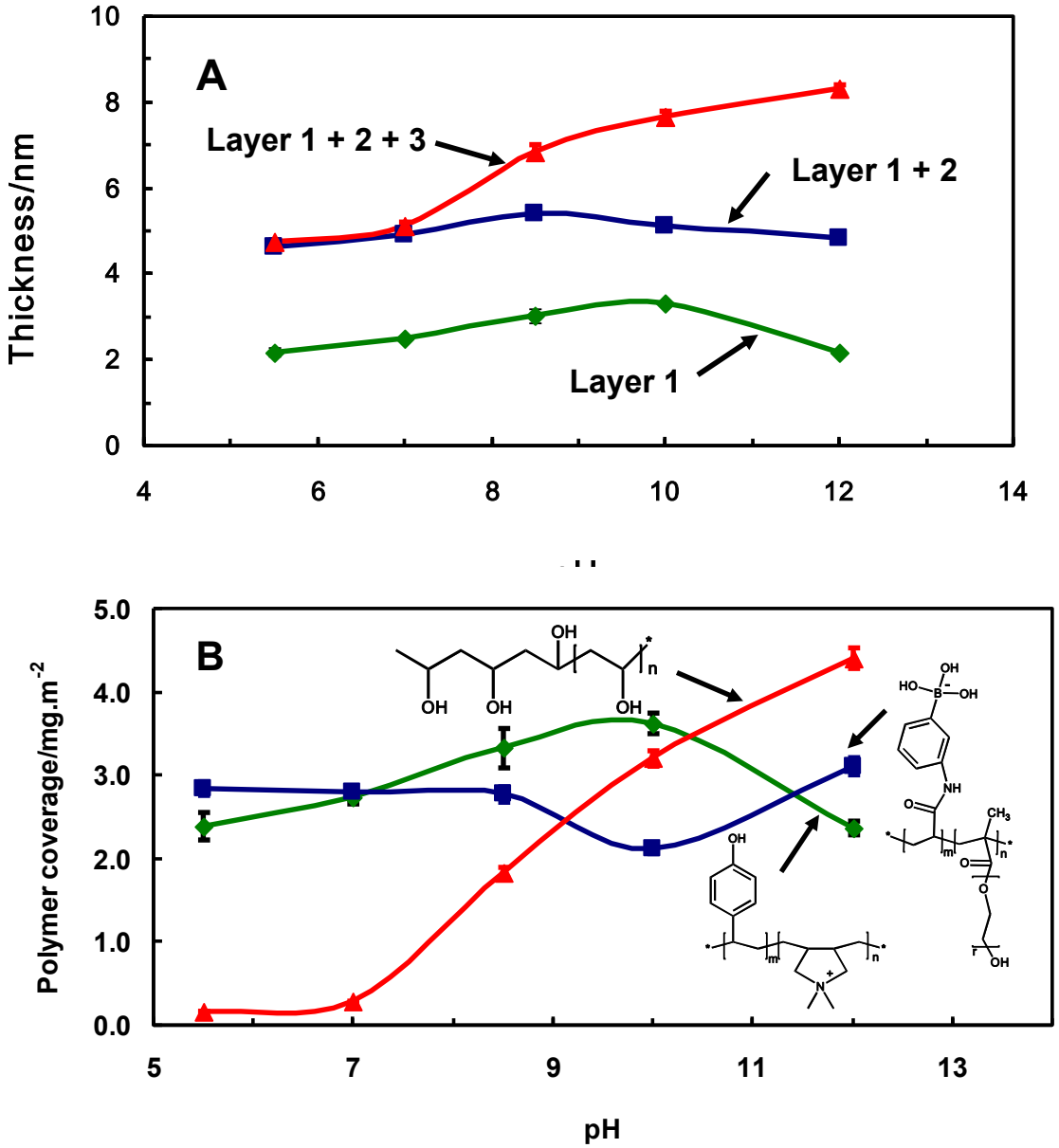

Figure 2 (A) Thicknesses of dry films assembled by LBL method on a silicon wafer were determined by ellipsometry. The pH mentioned in the figure refers to the pH at both adsorption and rinse. The laser wavelength was 632.8 nm and the incident angle was 70 degrees. The measurements were performed under ambient laboratory conditions and all data are an average of three measurements. (B) Polymer adsorption densities of trilayer polymers on a silicon wafer. The following polymer densities were used to calculate the coverage of that layers - layer 1 (Ph-DADMAC) 1.09 g/cm^3, layer 2 (APBA-PEG) 1.17 g/cm^3, and layer 3 (PVA) 1.27 g/cm^3.

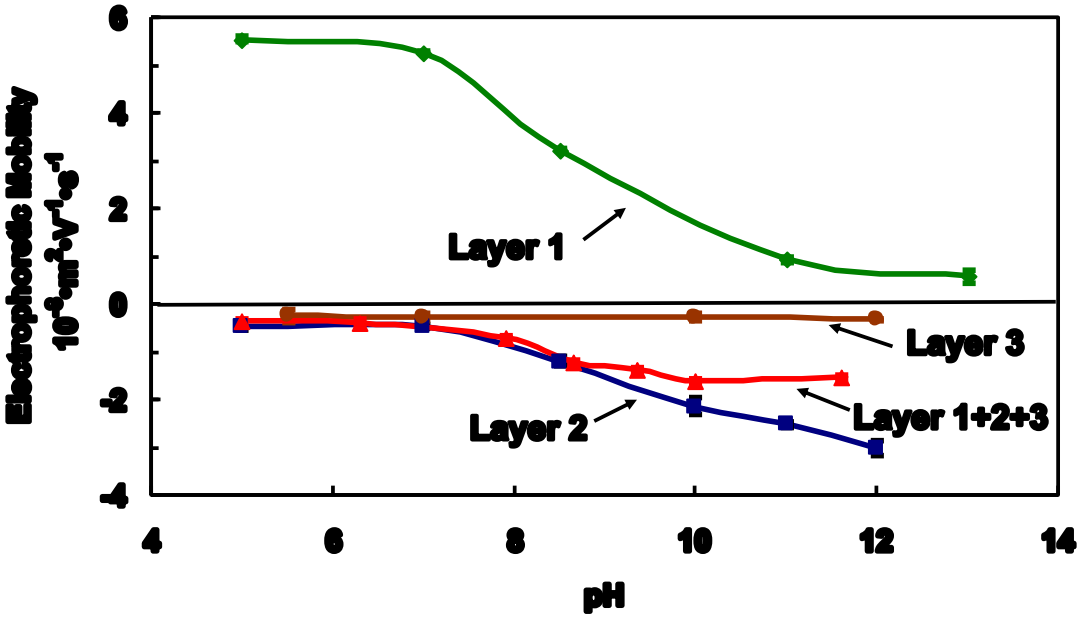

Figure 3 Electrophoretic mobilities of polystyrene particles (Diameter 500nm) adsorbed with trilayer polymers. All measurements were performed in 2 mM NaCl aqueous solutions at 25 °C. Layer 1, layer 2 and layer 3 polymers were adsorbed onto the latex particles separately. Trilayer polymers were also adsorbed onto the particles by LBL method.

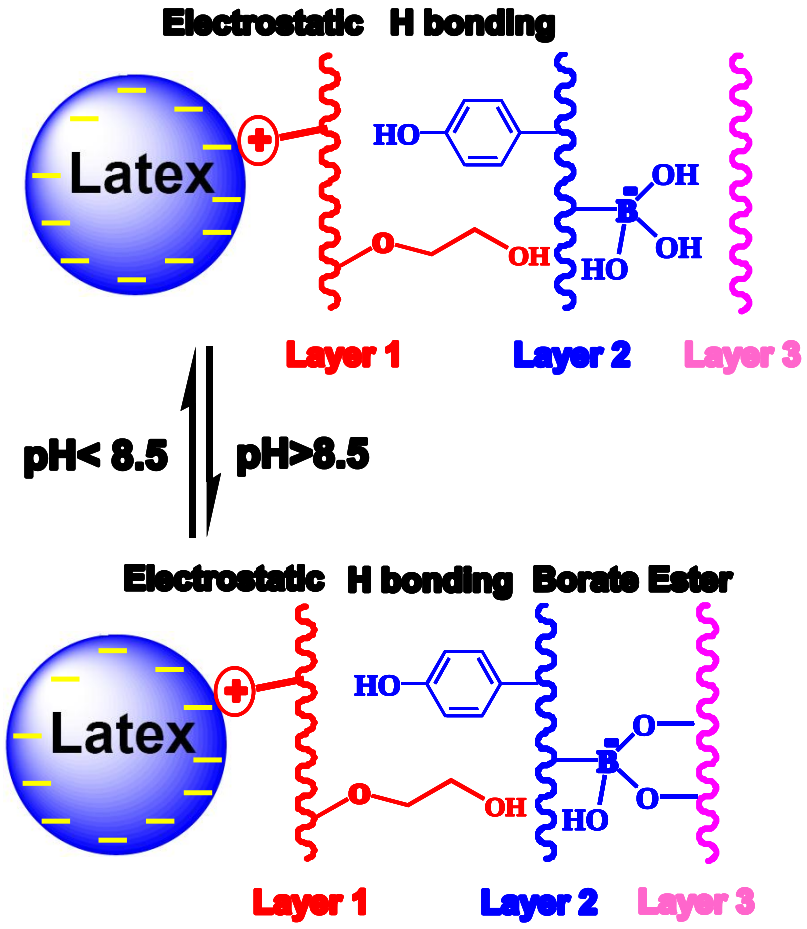

Figure 4 Schematic trilayer adsorption on a polystyrene particle.

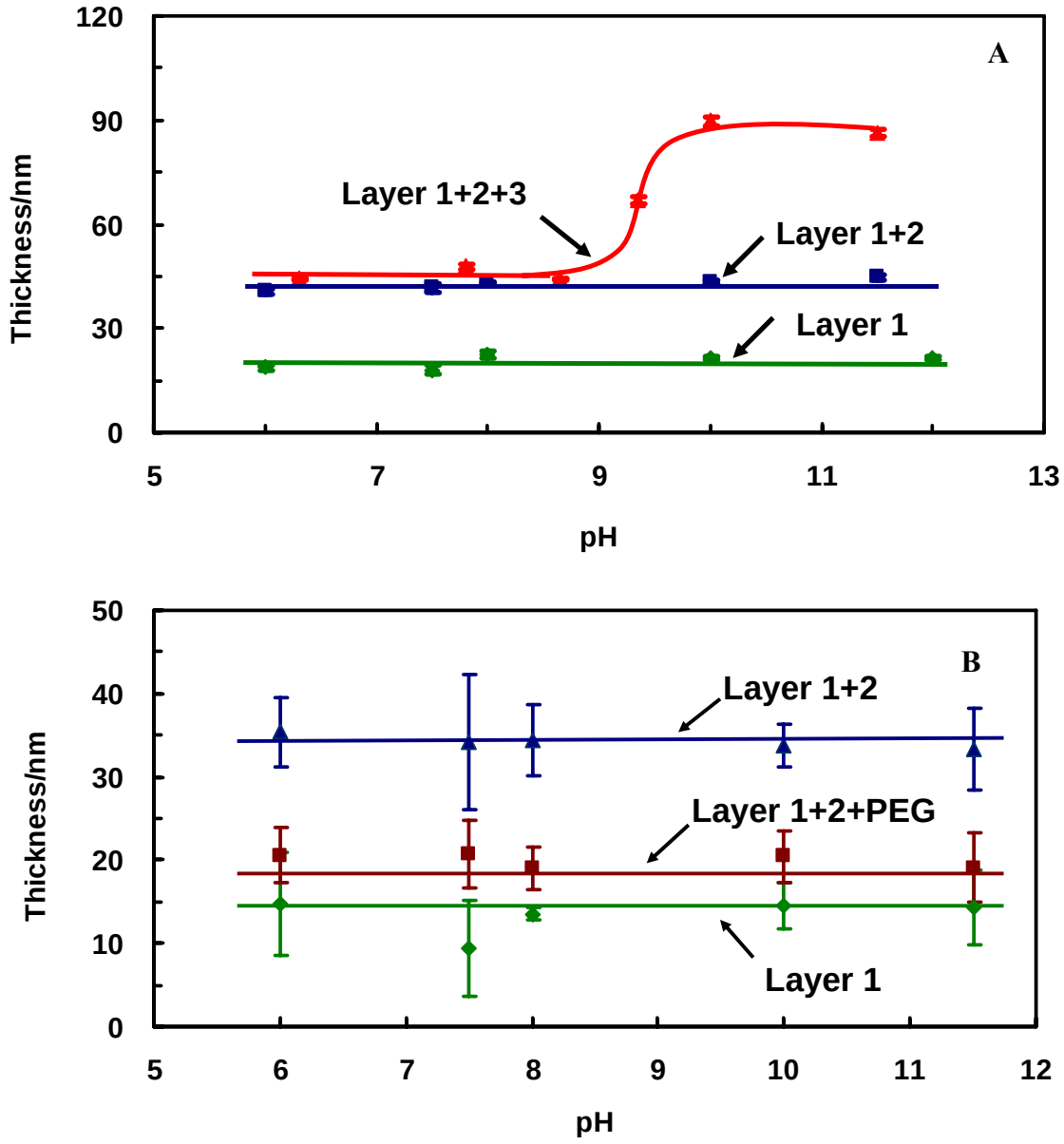

Figure 1 (A) Thicknesses of monolayer, bilayer and trilayer polymers adsorbed on a 500 nm polystyrene particle in aqueous solutions. (B)Thicknesses of monolayer, bilayer and bilayer/PEG (Mw 600 Da) adsorbed on a 500 nm polystyrene particle in aqueous solutions. All measurements were conducted in 2 mM NaCl solutions at 25 °C.

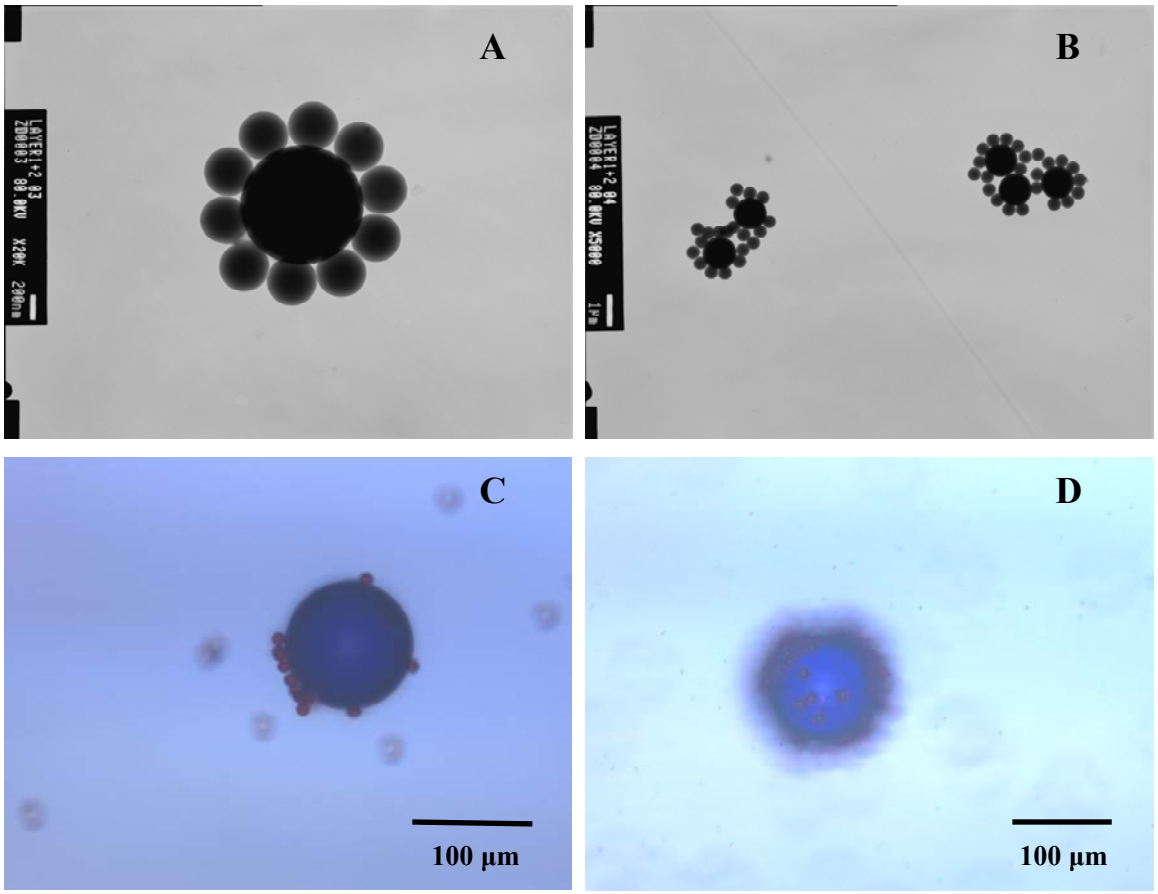

Figure 6 A and B are transmission electron microscopy images of 1000 nm polystyrene particles covered with layer 1 polymers and 500 nm polystyrene particles covered with layer 2 polymers at pH=7. C and D are microscopy images of blue polystyrene particles (100 µm) covered with layer 1 polymers and red polystyrene particles (10 µm) covered with layer 2 polymers at pH=7 in water.

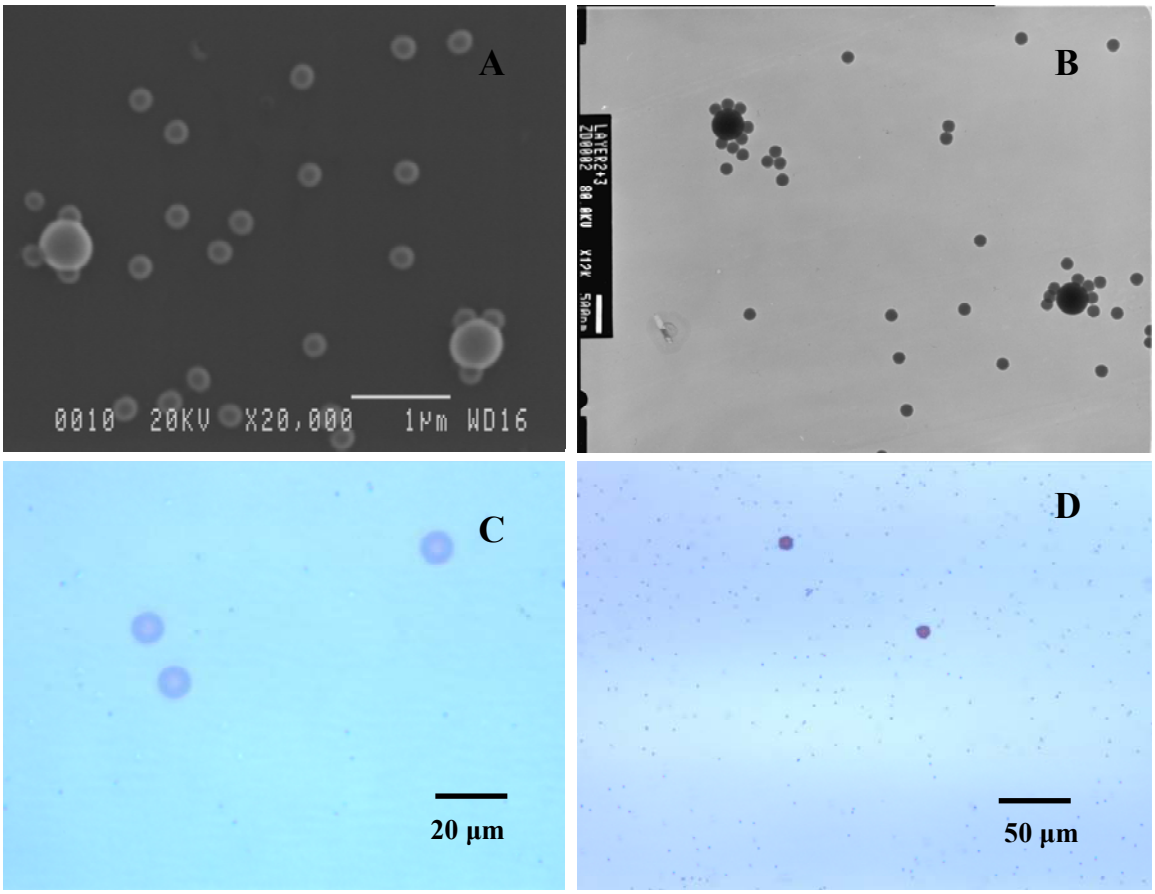

Figure 7 A is a scanning electron microscopy image of 500 nm polystyrene particles covered with layer 2 polymers and 200 nm polystyrene particles covered with layer 3 polymers at pH=10. B is a transmission electron microscopy image of 500 nm polystyrene particles covered with layer 2 polymers and 200 nm polystyrene particles covered with layer 3 polymers at pH=10. C and D are microscopy images of 10 μm polystyrene particles covered with layer 2 polymers and 1 μm polystyrene particles covered with layer 3 polymers in water. The insets are zoomed figures obtained at the same experimental conditions.

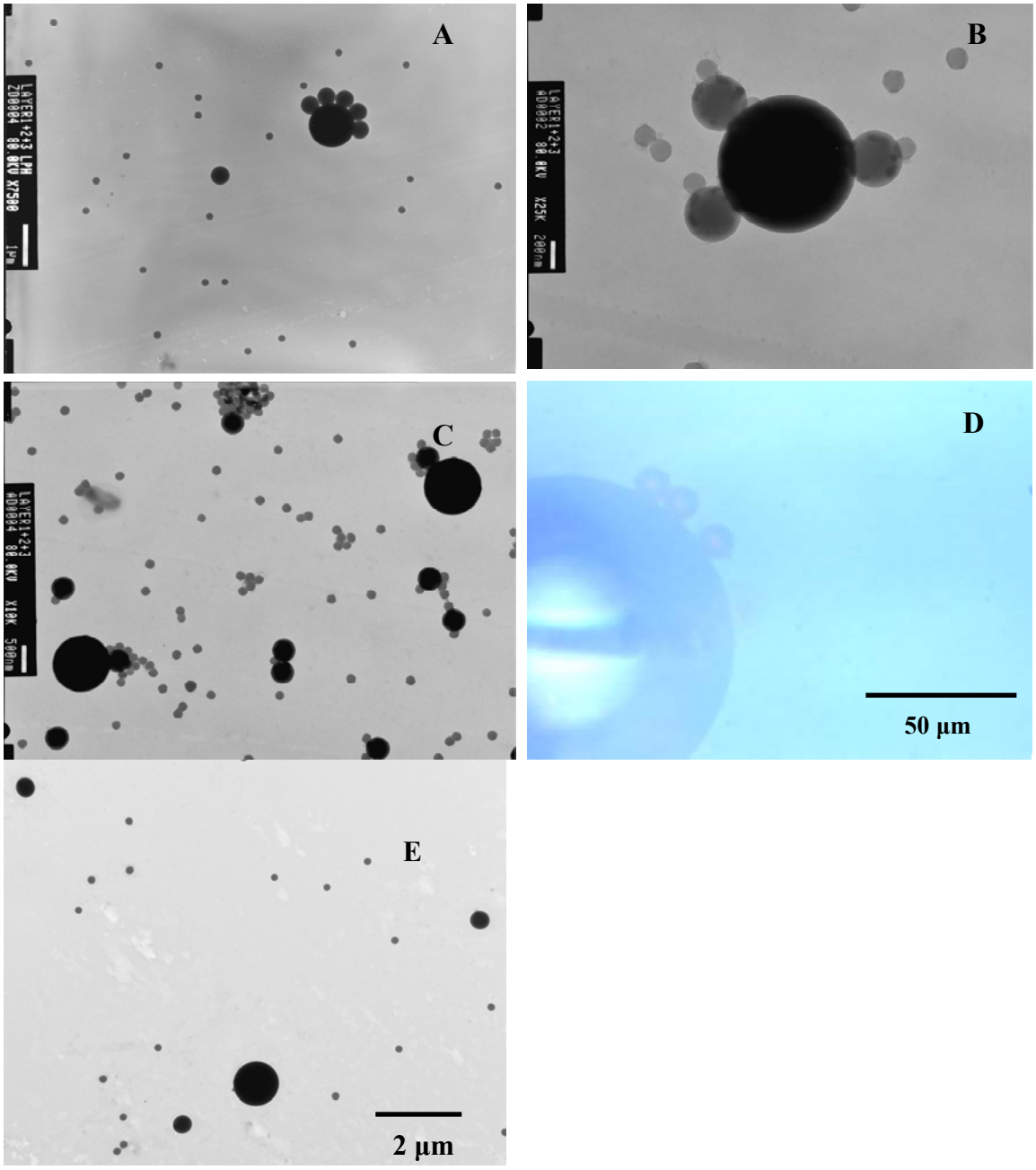

Figure 8 Microscope images of reversible assembly of polystyrene particles adsorbed with polymers. Ph-DADMAC, APBA-PEG and PVA were adsorbed on polystyrene latexes with diameters 1 µm/500 nm/200 nm (A-C) or 100 µm/10 µm/1µm in aqueous solutions (D). (E) is a control experiment, showing three polystyrene latexes with diameters 1 µm/500 nm/200 nm.

References

1. Decher, G., Fuzzy nanoassemblies: Toward layered polymeric multicomposites. *Science* 1997, *277* (5330), 1232-1237.

2. Zhang, X.; Shen, J. C., Self-assembled ultrathin films: From layered nanoarchitectures to functional assemblies. *Advanced Materials* 1999, *11* (13), 1139-1143.

3. Ariga, K.; Lvov, Y.; Kunitake, T., Assembling alternate dye-polyion molecular films by electrostatic layer-by-layer adsorption. *Journal of the American Chemical Society* 1997, *119* (9), 2224-2231.

4. Van Cott, K. E.; Guzy, M.; Neyman, P.; Brands, C.; Heflin, J. R.; Gibson, H. W.; Davis, R. M., Layer-by-layer deposition and ordering of low-molecular-weight dye molecules for second-order nonlinear optics (vol 41, pg 3236, 2002). *Angewandte Chemie-International Edition* 2002, *41* (19), 3719-3722.

5. Schmitt, J.; Decher, G.; Dressick, W. J.; Brandow, S. L.; Geer, R. E.; Shashidhar, R.; Calvert, J. M., Metal nanoparticle/polymer superlattice films: Fabrication and control of layer structure. *Advanced Materials* 1997, *9* (1), 61-65.

6. Sun, Y. P.; Hao, E.; Zhang, X.; Yang, B.; Shen, J. C.; Chi, L. F.; Fuchs, H., Buildup of composite films containing tio2/pbs nanoparticles and polyelectrolytes based on electrostatic interaction. *Langmuir* 1997, *13* (19), 5168-5174.

7. Caruso, F.; Furlong, D. N.; Ariga, K.; Ichinose, I.; Kunitake, T., Characterization of polyelectrolyte-protein multilayer films by atomic force microscopy, scanning electron microscopy, and fourier transform infrared reflection-absorption spectroscopy. *Langmuir* 1998, *14* (16), 4559-4565.

8. Lvov, Y.; Ariga, K.; Ichinose, I.; Kunitake, T., Assembly of multicomponent protein films by means of electrostatic layer-by-layer adsorption. *Journal of the American Chemical Society* 1995, *117* (22), 6117-6123.

9. Lu, C.; Pelton, R., Peo flocculation of polystyrene-core poly(vinylphenol)-shell latex: An example of ideal bridging. *Langmuir* 2001, *17* (25), 7770-7776.

10. Lu, C.; Pelton, R., Factors influencing the size of peo complexes with a tyrosine-rich polypeptide. *Langmuir* 2004, *20* (10), 3962-3968.

11. Yang, H. C.; Aoki, K.; Hong, H. G.; Sackett, D. D.; Arendt, M. F.; Yau, S. L.; Bell, C. M.; Mallouk, T. E., Growth and characterization of metal(ii) alkanebisphosphonate multilayer thin-films on gold surfaces. *Journal of the American Chemical Society* 1993, *115* (25), 11855-11862.

12. Chan, E. W. L.; Lee, D. C.; Ng, M. K.; Wu, G. H.; Lee, K. Y. C.; Yu, L. P., A novel layer-by-layer approach to immobilization of polymers and nanoclusters. *Journal of the American Chemical Society* 2002, *124* (41), 12238-12243.

13. Zhang, F.; Jia, Z.; Srinivasan, M. P., Application of direct covalent molecular assembly in the fabrication of polyimide ultrathin films. *Langmuir* 2005, *21* (8), 3389-3395.

14. Cong, R. J.; Bain, A. D.; Pelton, R., An nmr investigation of the interaction of polyethylene oxide with water-soluble poly(vinyl phenol-co-potassium styrene sulfonate). *J. Polym. Sci. Pt. B-Polym. Phys.* 2000, *38* (10), 1276-1284.

15. Lu, C.; Richardson, R.; Pelton, R.; Cosgrove, T.; Dalnoki-Veress, K., Peo penetration into water-plasticized poly(vinylphenol) thin films. *Macromolecules* 2004, *37* (2), 494-500.

16. Cong, R. J.; Pelton, R., The influence of peo/poly(vinyl phenol-co-styrene sulfonate) aqueous complex structure on flocculation. *Journal of Colloid and Interface Science* 2003, *261* (1), 65-73.

17. Cong, R. J.; Pelton, R.; Russo, P.; Doucet, G., Factors affecting the size of aqueous poly(vinylphenol-co-potassium styrenesulfonate)/poly(ethylene oxide) complexes. *Macromolecules* 2003, *36* (1), 204-209.

18. Niwa, M.; Sawada, T.; Higashi, N., Surface monolayers of polymeric amphiphiles carrying a copolymer segment composed of phenylboronic acid and amine. Interaction with saccharides at the air-water interface. *Langmuir* 1998, *14* (14), 3916-3920.

19. Zhang, D.; Tanaka, H.; Pelton, R., Polymer assembly exploiting three independent interactions. *Langmuir* 2007, *23* (17), 8806-8809.

20. Kharlampieva, E.; Kozlovskaya, V.; Tyutina, J.; Sukhishvili, S. A., Hydrogen-bonded multilayers of thermoresponsive polymers. *Macromolecules* 2005, *38* (25), 10523-10531.

21. Zhang, H. Y.; Wang, Z. Q.; Zhang, Y. Q.; Zhang, X., Hydrogen-bonding-directed layer-by-layer assembly of poly(4-vinylpyridine) and poly(4-vinylphenol): Effect of solvent composition on multilayer buildup. *Langmuir* 2004, *20* (21), 9366-9370.

22. McGhie, T. K.; Markham, K. R., Separation of flavonols by capillary electrophoresis - the effect of structure on electrophoretic mobility. *Phytochem. Anal.* 1994, *5* (3), 121-126.

23. Shiratori, S. S.; Rubner, M. F., Ph-dependent thickness behavior of sequentially adsorbed layers of weak polyelectrolytes. *Macromolecules* 2000, *33* (11), 4213-4219.

24. Xiao, H. N.; Pelton, R.; Hamielec, A., The association of aqueous phenolic resin with polyethylene oxide and poly(acrylamide-co-ethylene glycol). *J. Polym. Sci. Pol. Chem.* 1995, *33* (15), 2605-2612.

25. Bailey, F. E.; Callard, R. W.; Callard, R. W., Some factors affecting the molecular association of poly(ethylene oxide) and poly(acrylic acid) in aqueous solution. *J. Polym. Sci. Pol. Chem.* 1964, *2*, 845-851.

26. Dubas, S. T.; Schlenoff, J. B., Polyelectrolyte multilayers containing a weak polyacid: Construction and deconstruction. *Macromolecules* 2001, *34* (11), 3736-3740.

27. Pelton, R.; Xiao, H. N.; Brook, N. A.; Hamielec, A., Flocculation of polystyrene latex with mixtures of poly(p-vinylphenol) and poly(ethylene oxide). *Langmuir* 1996, *12* (24), 5756-5762.

Supporting Information

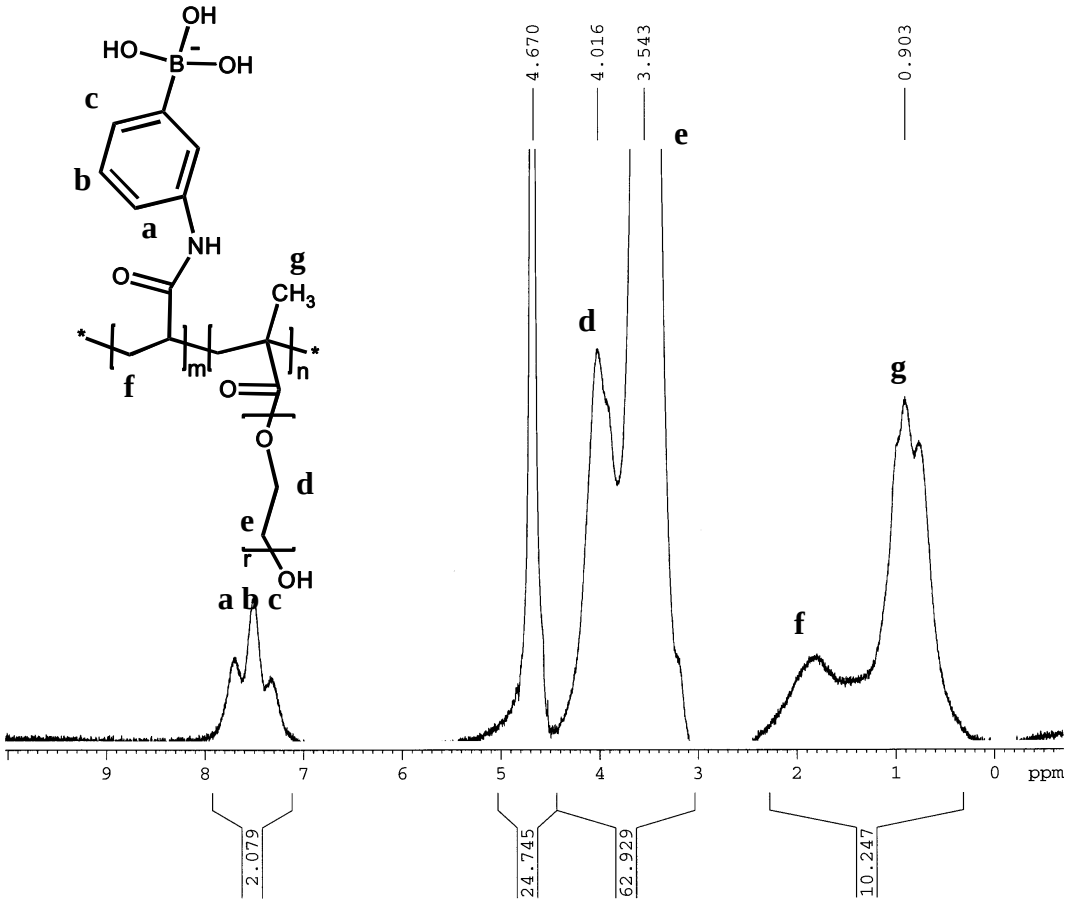

Figure S1 ^{1}H NMR spectra of layer 2 polymer APBA-PEG

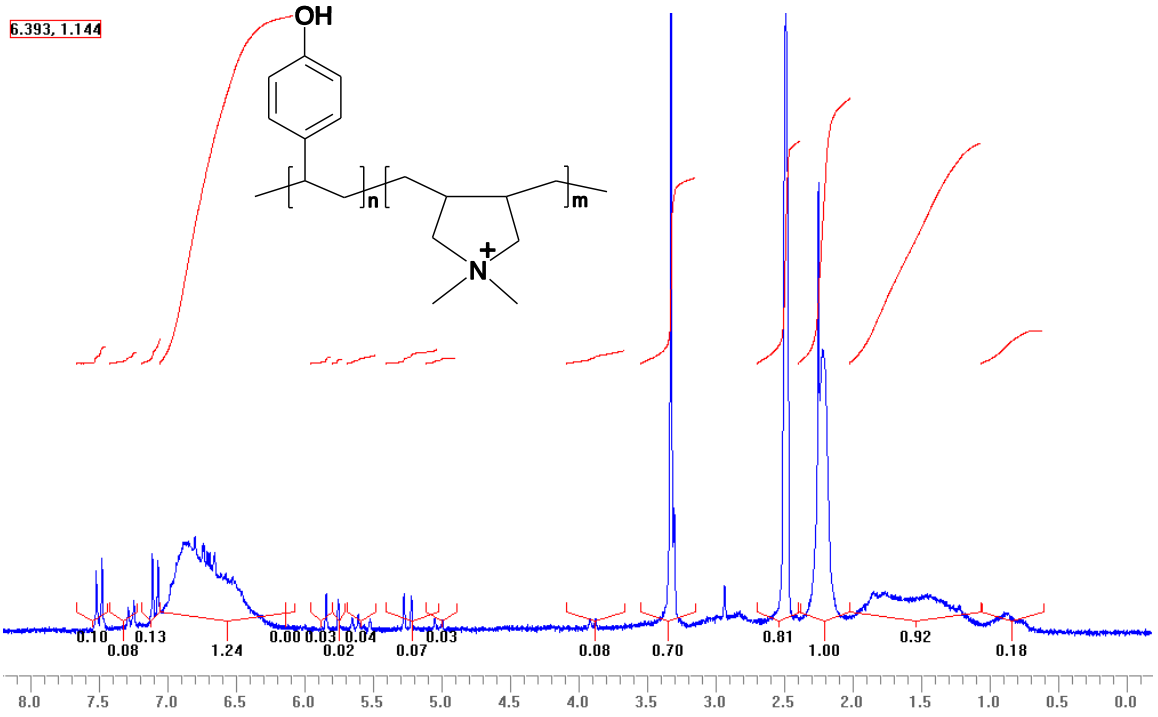

Figure S2 ^{1}H NMR spectra of layer 1 polymer Ph-DADMAC

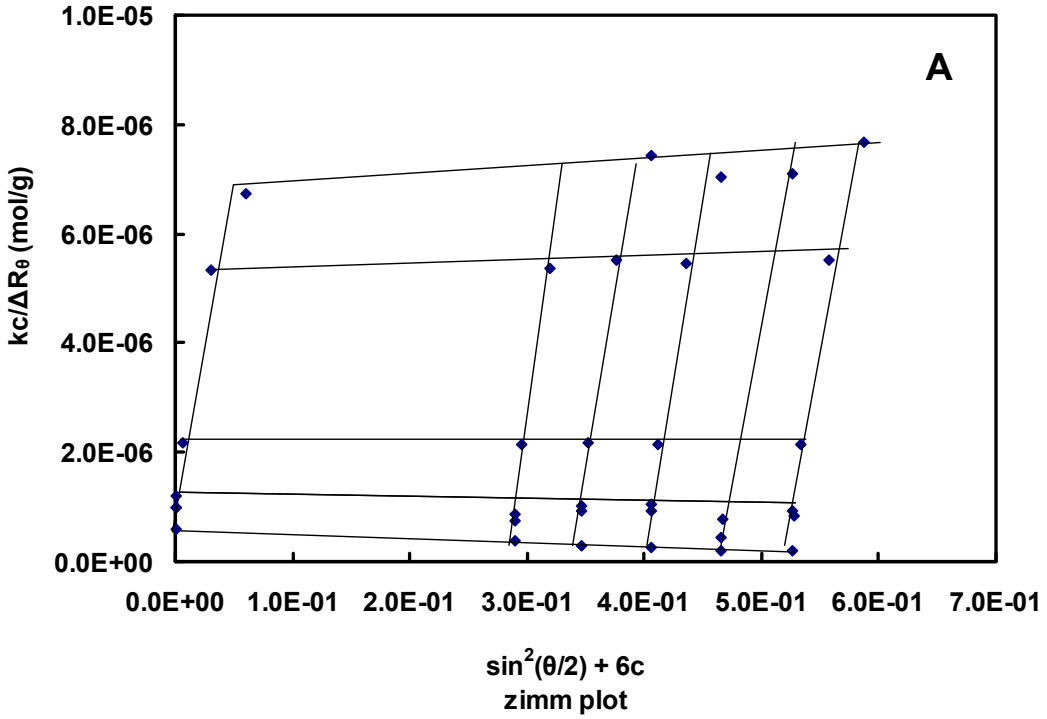

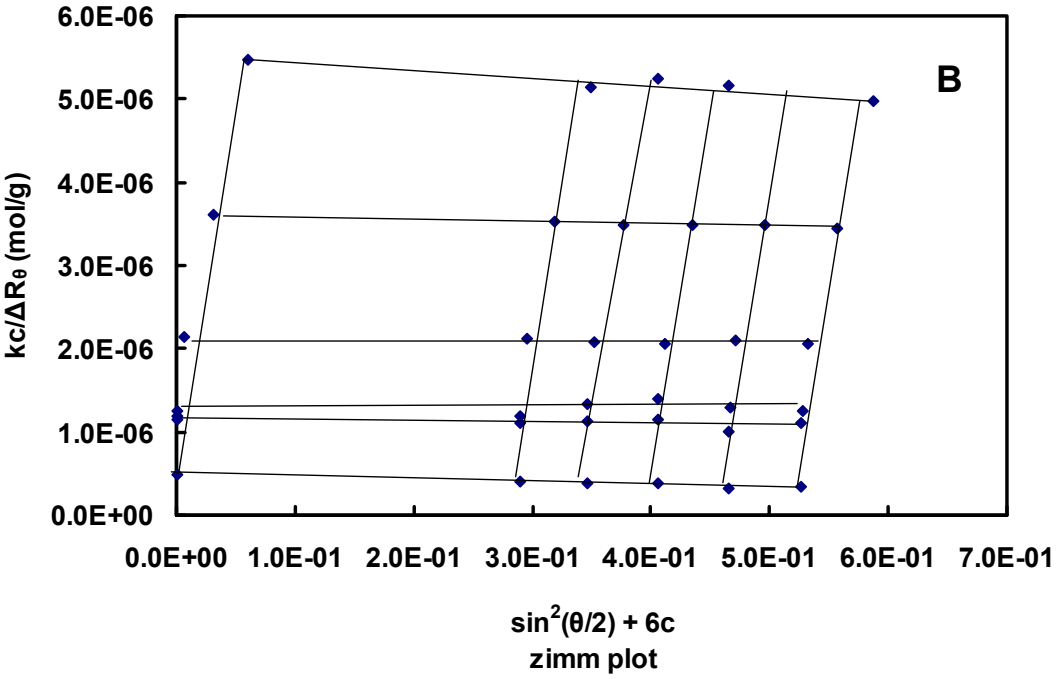

Figure S3 Zimm plot of total intensity light-scattering data from solutions of (A) layer 1 polymer (APBA-PEG) and (B) layer 2 polymer (Ph-DADMAC)

Chapter 4 Controlling Deposition and Release of Polyol-Stabilized Latex on Boronic Acid-Derivatized Cellulose

In Chapter 4, Dr. Armes and his student Kate L. Thompson prepared poly(glycerol monomethacrylate)-stabilized polystyrene (PGMA-PS) latex particles. I conducted all the other experiments and calculations. Dr. Pelton revised my manuscript and offered some useful discussion and good advices.

Langmuir
Article
pubs.acs.org/Langmuir

Controlling Deposition and Release of Polyol-Stabilized Latex on Boronic Acid-Derivatized Cellulose

Dan Zhang,[†] Kate L. Thompson,[‡] Robert Pelton,*[,†] and Steven P. Armes[‡]

[†]*Department of Chemical Engineering McMaster University, Hamilton, Ontario, Canada, L8S 4L7, and* [‡]*Department of Chemistry, University of Sheffield, Brook Hill, Sheffield, South Yorkshire, S3 7HF United Kingdom*

Received August 30, 2010. Revised Manuscript Received September 26, 2010

Poly(glycerol monomethacrylate)-stabilized polystyrene (PGMA-PS) latex particles undergo specific, pH-dependent adsorption onto regenerated cellulose film bearing surface phenylboronic acid groups (cellulose-PBA). Deposition occurs at pH 10 and is driven by the boronate ester formation with the polyol latex surface coating. In contrast, no deposition occurs at pH 4, and previously deposited particles can be readily desorbed at this lower pH. In control experiments, conventional anionic sulfate-stabilized polystyrene latex did not deposit onto the hydrophilic cellulose surface. The distribution of boronate groups in the cellulose was determined by exposure to Alizarin Red S dye, which forms a fluorescent complex with phenylboronic acid; confocal microscopy was used to determine a surface density of 3 nm^2 per boronic acid group on the cellulose surface. Although the boronic acid binding constant with PGMA is relatively low (5.4 L/mol), the cooperative interactions between multiple PBA surface sites and the many PGMA chains per latex particle are sufficient to induce specific latex adsorption, providing a convenient new tool for controlling nanoparticle deposition on surfaces.

Introduction

Self-assembly is critical for the manufacture of low cost nanostructured materials from nanoparticle dispersions. A conventional latex paint coating is a good example of a self-assembled nanostructured material. During drying, surface tension forces the nanoparticles together within the paint film, causing the softer polymeric components to sinter. At the other extreme of complexity, biological structures depend upon specific recognition events to drive assembly, including enzyme−substrate, antibody−antigen, and DNA−duplex formation. In this paper we demonstrate a new approach for controlling the deposition (and removal) of nanoparticles on surfaces, which may allow us to get closer to the complexity of biological assembly.

Our approach is based upon the pH-dependent condensation of borate ions with polyols. Specifically, we demonstrate the pH dependent deposition of poly(glycerol monomethacrylate), (PGMA)-coated polymer colloids onto regenerated cellulose film derivatized with phenylboronic acid groups. The structure of the phenylbornate-PGMA esters is shown in Figure 1 and the binding constant is 5.4 L/mol,[1] which is low. Boronate-polyol condensation is an enthalpy driven process[2,3] and the solution pH is a critical parameter. It is generally accepted,[4] although not unanimously,[5] that the boronate ion, rather than the uncharged

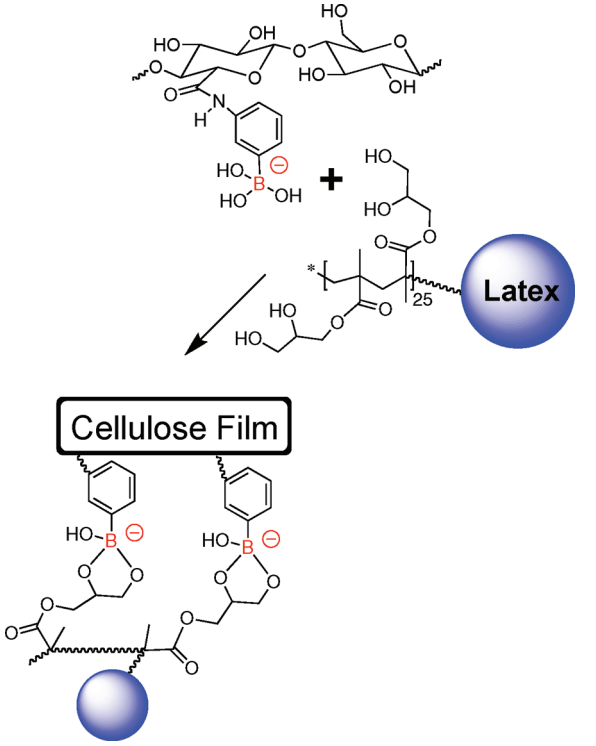

Figure 1. Reaction of phenylboronate-derivatized cellulose with the PGMA stabilizer chains coating on the latex particle surface.

*Corresponding author. Tel: (905) 529 7070 ext. 27045. Fax: (905) 528 5114. E-mail: peltonrh@mcmaster.ca.

(1) Keita, G.; Ricard, A.; Audebert, R. Viscosity behavior of poly(glyceryl methacrylate) in the presence of borate and phenylboronate ions. *J. Polym. Sci., Part B: Polym. Phys.* **1995**, *33*, 1015–1022.

(2) Pizer, R.; Ricatto, P. J. Thermodynamics of several 1−1 and 1−2 complexation reactions of the borate ion with bidentate ligands - b-11 nmr spectroscopic studies. *Inorg. Chem.* **1994**, *33*, 2402–2406.

(3) Torun, Z.; Dudak, F. C.; Bas, D.; Tamer, U.; Boyaci, I. H. Thermodynamic analysis of the interaction between 3-aminophenylboronic acid and monosaccharides for development of biosensor. *Sens. Actuators, B* **2009**, *140*, 597–602.

(4) Springsteen, G.; Wang, B. H. A detailed examination of boronic acid-diol complexation. *Tetrahedron* **2002**, *58*, 5291–5300.

(5) Iwatsuki, S.; Nakajima, S.; Inamo, M.; Takagi, H. D.; Ishihara, K. Which is reactive in alkaline solution, boronate ion or boronic acid? Kinetic evidence for reactive trigonal boronic acid in an alkaline solution. *Inorg. Chem.* **2007**, *46*, 354–356.

(6) Matsumoto, A.; Ikeda, S.; Harada, A.; Kataoka, K. Glucose-responsive polymer bearing a novel phenylborate derivative as a glucose-sensing moiety operating at physiological ph conditions. *Biomacromolecules* **2003**, *4*, 1410–1416.

form of boronic acid, is the reactive species. Thus the reaction shown in Figure 1 requires pH values either near or above the pK_a of phenylboronic acid adduct (8.9).[6]

Recently Thompson et al. reported the synthesis of novel sterically stabilized polystyrene latexes using a near-monodisperse PGMA macromonomer as a reactive steric stabilizer.[7] Herein we report the pH-dependent adsorption of these PGMA-stabilized PS latexes onto cellulose surfaces bearing phenylboronic acid groups (cellulose-PBA).

Experimental Section

Materials. NaCl, NaBr, NaClO aqueous solution (~10 wt %), 3-aminophenylboronic acid, *N*-(3-dimethylaminopropyl)-*N*′-ethylcarbodiimide hydrochloride (EDC), 2,2′-azobisisobutyronitrile (AIBN), and 2,2,6,6-tetramethylpiperidine-1-oxyl (TEMPO) were obtained from Aldrich and were used without further purification. The styrene and *n*-butyl acrylate monomers were purified by passing through a column of basic alumina before use. An anionic 1 μm polystyrene latex was purchased from Fluka. Polyvinylamine (PVAm) with a molecular weight of 15 000 Da was obtained from BASF (Germany). To ensure complete hydrolysis from poly(*N*-vinyl formamide), this polymer precursor was treated with 5% NaOH at 70 °C under nitrogen flow for 48 h. The product was dialyzed against water for two weeks using cellulose dialysis tubing (3500 Da molecular weight cutoff, Spectrum Laboratories, Inc.) and freeze-dried. All aqueous solutions were prepared with Milli-Q water.

Latex Syntheses. Two PGMA-stabilized latexes with either a high T_g polystyrene core or a low T_g poly(styrene-*co*-*n*-butyl acrylate) core were prepared according to the general protocol recently reported by Thompson et al.[7] The mean degree of polymerization of the PGMA macromonomer was 50 as judged by ^{1}H NMR spectroscopy and GPC analysis (DMF eluent; poly(methyl methacrylate) calibration standards) indicate a M_w/M_n of 1.21. The *n*-butyl acrylate mass content of the copolymer latex was chosen to be approximately 50%, which reduces its T_g to below room temperature. This film-forming copolymer latex also contained ~1.0 wt % fluorescein methacrylate comonomer to facilitate confocal microscopy studies.

$PGMA_{50}$-PS Latex Synthesis. $PGMA_{50}$ macromonomer (0.50 g) was dissolved in water (44.5 g) in a 100 mL round-bottomed flask equipped with a magnetic stirrer bar. This solution was purged with N_2 for 30 min then heated to 70 °C in an oil bath. A solution of AIBN (0.050 g) dissolved in styrene (5.0 g) was then injected into the reaction solution. The reaction was stirred at 70 °C for 24 h. This high T_g latex was purified by three centrifugation/redispersion cycles, replacing each supernatant with deionized water. This high T_g polystyrene latex is denoted as PGMA-PS.

$PGMA_{50}$-P(S-nBuA) Copolymer Latex Synthesis. $PGMA_{50}$ macromonomer (0.50 g) and fluorescein-*o*-methacrylate (0.050 g) were dissolved in water (44.5 g) in a 100 mL round-bottomed flask equipped with a magnetic stirrer bar. This solution was purged with N_2 for 30 min then heated to 70 °C in an oil bath. A solution of AIBN (0.050 g) dissolved in the 1:1 styrene/*n*-butyl acrylate mixture (2.5 g of each monomer; total mass = 5.0 g) was then injected into the reaction solution. The reaction was stirred at 70 °C for 24 h. This low T_g copolymer latex was purified by exhaustive dialysis against deionized water. This low T_g fluorescently labeled poly(styrene-*co*-*n*-butyl acrylate) copolymer latex is denoted as PGMA-P(S-nBuA).

Cellulose−PBA Preparation. Regenerated cellulose dialysis tubing (No. 132682, 12k Da molecular weight cutoff, Spectrum Laboratories, Inc.) was cut into 1 × 3 cm strips and then soaked in water at room temperature for 24 h to remove the glycerin plasticizer. Subsequently, they were rinsed three times with water and stored wet at 4 °C. In order to introduce conjugation sites, the cellulose films were oxidized by TEMPO-mediated oxidation according to Anelli,[8] which almost exclusively oxidizes C-6 hydroxyls to carboxyl groups.[9,10] Cellulose strips (1.0 g) were suspended in 250 mL of water at room temperature. TEMPO (0.01 g), NaBr (0.10 g), and 10 wt % NaClO solution (16 mL) were subsequently added, and the solution pH was maintained at 10.5 with 1 M NaOH. After reaction for 2 h at room temperature, this oxidation reaction was quenched with excess ethanol. Previous work performed in similar conditions showed that the content of carboxyl groups was ~0.02 meq/g dry cellulose.[11]

Cellulose−COOH (1 g) was derivatized with 3-aminophenylboronic acid (0.20 g) using EDC (5.40 g), with all reagents being dispersed in 200 mL water at pH 6.0. The mixture was stirred at 25 °C for 3 h and then quenched by exhaustive washing with Milli-Q water. A control experiment was conducted without EDC and ARS analysis (see below) confirmed that any physically adsorbed 3-aminophenylboronic acid was washed away.

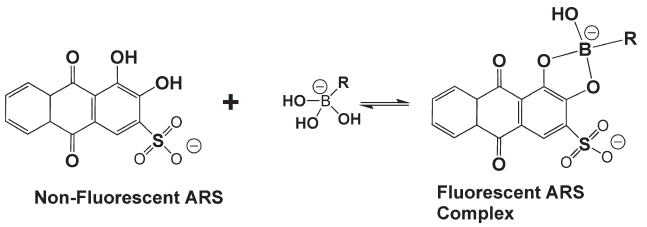

Figure 2. Alizarin Red S (ARS), which fluoresces only when present as a boronate complex.[4]

The total phenyl boronate content of the film and the distribution of boronate groups through the thickness of the film was measured in two types of experiments involving Alizarin Red S (ARS). Figure 2 shows the condensation product formed between ARS and a boronate anion.[4,12] The ARS−boronate adduct fluoresces whereas the ARS dye alone does not. To measure the total content of phenylboronic acid moieties in the cellulose, the films were soaked for 2 h at room temperature in a solution of 0.25 g/L ARS in 2 mM NaCl at pH 11. The treated films were gently rinsed by dipping five times into 2 mM NaCl solution at pH 11 to remove uncondensed ARS. In order to desorb all of the bound ARS, the cellulose films were soaked into 10 mL of 2 mM NaCl solution at pH 2.75 for 2 h. The absorbance of the ARS dye in the supernatant solution was measured at 420 nm and the corresponding ARS concentration was determined from the linear calibration curve.

The calculation of the total phenylboronic acid content was made as follows. The reaction is shown in Figure 2 where R is a phenyl group bounded to cellulose (see Figure 1). The fraction of phenylboronate groups that was condensed with ARS was calculated using the published equilibrium constant for the condensation of ARS with phenylboronic acid, which was 1300 L/mol.[4] Furthermore, we assumed ideal solution behavior and that at pH 11 all of the phenylboronic acid was present as boronate species. Under these conditions, 48% of phenylboronate species should be present as ARS adducts. Thus the total content of phenylboronic acid in the cellulose film was estimated to be 0.012 meq/g.

(7) Thompson, K. L.; Armes, S. P.; York, D. W.; Burdis, J. A. Synthesis of sterically-stabilized latexes using well-defined poly(glycerol monomethacrylate) macromonomers. *Macromolecules* **2010**, *43*, 2169–2177.

(8) Anelli, P. L.; Biffi, C.; Montanari, F.; Quici, S. Fast and selective oxidation of primary alcohols to aldehydes or to carboxylic-acids and of secondary alcohols to ketones mediated by oxoammonium salts under 2-phase conditions. *J. Org. Chem.* **1987**, *52*, 2559–2562.

(9) Kitaoka, T.; Isogai, A.; Onabe, F. Chemical modification of pulp fibers by tempo-mediated oxidation. *Nordic Pulp Paper Res. J.* **1999**, *14*, 279–284.

(10) Saito, T.; Shibata, I.; Isogai, A.; Suguri, N.; Sumikawa, N. Distribution of carboxylate groups introduced into cotton linters by the tempo-mediated oxidation. *Carbohydr. Polym.* **2005**, *61*, 414–419.

(11) Kurosu, K.; Pelton, R. Simple lysine-containing polypeptide and polyvinylamine adhesives for wet cellulose. *J. Pulp Paper Sci.* **2004**, *30*, 228–232.

(12) Elmas, B.; Senel, S.; Tuncel, A. A new thermosensitive fluorescent probe for diol sensing: Poly(n-isopropylacrylamide-co-vinylphenylboronic acid)-alizarin red s complex. *React. Funct. Polym.* **2007**, *67*, 87–96.

The ARS dye was also used to determine the distribution of phenylboronate groups throughout the cellulose film thickness. A total of 50 mL of 0.25 g/L ARS solution in 2 mM NaCl was prepared, and the pH of the solution was adjusted to 9.0 with 0.1 M NaOH. The cellulose films were immersed into the solution for 2 h and then gently rinsed by dipping five times into 2 mM NaCl solution at pH 9.0 to remove any ARS not condensed with borate. The cellulose films were then cut into slices and the cross section was viewed under a coverslip with a Zeiss LSM 510 laser scanning confocal microscope at a wavelength of 488 nm. Images were captured at a depth of 5 μm below the cut surface.

Latex Deposition Experiments. Aqueous latex (PGMA-PS latex or the film-forming PGMA-P(S-nBuA) latex) was diluted with 2 mM NaCl solution to give a concentration of 0.01 g/L. Two cellulose membranes were immersed into 100 mL of a latex suspension for 2 h. The pH was adjusted with 0.1 M NaOH or 0.1 M HCl to either pH 4.0 or 10.5. Thereafter, cellulose films were gently rinsed by dipping five times into 2 mM NaCl solution at either pH 4.0 or 10.5 to remove nonadsorbed latex particles.

Latex deposition onto cellulose films was monitored by either confocal laser scanning microscopy (CLSM) or by scanning electron microscopy (SEM). In CLSM, wet samples were viewed under a coverslip using a Zeiss LSM 510 laser scanning confocal microscope employing 488 nm laser excitation. SEM images of dried, gold-coated cellulose samples were obtained with an EOL JSM-840 SEM instrument.

The specific deposition of PGMA coated particles onto cellulose-boronate surfaces was further demonstrated by deposition experiments involving a mixture of PGMA particles and larger anionic polystyrene particles. Cellulose substrates were immersed in a mixed dispersion of 0.02 g/L polystyrene latex and 0.01 g/L PS-PGMA latex in 2 mM NaCl and after 4 h the films were removed and rinsed with deionized water. Two cellulose substrates were employed: the cellulose−boronate (deposition conducted at pH 10.5), described above, and unmodified cellulose that was soaked in 0.2 g/L PVAm (M_w = 15k) for four hours and exhaustively rinsed, leaving an adsorbed monolayer of the highly cationic PVAm (deposition at pH 6.5). After latex deposition and rinsing, the cellulose surfaces were characterized by SEM.

Microelectrophoresis. Electrophoretic mobilities were determined using a Brookhaven ZetaPlus zeta potential analyzer operating in phase analysis light scattering mode with BIC Pals Zeta Potential Analyzer software (version 2.5). Data were averaged over 10 cycles, with each cycle consisting of 15 scans.

Dynamic Light Scattering. Particle sizes were measured using a Brookhaven dynamic light scattering instrument equipped with a BI-9000AT autocorrelator, a 35 mW laser operating at a wavelength of 633 nm, and a scattering angle of 90°. Data were acquired using BIC dynamic light scattering software 9kdlsw32 (version 3.34). The sample cell temperature was maintained at 25 °C with a NESLAB water bath. Data were analyzed using the CONTIN method and the reported z-average particle diameters are an average of at least three measurements.

Results and Discussion

Regenerated cellulose dialysis membranes were oxidized to introduce carboxyl groups at the C6 position and the carboxylated films derivatized with 3-aminophenylboronic acid to give cellulose-PBA. The conjugation chemistry is shown in Figure 1. The total content of phenylboronic moieties in the cellulose films was 0.012 meq/g. This value was determined by ARS dye binding (see Figure 2) at pH 11, washing the film, and releasing the dye at low pH for spectrophotometric analysis.

The distribution of the phenylboronate-ARS complex through the thickness of the cellulose film was assessed by laser scanning confocal microscopy and the result are shown in Figure 3. Also shown is a plot of color intensity versus position through the film. Only the boronate groups near the surface are available to interact with the latex particles. The density of surface boronate groups was estimated to be 3 nm^2 per group based on the following analysis. The empirical intensity function in Figure 3 was integrated to give the total area under the curve and the area corresponding to the first 5 nm on each surface. The ratio of these two areas (3.4×10^{-4}) was taken as the fraction of the total phenylboronate groups present near the surface.

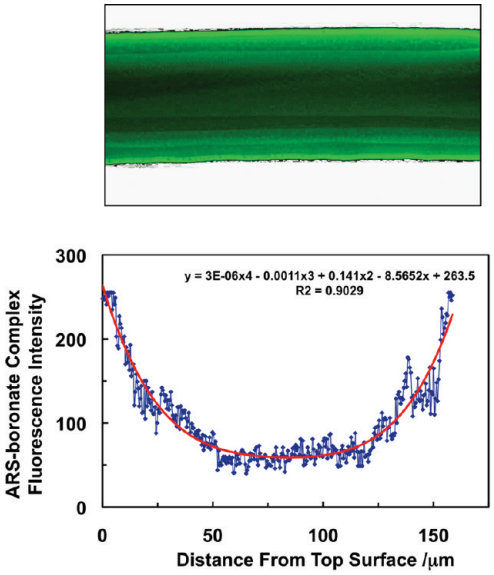

Figure 3. Laser scanning confocal micrograph of cellulose-PBA treated with ARS dye at pH 9. The fluorescence intensity (488 nm) of the ARS-boronate complex is plotted as function of distance through the film. The red line is an empirical fit of the data. The X, Y, and Z resolutions of the confocal micrographs were 450, 450, and 400 nm respectively.

Table 1. Summary of the Mean Intensity-Average Diameter, Macromonomer Content, Adsorbed Amount, and Area Occupied Per Macromonomer Chain for the Two Latexes Used in This Study[a]

	diameter (at pH 10.5)/nm	$PGMA_{50}$ content/ wt %	Γ/mg m^{-2}	area per PGMA chain/nm^2
PGMA-PS	206	9	3.2	25
PGMA-P(S-BuA)	215	8	4.3	19

[a] The macromonomer content of both latexes was determined by ^{1}H NMR spectroscopy by dissolving the particles in d5-pyridine.

Properties of the two latexes used in this work are summarized in Table 1. Assuming that all of the macromonomer chains are located on the particle surface, the area per stabilizing PGMA chain was estimated to be 25 nm^2 (Γ = 3.2 mg m^2) for the PGMA-PS latex and 19 nm^2 (Γ = 4.3 mg m^{-2}) for the PGMA-P(S-nBuA) latex. The electrophoretic mobilities of the PGMA-PS latex were −0.07 at pH 4 and −0.82 at pH 10.5. Similarly, the mobility of the PGMA-P(S-nBuA) latex was −0.21 at pH 4 and −1.30 at pH 10.5. Finally, the hydrodynamic diameters of these two latexes at pH 10.5 were 206 and 215 nm, respectively.

Confocal laser scanning microscopy was used to monitor the specific deposition of the fluorescently labeled PGMA-P(S-nBuA) onto cellulose−boronate films; the results are summarized in Figure 4. Image A shows a top view of the initial cellulose−PBA film before latex deposition. The pristine film has very little background florescence. Image B shows the film obtained after PGMA-P(S-nBuA) deposition, followed by rinsing at pH 10.5. The latex particles are uniformly deposited onto the film. The vertical band of enhanced fluorescence corresponds to the film edge. Image C

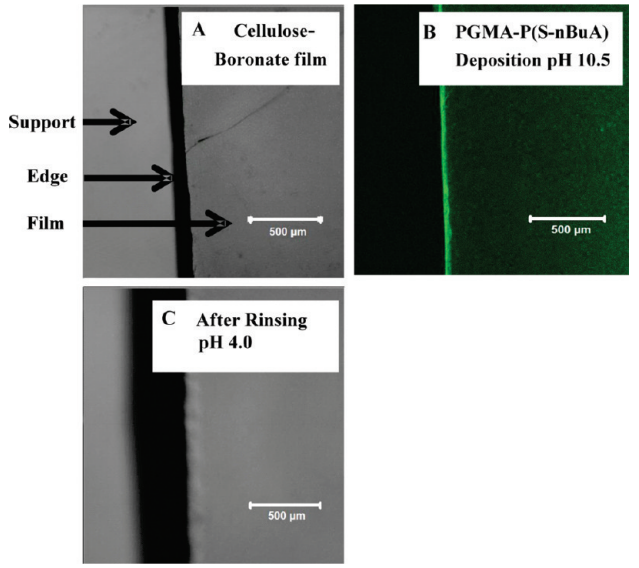

Figure 4. Confocal images obtained for PGMA-P(S-nBuA) latex adsorbed onto cellulose−PBA films excited with a 488 nm laser: (A) blank, cellulose−PBA, (B) adsorption at pH 10.5 and rinsed with dilute aqueous NaOH (also at pH 10.5), and (C) adsorption at pH 10.5 and rinsed with dilute aqueous HCl (pH 4.0).

shows the film after latex deposition at pH 10.5, followed by gentle rinsing with dilute HCl (pH 4). This mild acid rinse removed essentially all of the surface-bound copolymer latex.

SEM was also used to monitor latex adsorption at pH 10.5. The results are shown in Figure 5 as the A series of micrographs for the low T_g PGMA-P(S-nBuA) latex and the B series for the high T_g PGMA-PS latex. A-1 and B-1show unmodified cellulose films after exposure to the latexes and subsequent gentle rinsing at pH 10.5. There is no evidence of any particle deposition under these conditions.

Images A-2 and B-2 show cellulose−PBA films after exposure to latex and rinsing at pH 10.5. A-2 shows significant deposition of the PGMA-P(S-nBuA) copolymer latex particles. Many large features suggest that the low T_g particles coalesced during drying. In contrast, the corresponding experiment for the high T_g PGMA-PS particles produced a uniform coating of mainly individual particles. Close inspection revealed submonolayer latex coverage, possibly due to blocking effects.[13]

Images A-3 and B-3 show cellulose−PBA films after deposition at pH 10.5 and subsequent rinsing at pH 4. Note that the samples were not dried before washing so the low T_g latex particles did not have an opportunity to coalesce. Most of the particles were removed by washing at pH 4; however, some larger debris remained.

Finally, images A-4 and B-4 show cellulose−PBA films after latex particle exposure and washing both at pH 4. There was little evidence of adsorbed latex particles. Taken as a whole, the results in Figure 5 support the scenario depicted in Figure 1: phenylboronate−PGMA condensation drives latex adsorption at high pH, with no latex deposition occurring at low pH.

To further demonstrate the ability of phenylboronate−PGMA condensation to promote specific adsorption, experiments were performed with a binary latex mixture consisting of PGMA-PS (206 nm) and larger surfactant-free, anionic polystyrene particles (1000 nm). Figure 6 shows an SEM image of a cellulose−PBA film after exposure to the latex mixture. Many small PGMA-PS particles are visible, but there is just a single large polystyrene

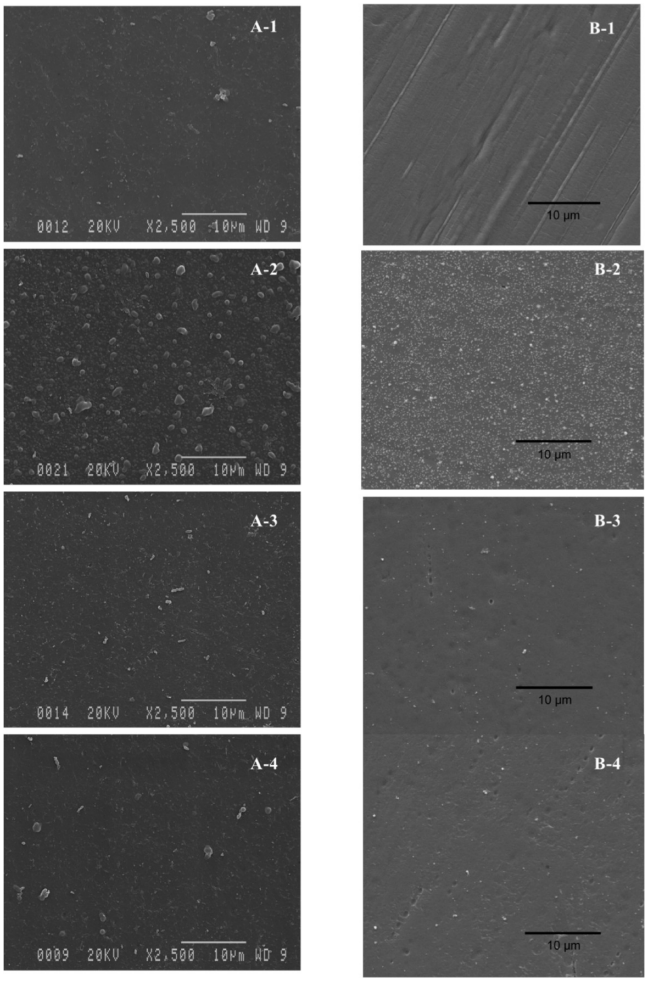

Figure 5. SEM images of low T_g PGMA-P(S-nBuA) latex (A series) and high T_g PGMA-PS latex (B series) adsorbed on cellulose-PBA films: (A-1, B-1) control experiment: latexes adsorption on pure cellulose films at pH 10.5, (A-2, B-2) adsorption onto cellulose−PBA at pH 10.5 and rinsed with pH 10.5 NaOH solution, (A-3, B-3) adsorption onto cellulose−PBA at pH 10.5 and rinsed with pH 4.0 HCl solution, and (A-4, B-4) adsorption onto cellulose−PBA at pH 4.0 and rinsed with pH 4.0 HCl solution.

particle adsorbed at the surface. Other images showed no large polystyrene particles at all.

Since the number concentration of the large spheres was lower than the small spheres, it could be argued that the small spheres occupy all of the surface sites before the larger spheres have a chance to deposit: a kinetic argument. The following control experiment illustrates that in cases where both sizes of spheres have a tendency to adsorb, both could be observed under these conditions.

As a control experiment, a cellulose film with an adsorbed monolayer of 15 kDa polyvinylamine (PVAm) was immersed in binary latex mixture at pH 6.5. PVAm adsorbs onto cellulose giving a coverage of about 1.5 mg/m^2,[14] and at this pH the degree of ionization of the PVAm is approximately 50%.[15] Therefore the cellulose-PVM surface is highly cationic and should induce adsorption of both the negatively charged latexes at pH 6.5. The SEM images in Figure 7 do indeed confirm latex monolayer coverage. The cellulose surface is covered with more PS-PGMA than with the larger charge-stabilized polystyrene

(13) Van De Ven, T. G. M. The capture of colloidal particles on surfaces and in porous material: Basic principles. *Colloids Surf. A* **1998**, *138*, 207–216.

(14) Chen, W.; Leung, V.; Kroener, H.; Pelton, R. Polyvinylamine-phenylboronic acid adhesion to cellulose hydrogel. *Langmuir* **2009**, *25*, 6863–6868.

(15) Katchalsky, A.; Mazur, J.; Spitnik, P. Polybase properties of poly-(vinylamine). *J. Polym. Sci.* **1957**, *23*, 513–30.

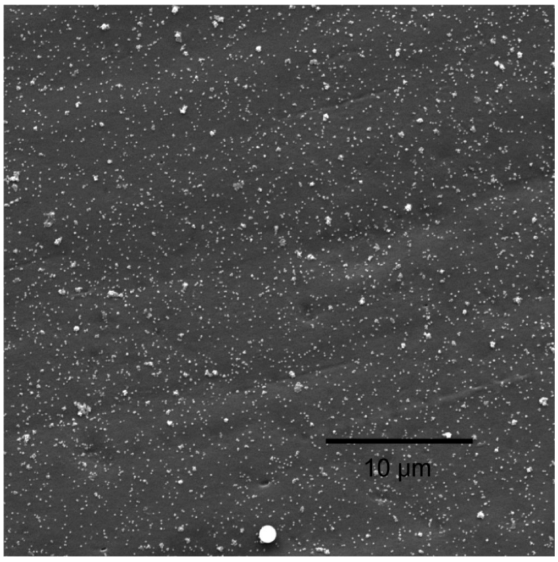

Figure 6. SEM of cellulose-PBA after exposure to a mixture of PGMA-PS latex (206 nm) and anionic charge-stabilized polystyrene latex (1000 nm) in 2 mM NaCl at pH 10.5. There is just one adsorbed 1000 nm polystyrene particle (see bottom center of the image).

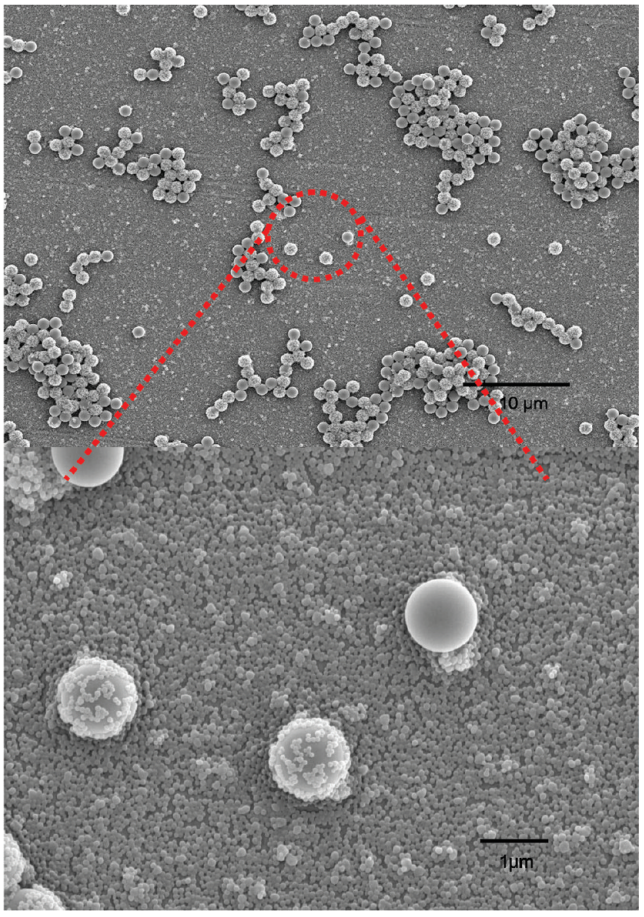

Figure 7. SEM image of the PVAm-coated cellulose film after exposure to a mixture of 0.01 g/L PGMA-PS (206 nm) and 0.2 g/L anionic polystyrene latex (1000 nm) in 2 mM NaCl at pH 6.5. The highly cationic surface was completely covered by both latexes.

particles, reflecting the higher number concentration of small particles in the mixed latex dispersion. Some of the larger polystyrene particles are coated with smaller PGMA-PS particles whereas other adsorbed large particles are bare. Tanaka showed that during Brownian encounters of polystyrene latex with cellulose, cationic polyacrylamide adsorbed onto cellulose was partially transferred onto the latex surfaces.[16,17] Thus we suggest that the large polystyrene particles covered with PGMA-PS pick up PVAm by weakly interacting with the cellulose surface, providing cationic adsorption sites for subsequent deposition of PGMA-PS.

Close comparison of the distribution of PGMA-PS particles on the PVM-coated cellulose-polyvinylamine surface with the cellulose−PBA surface (i.e., Figure 7 vs Figure 6) reveals an important distinction. On the cationic PVAm-coated cellulose surface, the binary latex mixture formed a dense mixed monolayer of small and large particles. In contrast, on cellulose-PBA the particle coating was sparse. Perhaps the particle distribution reflects the requirement for higher density patches of boronic groups for particle adhesion. We propose that the relatively weak nature of the boronate-PGMA interaction requires many contacts per particle. Keita et al. reported that the binding constant between phenylboronic acid and PGMA was 5.4 L/mol, which corresponds to a free energy change of only 4.2 kJ/mol (or −1.6 kT per complex).[1] It is remarkable that such a low energy interaction could drive latex deposition. We suggest that, like H-bonding and hydrophobic driven polymer adsorption, the cooperative effect of multiple, simultaneous weak bonds suffice to give latex particle attachment.

Clearly boronate−PGMA interactions are not the best way to achieve high densities of strongly adhering latex particles. On the other hand, for applications requiring specificity and reversibility such as temporary surface blocking, latex deposition driven by boronate−PGMA bonding could be ideal.

Conclusions

The main conclusions from this work are as follows:

(1) Latex particles stabilized with a poly(glycerol monomethacrylate) chains exhibit specific, pH-dependent adsorption and desorption from cellulose films derivatized with phenylboronic acid. Specific adsorption of PGMA-coated particles onto negatively charged cellulose was observed at pH 10.5, whereas complete particle removal was achieved at pH 4.

(2) Although the PGMA-borate binding constant is only 5.4 L/mol (1.6 kT per complex), we conclude that the cooperative effect of multiple PGMA-surface contacts promotes specific latex deposition and adhesion.

(3) We have developed a new quantitative method for measuring the content and distribution of phenylboronic acid groups in derivatized cellulose hydrogel based on measuring the total uptake of Alizarin Red S dye and the subsequent confocal laser scanning microscopic imaging of the dye distribution.

Acknowledgment. The authors thank the Natural Sciences and Engineering Research Council of Canada for funding this work. The authors also thank the Canada Foundation for Innovation. RP holds the Canada Research Chair in Interfacial Technologies. K.L.T. and S.P.A. thank both the EPSRC and P&G for funding a Ph.D. CASE studentship for K.L.T.

(16) Tanaka, H.; Swerin, A.; Odberg, L. Cleavage of polymer-chains during transfer of cationic polyacrylamide from cellulose fibers to polystyrene latex. *J. Colloid Interface Sci.* **1992**, *153*, 13–22.

(17) Tanaka, H.; Odberg, L. Transfer of cationic polymers from cellulose fibers to polystyrene latex. *J. Colloid Interface Sci.* **1992**, *149*, 40–48.

Chapter 5 Concluding Remarks

In this thesis, the interaction of boronic acid with polyols was investigated. The formation of boronic esters is reversible and pH-dependent. Boronate groups are well known to complex with 1,2- or 1,3-diols at high pH, although the interaction pH value can be lowered by locating an amine group near the boronic acid group. Hence, the property of the boronic ester was employed to exploit multilayer self-assembly films by three independent interactions. To exploit these interactions, I prepared and characterized copolymers containing pairs of non-interacting groups, thus each bifunctional polymer can specifically interact with two other types of polymers/substrates. The ultimate goal was to employ independent polymer/polymer interactions to prepare complex assemblies in one step.

The utility of multiple, independent interactions was also demonstrated by formation of complex latex aggregates. Monodispersed polystyrene particles with different diameters were used as building blocks. Poly(vinyl alcohol) and two novel bifunctional copolymers were adsorbed onto three sizes of polystyrene particles. Particle-particle interactions were turned on by raising pH resulting in well-defined composite particles.

To further exploit the interaction of boronic acid and polyols, poly(glycerol monomethacrylate)- stabilized polystyrene (PGMA-PS) latex particles were employed to have specific, pH-dependent adsorption onto regenerated cellulose film bearing surface phenylboronic acid groups (cellulose-PBA). The cellulose-PBA films were prepared in two steps: 1) regenerated cellulose dialysis membranes were oxidized to introduce carboxyl groups at the C6 position and then 2) the carboxylated cellulose films (cellulose-COOH) derivatized with 3-aminophenylboronic acid to give cellulose-PBA. It is a new approach to control the adsorption and desorption of nanoparticles on surfaces, especially for some applications requiring specificity and reversibility such as temporary surface binding.

The research objectives proposed in Chapter 1 were fulfilled and the major contributions of my work are listed as follows:

1. It is the first time that three independent polymer-polymer interactions, based on 1) electrostatic attraction, 2) hydrogen bonding, and 3) boronate ester formation were used simultaneously to form layer-by-layer adsorbed polymers. For a polymer assembly system, the substrate/layer 1 interaction is electrostatic complexation,

the layer 1/layer 2 interaction is PEG/phenolic complexation, and the layer 2/layer 3 interaction is boronate/cis diol complexation.

2. A series of new bifunctional copolymers are of water solubility and the absence of interaction between layer-one and layer-three polymer, which makes the multilayer assembly in one step feasible. This approach offers the possibility of large-scale, low cost, directed assembly in water.

3. Three independent interactions were also employed to control the self-assembly of three types of nanoparticles. Specifically, copolymers Ph-DADMAC, APBA-PEG and polyvinylalcohol (PVA) were adsorbed on monodispersed polystyrene latexes with diameters 1μm, 500 nm and 200 nm respectively. The particles self assembled to form hierarchical structures. Furthermore, pH could be used to turn on or off the interaction of phenyl boronate polymers with polyvinylalcohol.

4. In the trilayer polymer system, each of the three types of polymer-polymer interactions can be "turned off" independently: boronate esters are hydrolyzed by lowering pH; hydrogen bonding of PEG containing copolymers and phenol containing copolymers is disrupted by low molecular weight PEG addition; and electrostatic adsorption on the substrate is reversed by electrolyte addition.

5. The crystal structure of the compound, [3-(Propenamido)phenyl]boronic acid, was studied as a potential precursor for use in affinity chromatography and saccharide sensing.

6. A quantitative method for measuring the content and distribution of phenylboronic acid groups in derivatized cellulose hydrogels was developed. It is based on measuring the total uptake of Alizarin Red S dye and the subsequent confocal laser scanning microscopic imaging of the dye distribution.

7. Poly(glycerol monomethacrylate) (PGMA)-stabilized polystyrene latex particles displayed a reversible binding towards cellulose films derivatized with phenylboronic acid. Specific adsorption of PGMA-coated particles onto negatively charged cellulose was observed at pH 10.5, whereas complete particle removal was achieved at pH 4.

8. Although the binding constant of PGMA-borate is low (5.4 L/mol), we conclude that the cooperative effect of multiple PGMA-surface contacts promotes specific latex deposition and adhesion.

Appendix A

In this paper, I prepared the compound [3-(Propenamido)phenyl]boronic acid and its single crystal. Dr. Harrington did the SAXD examination of the crystal. I completed the data analysis and wrote the paper. Dr. Pelton and Dr. Tanaka contributed some helpful discussion on this paper.

Acta Crystallographica Section E
Structure Reports Online
ISSN 1600-5368

[3-(Propenamido)phenyl]boronic acid

Dan Zhang,[a] Laura E. Harrington,[b]* Hiroo Tanaka[a] and Robert Pelton[a]

[a]Department of Chemical Engineering, JHE-136, McMaster University, Hamilton, Ontario, Canada L8S 4L7, and [b]Department of Chemistry, McMaster University, 1280 Main Street W., Hamilton, Ontario, Canada L8S 4M1
Correspondence e-mail: harrinl@mcmaster.ca

Received 28 August 2007; accepted 1 November 2007

Key indicators: single-crystal X-ray study; T = 295 K; mean σ(C–C) = 0.003 Å; R factor = 0.038; wR factor = 0.108; data-to-parameter ratio = 9.6.

The title compound, $C_9H_{10}BNO_3$, was synthesized for investigation as a potential precursor for use in affinity chromatography and glucose sensing. Weak N—H···O and O—H···O hydrogen-bonding interactions are observed in the molecular structure. The dihedral angle between the benzene ring and the BO_2 plane is 35.1 (2)°.

Related literature

For related literature, see: Zhang *et al.* (2007); Chen *et al.* (2006); Deutsch & Osoling (1949).

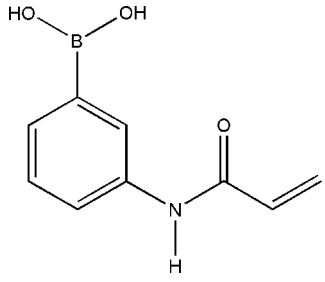

Experimental

Crystal data

$C_9H_{10}BNO_3$
M_r = 190.99
Orthorhombic, *Fdd*2
a = 18.626 (4) Å
b = 42.112 (8) Å
c = 5.0536 (10) Å
V = 3963.9 (13) Å^3
Z = 16
Mo $K\alpha$ radiation
μ = 0.09 mm^{-1}
T = 295 (2) K
0.43 × 0.18 × 0.12 mm

Data collection

Bruker APEXII CCD diffractometer
Absorption correction: numerical (*APEX2*; Bruker, 2006)
T_{min} = 0.87, T_{max} = 0.99
14806 measured reflections
1657 independent reflections
1279 reflections with $I > 2\sigma(I)$
R_{int} = 0.035

Refinement

$R[F^2 > 2\sigma(F^2)]$ = 0.039
$wR(F^2)$ = 0.108
S = 1.04
1657 reflections
172 parameters
1 restraint
H atoms treated by a mixture of independent and constrained refinement
$\Delta\rho_{max}$ = 0.17 e Å^{-3}
$\Delta\rho_{min}$ = −0.12 e Å^{-3}

Table 1
Hydrogen-bond geometry (Å, °).

D—H···A	D—H	H···A	D···A	D—H···A
O2—H2A···O2^{i}	0.77 (7)	2.02 (7)	2.759 (3)	163 (7)
O2—H2B···O3^{ii}	0.77 (8)	2.10 (9)	2.748 (3)	143 (7)
O3—H3A···O2^{iii}	0.75 (8)	2.24 (8)	2.748 (3)	126 (7)
O3—H3B···O3^{i}	0.87 (5)	1.88 (5)	2.746 (3)	173 (6)
N1—H1A···O1^{iv}	0.93 (3)	1.98 (3)	2.911 (3)	172 (2)

Symmetry codes: (i) $-x+1, -y, z$; (ii) $x, y, z-1$; (iii) $x, y, z+1$; (iv) $x-\frac{1}{4}, -y+\frac{1}{4}, z-\frac{1}{4}$.

Data collection: *APEX2* (Bruker, 2006); cell refinement: *APEX2*; data reduction: *APEX2*; program(s) used to solve structure: *SHELXS97* (Sheldrick, 1997); program(s) used to refine structure: *SHELXL97* (Sheldrick, 1997); molecular graphics: *SHELXTL* (Bruker, 2000) and *Mercury* (Macrae *et al.*, 2006); software used to prepare material for publication: *SHELXTL*.

We acknowledge the Canadian Government (NSERC) for funding.

Supplementary data and figures for this paper are available from the IUCr electronic archives (Reference: KJ2069).

References

Bruker (2000). *SHELXTL*. Version 6.10. Bruker AXS Inc., Madison, Wisconsin, USA.
Bruker (2006). *APEX2*. Version 2.1-0. Bruker AXS Inc., Madison, Wisconsin, USA.
Chen, W., Lu, C. & Pelton, R. (2006). *Biomacromolecules*, **7**, 701–702.
Deutsch, A. & Osoling, S. (1949). *J. Am. Chem. Soc.* **71**, 1637–1640.
Macrae, C. F., Edgington, P. R., McCabe, P., Pidcock, E., Shields, G. P., Taylor, R., Towler, M. & van de Streek, J. (2006). *J. Appl. Cryst.* **39**, 453–457.
Sheldrick, G. M. (1997). *SHELXS97* and *SHELXL97*. University of Göttingen, Germany.
Zhang, D., Tanaka, H. & Pelton, R. (2007). *Langmuir*, **23**, 8806–8809.

  doi:10.1107/S1600536807055389

supplementary materials

Acta Cryst. (2007). E**63**, o4628 [**doi:10.1107/S1600536807055389**]

[3-(Propenamido)phenyl]boronic acid

D. Zhang, L. E. Harrington, H. Tanaka and R. Pelton

Comment

The title compound is a monomer containing a boronate group, which can form complexes with *cis* diols at pH values above 9 (Deutsch & Osoling, 1949). This interaction can be employed for affinity chromatography and glucose sensing (Chen *et al.*, 2006).

The molecular structure of the title compound is illustrated in Fig.1. Weak N—H···O and O—H···O hydrogen bonding interactions are observed in the molecular structure which help to stabilize the crystal structure and forming an infinite threedimensional network, as illustrated in the packing diagram displayed in Fig. 2. The dihedral angle between the benzene ring and the plane composed of O2—B1—O3 is 35.12(0.23)°.

Experimental

The synthesis of (I) was described previously (Zhang *et al.*, 2007). Single crystals suitable for X-ray analysis were obtained by slow evaporation of a water solution at room temperature.

Refinement

Friedel pairs were merged prior to refinement using *SHELXTL* (Bruker, 2000). The positions of the H atoms were determined using the difference map and were refined isotropically. The H atoms on O2 and O3 were disordered over 2 sites with 50% occupancy in each site. The disordered H atoms were refined with one common U_{iso}.

Figures

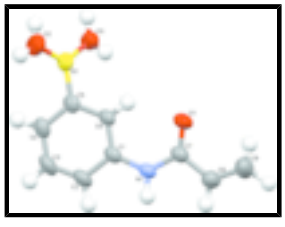

Fig. 1. The molecular structure of (I), showing the atom-labelling scheme. Displacement ellipsoids are drawn at the 50% probability level. H atoms are represented by circles of arbitrary size. Only one component of the disorder is shown.

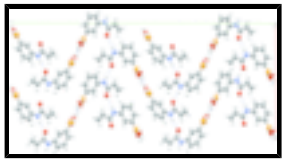

Fig. 2. The crystal packing of (II), viewed along the *c* axis. Only one component of the disorder is shown. H-bonds are shown as dashed lines.

[3-(Propenamido)phenyl]boronic acid

Crystal data

$C_9H_{10}BNO_3$	F_{000} = 1600
M_r = 190.99	D_x = 1.280 Mg m^{-3}
Orthorhombic, *Fdd*2	Mo *K*α radiation λ = 0.71073 Å
Hall symbol: F 2 -2d	Cell parameters from 2853 reflections
a = 18.626 (4) Å	θ = 2.4–25.1°
b = 42.112 (8) Å	μ = 0.09 mm^{-1}
c = 5.0536 (10) Å	*T* = 295 (2) K
V = 3963.9 (13) Å^3	Needle, colourless
Z = 16	0.43 × 0.18 × 0.12 mm

Data collection

Bruker APEXII CCD diffractometer	1657 independent reflections
Radiation source: fine-focus sealed tube	1279 reflections with $I > 2\sigma(I)$
Monochromator: graphite	R_{int} = 0.035
T = 295(2) K	θ_{max} = 30.5°
φ and ω scans	θ_{min} = 1.9°
Absorption correction: numerical (face correction with APEX2; Bruker, 2006)	*h* = −26→25
T_{min} = 0.87, T_{max} = 0.99	*k* = −59→59
14806 measured reflections	*l* = −7→2

Refinement

Refinement on F^2	Hydrogen site location: inferred from neighbouring sites
Least-squares matrix: full	H atoms treated by a mixture of independent and constrained refinement
$R[F^2 > 2\sigma(F^2)]$ = 0.039	$w = 1/[\sigma^2(F_o^2) + (0.0606P)^2 + 0.5557P]$ where $P = (F_o^2 + 2F_c^2)/3$
$wR(F^2)$ = 0.108	$(\Delta/\sigma)_{max}$ = 0.007
S = 1.04	$\Delta\rho_{max}$ = 0.17 e Å^{-3}
1657 reflections	$\Delta\rho_{min}$ = −0.12 e Å^{-3}
172 parameters	Extinction correction: none
1 restraint	
Primary atom site location: structure-invariant direct methods	
Secondary atom site location: difference Fourier map	

Special details

Geometry. All e.s.d.'s (except the e.s.d. in the dihedral angle between two l.s. planes) are estimated using the full covariance matrix. The cell e.s.d.'s are taken into account individually in the estimation of e.s.d.'s in distances, angles and torsion angles; correlations between e.s.d.'s in cell parameters are only used when they are defined by crystal symmetry. An approximate (isotropic) treatment of cell e.s.d.'s is used for estimating e.s.d.'s involving l.s. planes.

Refinement. Refinement of F^2 against ALL reflections. The weighted *R*-factor *wR* and goodness of fit S are based on F^2, conventional *R*-factors *R* are based on F, with F set to zero for negative F^2. The threshold expression of $F^2 > 2\text{sigma}(F^2)$ is used only for calculating *R*-factors(gt) *etc*. and is not relevant to the choice of reflections for refinement. *R*-factors based on F^2 are statistically about twice as large as those based on F, and R– factors based on ALL data will be even larger.

Fractional atomic coordinates and isotropic or equivalent isotropic displacement parameters (Å^2)

	x	*y*	*z*	U_{iso}*/U_{eq}	Occ. (<1)
O1	0.34232 (7)	0.11569 (4)	1.1454 (4)	0.0653 (5)	
O2	0.43076 (12)	0.01158 (6)	0.3738 (4)	0.0779 (6)	
H2A	0.466 (3)	0.0024 (17)	0.394 (16)	0.082 (10)*	0.50
H2B	0.413 (4)	0.0131 (15)	0.237 (17)	0.082 (10)*	0.50
O3	0.43531 (9)	0.01566 (4)	0.8312 (3)	0.0569 (4)	
H3A	0.414 (4)	0.0220 (15)	0.944 (17)	0.082 (10)*	0.50
H3B	0.478 (3)	0.0072 (14)	0.827 (14)	0.082 (10)*	0.50
N1	0.23312 (9)	0.10547 (4)	0.9628 (3)	0.0476 (4)	
H1A	0.1859 (16)	0.1131 (6)	0.949 (6)	0.072 (8)*	
B1	0.39944 (13)	0.02160 (6)	0.6027 (5)	0.0469 (5)	
C1	0.24915 (10)	0.08023 (4)	0.7901 (4)	0.0442 (4)	
C2	0.19502 (12)	0.07111 (5)	0.6107 (5)	0.0567 (5)	
H2	0.1493 (13)	0.0830 (5)	0.624 (6)	0.059 (6)*	
C3	0.20685 (14)	0.04743 (6)	0.4318 (5)	0.0633 (6)	
H3	0.1704 (15)	0.0419 (6)	0.324 (7)	0.068 (7)*	
C4	0.27236 (13)	0.03202 (5)	0.4223 (4)	0.0543 (5)	
H4	0.2783 (13)	0.0162 (6)	0.288 (6)	0.060 (7)*	
C5	0.32638 (10)	0.03966 (4)	0.6037 (4)	0.0447 (4)	
C6	0.31372 (10)	0.06372 (5)	0.7880 (4)	0.0433 (4)	
H6	0.3479 (12)	0.0696 (5)	0.914 (5)	0.055 (6)*	
C7	0.27804 (10)	0.12142 (5)	1.1262 (4)	0.0478 (4)	
C8	0.24262 (14)	0.14649 (6)	1.2856 (6)	0.0646 (6)	
H8	0.1923 (18)	0.1488 (7)	1.258 (8)	0.085 (9)*	
C9	0.2770 (2)	0.16236 (8)	1.4653 (8)	0.0938 (11)	
H9A	0.2548 (17)	0.1772 (8)	1.613 (9)	0.101 (10)*	
H9B	0.322 (2)	0.1570 (8)	1.511 (9)	0.105 (12)*	

Atomic displacement parameters (Å^2)

	U^{11}	U^{22}	U^{33}	U^{12}	U^{13}	U^{23}
O1	0.0357 (7)	0.0729 (9)	0.0873 (12)	0.0017 (6)	−0.0151 (8)	−0.0233 (9)
O2	0.0824 (15)	0.1155 (17)	0.0359 (9)	0.0226 (11)	0.0051 (9)	−0.0134 (10)

O3	0.0593 (10)	0.0778 (11)	0.0334 (7)	0.0152 (8)	−0.0019 (6)	−0.0005 (7)
N1	0.0334 (8)	0.0568 (9)	0.0526 (9)	0.0036 (7)	−0.0099 (7)	−0.0050 (8)
B1	0.0551 (12)	0.0549 (11)	0.0307 (8)	0.0020 (9)	0.0008 (8)	−0.0002 (9)
C1	0.0394 (9)	0.0505 (10)	0.0427 (9)	−0.0035 (8)	−0.0090 (7)	0.0036 (8)
C2	0.0463 (11)	0.0635 (12)	0.0602 (13)	−0.0005 (10)	−0.0215 (10)	−0.0013 (11)
C3	0.0607 (13)	0.0686 (14)	0.0606 (13)	−0.0068 (11)	−0.0281 (11)	−0.0065 (11)
C4	0.0648 (13)	0.0559 (11)	0.0421 (10)	−0.0038 (10)	−0.0128 (9)	−0.0034 (9)
C5	0.0507 (10)	0.0511 (10)	0.0324 (8)	−0.0022 (8)	−0.0017 (7)	0.0052 (8)
C6	0.0380 (9)	0.0550 (11)	0.0370 (9)	−0.0014 (8)	−0.0066 (7)	−0.0001 (7)
C7	0.0381 (9)	0.0530 (10)	0.0522 (10)	−0.0016 (8)	−0.0076 (8)	−0.0007 (9)
C8	0.0525 (13)	0.0653 (13)	0.0760 (17)	0.0114 (11)	−0.0125 (12)	−0.0159 (12)
C9	0.081 (2)	0.097 (2)	0.104 (3)	0.0237 (17)	−0.0317 (18)	−0.049 (2)

Geometric parameters (Å, °)

O1—C7	1.225 (2)	C2—C3	1.364 (4)
O2—B1	1.363 (3)	C2—H2	0.99 (2)
O2—H2A	0.76 (7)	C3—C4	1.383 (4)
O2—H2B	0.77 (8)	C3—H3	0.90 (3)
O3—B1	1.357 (3)	C4—C5	1.399 (3)
O3—H3A	0.74 (8)	C4—H4	0.96 (3)
O3—H3B	0.87 (5)	C5—C6	1.396 (3)
N1—C7	1.354 (3)	C6—H6	0.93 (3)
N1—C1	1.407 (3)	C7—C8	1.483 (3)
N1—H1A	0.94 (3)	C8—C9	1.297 (4)
B1—C5	1.559 (3)	C8—H8	0.95 (3)
C1—C6	1.389 (3)	C9—H9A	1.06 (4)
C1—C2	1.409 (3)	C9—H9B	0.89 (4)
B1—O2—H2A	114 (6)	C4—C3—H3	121.6 (17)
B1—O2—H2B	123 (6)	C3—C4—C5	120.3 (2)
H2A—O2—H2B	122 (8)	C3—C4—H4	116.9 (15)
B1—O3—H3A	109 (6)	C5—C4—H4	122.9 (15)
B1—O3—H3B	120 (5)	C6—C5—C4	118.86 (18)
H3A—O3—H3B	131 (7)	C6—C5—B1	120.24 (17)
C7—N1—C1	128.46 (17)	C4—C5—B1	120.90 (19)
C7—N1—H1A	117.1 (18)	C1—C6—C5	120.95 (16)
C1—N1—H1A	114.2 (18)	C1—C6—H6	117.0 (14)
O3—B1—O2	117.0 (2)	C5—C6—H6	122.0 (14)
O3—B1—C5	121.1 (2)	O1—C7—N1	123.7 (2)
O2—B1—C5	121.8 (2)	O1—C7—C8	122.2 (2)
C6—C1—N1	124.49 (16)	N1—C7—C8	114.19 (18)
C6—C1—C2	118.57 (19)	C9—C8—C7	121.8 (3)
N1—C1—C2	116.93 (18)	C9—C8—H8	122 (2)
C3—C2—C1	120.7 (2)	C7—C8—H8	116 (2)
C3—C2—H2	123.6 (16)	C8—C9—H9A	127.2 (19)
C1—C2—H2	115.7 (15)	C8—C9—H9B	121 (2)
C2—C3—C4	120.6 (2)	H9A—C9—H9B	109 (3)
C2—C3—H3	117.8 (18)		
C7—N1—C1—C6	10.7 (3)	O3—B1—C5—C4	−145.3 (2)

C7—N1—C1—C2	−170.2 (2)	O2—B1—C5—C4	35.9 (3)
C6—C1—C2—C3	−2.6 (3)	N1—C1—C6—C5	−177.70 (18)
N1—C1—C2—C3	178.2 (2)	C2—C1—C6—C5	3.2 (3)
C1—C2—C3—C4	−0.3 (4)	C4—C5—C6—C1	−0.9 (3)
C2—C3—C4—C5	2.6 (4)	B1—C5—C6—C1	179.45 (19)
C3—C4—C5—C6	−2.0 (3)	C1—N1—C7—O1	0.3 (3)
C3—C4—C5—B1	177.6 (2)	C1—N1—C7—C8	−178.9 (2)
O3—B1—C5—C6	34.3 (3)	O1—C7—C8—C9	−4.2 (4)
O2—B1—C5—C6	−144.5 (2)	N1—C7—C8—C9	174.9 (3)

Hydrogen-bond geometry (Å, °)

D—H···*A*	*D*—H	H···*A*	*D*···*A*	*D*—H···*A*
O2—H2A···O2^{i}	0.77 (7)	2.02 (7)	2.759 (3)	163 (7)
O2—H2B···O3^{ii}	0.77 (8)	2.10 (9)	2.748 (3)	143 (7)
O3—H3A···O2^{iii}	0.75 (8)	2.24 (8)	2.748 (3)	126 (7)
O3—H3B···O3^{i}	0.87 (5)	1.88 (5)	2.746 (3)	173 (6)
N1—H1A···O1^{iv}	0.93 (3)	1.98 (3)	2.911 (3)	172 (2)

Symmetry codes: (i) −*x*+1, −*y*, *z*; (ii) *x*, *y*, *z*−1; (iii) *x*, *y*, *z*+1; (iv) *x*−1/4, −*y*+1/4, *z*−1/4.

Fig. 1

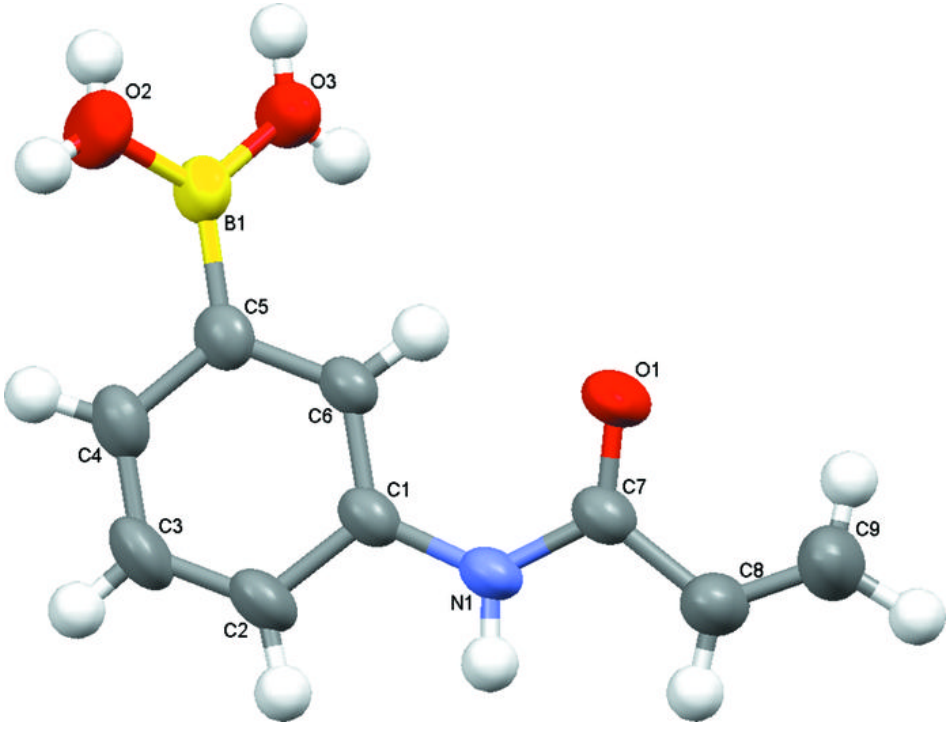

Fig. 2

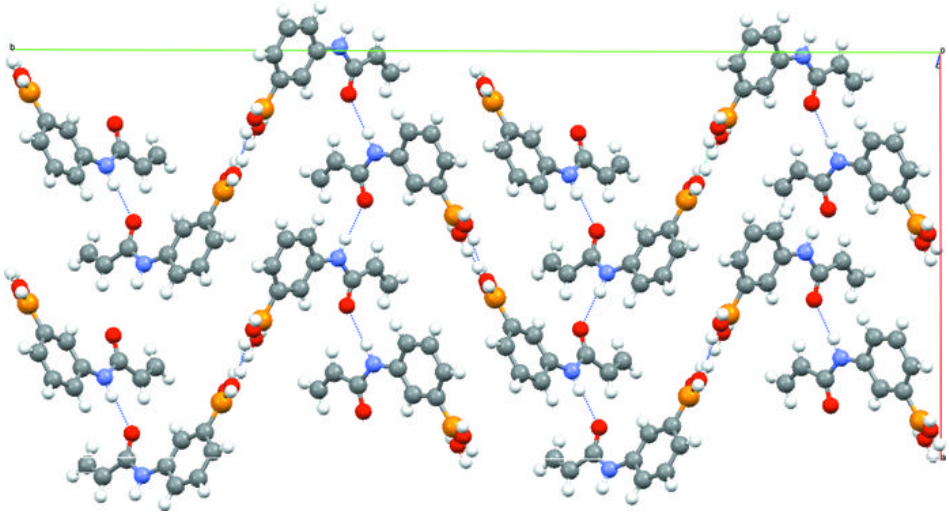

Appendix B Calculations of Properties of Cellulose-PBA Surface

Objectives:

1. To calculate the area for one borate group on cellulose surfaces at pH 9.0.

2. To calculate concentrations of free phenylboronic acid groups, phenylborate groups, and phenylborate bound ARS at pH 9.0.
.

Assumptions:

1. At pH 2.75, all bound ARS will desorb from cellulose film (no binding between ARS and phenyl borate or phenyl boronic acid)

2. At pH 11.0, all bound Boronic acid (pka=8.8) on cellulose films will be ionized.

Experimental:

1. The bound ARS was desorbed from cellulose-PBA films in 10 ml water with 2 mM NaCl at pH 2.75. UV-Vis method was used to detect the absorbence intensity of desorbed ARS in solution.
2. Meanwhile, a standard curve and an equation of ARS UV absorption was obtained.

3. The desorbed ARS concentration was then calculated. Also, the cellulose-PBA films was dried in a oven at 100 degree for 6 hours and then weighed (44.3 mg).

$$B(OH)_3 + OH^- \underset{}{\overset{Ka}{\rightleftharpoons}} B(OH)_4^-$$

$B(OH)_3$ is phenylbonic acid
pka of phenylboronic acid is 8.8

$$K_a = \frac{BOH}{B \cdot OH} \qquad (1)$$

B, phenyl borate concentration; BA, phenyl boronic acid concentation; OH, hydroxyl ion concentration

$$B(OH)_4^- + ARS \overset{K_1}{\rightleftharpoons} BA$$

$$K_1 = \frac{BA}{ARS \cdot BOH} \qquad (2)$$

BOH is concentration of free phenylborate groups, BA is concentration of phenylborate bound ARS,
ARS is concentration of free ARS.

$$ARS_T = ARS + BA$$

ARS balance

$$B_T = B + BOH + BA$$

Boron balance, B is concentration of free phenylboronic acid groups.

substitute boron balance to equation (1)

$$K_a = \frac{BOH}{(B_T - BOH - BA) \cdot OH} \text{ solve}, BOH \rightarrow -\frac{K_a \cdot OH \cdot (BA - B_T)}{K_a \cdot OH + 1}$$

substitute ARS balance to equation (2)

$$K_1 = \frac{BA}{(ARS_T - BA) BOH} \text{ solve}, BA \rightarrow \frac{ARS_T \cdot BOH \cdot K_1}{BOH \cdot K_1 + 1}$$

Calculation 1: Adsorbed ARS amount on cellulose films at pH 11.0

$\varepsilon := 19.381 \frac{L}{gm}$ UV absorption coefficient, see the figure below:

$ABS = 19.381 c_{ARS}$ c_{ARS}, mass concentration of ARS

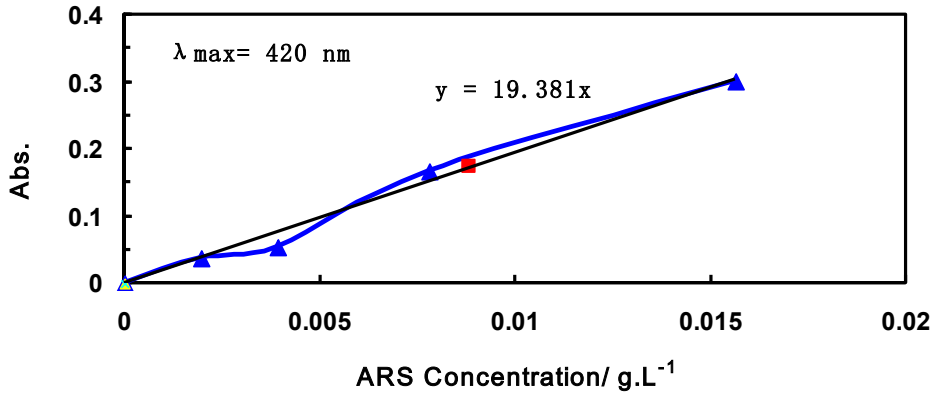

$ABS := 0.1718$ At pH 2.75, absorbance of desorbed ARS in 10mL 2mM NaCl

$c_{ARS} := \frac{ABS}{\varepsilon}$

$c_{ARS} = 8.864 \times 10^{-3} \cdot \frac{gm}{L}$ Desorbed ARS concentration

$w_{cell} := 44.3 mg$ Cellulose film weight

$M_{ARS} := 342.3 \frac{gm}{mol}$ ARS molecular weight

$V := 10 ml$ Volume of desorbed ARS solution

$m_{ARS} := \frac{c_{ARS} \cdot V}{M_{ARS}}$

$m_{ARS} = 2.59 \times 10^{-7} mol$ Amount of ARS in 10 mL 2mM NaCl solution

Calculation 2: Boron amount on cellulose films at pH 11.0

$BA := \frac{m_{ARS}}{V} = 2.59 \times 10^{-5} \cdot \frac{mol}{L}$ The bound ARS concentration with phenylborate on cellulose membrane

$K_1 := 1300 \frac{L}{mol}$ Binding constant of phenylborate and ARS, see reference: Wang B., Tetrahedron, 2002, 58, 5291-5300

$m_{ARST} := 0.25 \frac{gm}{L}$ Mass concentration of total added ARS in solution

$ARS_T := \frac{m_{ARST}}{M_{ARS}} = 7.304 \times 10^{-4} \cdot \frac{mol}{L}$ Molar concentration of total added ARS in solution

$BOH_T := \frac{BA}{K_1 \cdot (ARS_T - BA)} + BA$

$BOH_T = 5.417 \times 10^{-5} \cdot \frac{mol}{L}$ Total borate on cellulose film

$B_T := BOH_T = 5.417 \times 10^{-5} \cdot \frac{mol}{L}$ Total boron on cellulose film inside and outside

$\Gamma := \frac{B_T \cdot V}{w_{cell}}$ Total boron per gram of cellulose film

$\Gamma = 1.223 \times 10^{-5} \cdot \frac{mol}{gm}$

$eq := mol \qquad meq := 10^{-3} \cdot eq$

$\Gamma = 0.012 \cdot \frac{meq}{gm}$

Calculation 3: Calculation of phenyl borate on cellulose films at pH 9

$pH := 9$ $pKa := 8.8$

$K_a := 10^{14-pKa}\ \frac{L}{mol}$ Association constant of phenylboronic acid

$OH := 10^{-(14-pH)}\ \frac{mol}{L}$ $OH = 1 \times 10^{-5} \cdot \frac{mol}{L}$

$K_a = \frac{PB}{PBA \cdot OH}$ PB, phenyl borate concentration; PBA, phenyl boronic acid concentation; OH, hydroxyl ion concentration

$r = \frac{PB}{PBA}$ r is ratio of phenylborate to phenylboronate acid

$r := K_a \cdot OH$

$r = 1.585$

$p_{PB} := \frac{r}{1 + r} = 0.613$ Phenyl borate percentage of total phenyl boron at pH 9

$\Gamma_{PB} := \Gamma \cdot p_{PB} = 7.498 \times 10^{-3} \cdot \frac{meq}{gm}$ The milliequivalents of phenyl borate per gm of cellulose film at pH 9

Calculation 4: surface borate percentage of total borate, if the surface thickness is 5 nm and total thickness of cellulose films is 158.6 um. The equation was obtained from excel file.

$$\int_0^{0.005} \left(3\cdot 10^{-6}\cdot x^4 - 0.0011\cdot x^3 + 0.141x^2 - 8.5652\cdot x + 263.5\right) dx \rightarrow 1.317392940874828126$$

$$\int_0^{158.6} \left(3\cdot 10^{-6}\cdot x^4 - 0.0011\cdot x^3 + 0.141x^2 - 8.5652\cdot x + 263.5\right) dx \rightarrow 7780.728345901056$$

$$p_{surf} := \frac{2\left[\int_0^{0.005} \left(3\cdot 10^{-6}\cdot x^4 - 0.0011\cdot x^3 + 0.141x^2 - 8.5652\cdot x + 263.5\right) dx\right]}{\int_0^{158.6} \left(3\cdot 10^{-6}\cdot x^4 - 0.0011\cdot x^3 + 0.141x^2 - 8.5652\cdot x + 263.5\right) dx} = 3.386\times 10^{-4}$$

Surface borate percentage of total borate in cellulose film

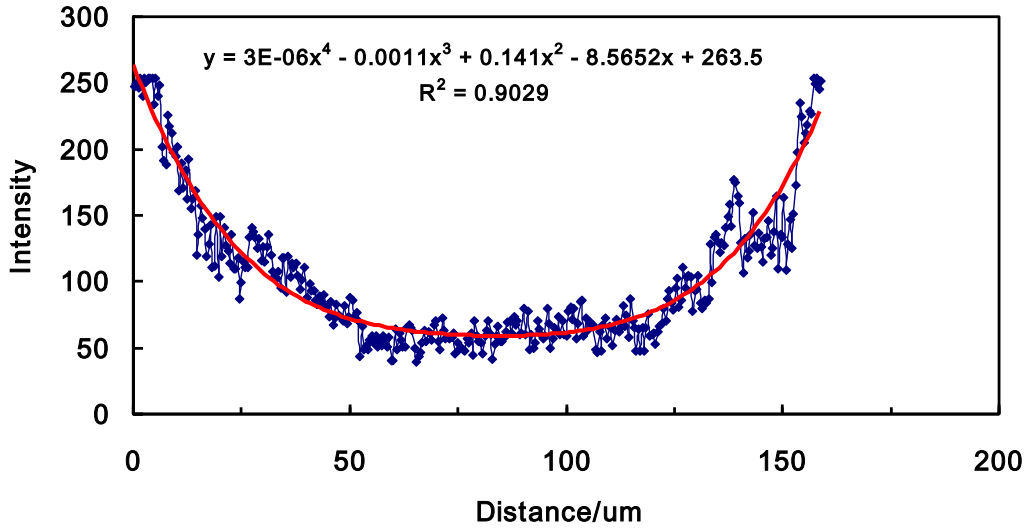

Calculation 5: Charge density of phenyl borate per exterior surface area

$S_{cell} := 2 cm^2$ Surface area of cellulose films

$\delta_{PB} := \frac{B_T \cdot V}{S_{cell}} \cdot p_{PB} \cdot p_{surf} = 5.624 \times 10^{-4} \cdot \frac{meq}{m^2}$

$N_A := 6.022 \cdot 10^{23} \frac{1}{mol}$ $e_o := 1.6 \cdot 10^{-19} C$

$\sigma_{PB} := \delta_{PB} \cdot N_A \cdot e_o = 0.054 \cdot \frac{C}{m^2}$

Charge density in Coulombs per square meter

Calculation 6: Calculation of the area for one borate group on cellulose surfaces at pH 9.0

$A_{PBT} := \frac{S_{cell}}{B_T \cdot V \cdot p_{surf} \cdot N_A} = 1.81 \cdot nm^2$ The area for each boron group on cellulose surfaces

$A_{PB} := \frac{S_{cell}}{B_T \cdot V \cdot p_{PB} \cdot p_{surf} \cdot N_A} = 2.953 \cdot nm^2$ The area for each borate group on cellulose surfaces

Calculation 7: Calculation of free boronate groups BOH and ester groups BA at pH 9.0

$B(OH)_3$ is phenylbonic acid
pka of phenylboronic acid is 8.8

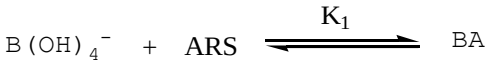

$B_T = B + BOH + BA$

Boron balance, B is concentration of free phenylboronic acid groups, BOH is concentration of free phenylborate groups, BA is concentration of phenylborate bound ARS.

$ARS_T = ARS + BA$

ARS balance, ARS is concentration of free ARS

Constants

$pH = 9$

$OH = 1 \times 10^{-5} \cdot \frac{mol}{L}$

$K_a := 10^{14-pKa} \frac{L}{mol} = 1.585 \times 10^{5} \cdot \frac{L}{mol}$

Association constant of phenylboronic acid

$B_T = 5.417 \times 10^{-5} \cdot \frac{mol}{L}$

$p_{PB} = 0.613$

$ARS_T = 7.304 \times 10^{-4} \cdot \frac{mol}{L}$ Total ARS added at pH 9

$K_1 := 1300 \frac{L}{mol}$

Initial guess

$BOH := 0.00001 \frac{mol}{L}$ $BA := 0.00001 \frac{mol}{L}$

Given

$BOH = \frac{K_a \cdot OH \cdot (B_T - BA)}{(K_a \cdot OH + 1)}$ $BOH \le B_T$

$BA = \frac{ARS_T \cdot BOH \cdot K_1}{(BOH \cdot K_1 + 1)}$ $BA \le B_T$

$f(B_T, ARS_T, OH) := Find(BOH, BA)$

$f(B_T, ARS_T, OH) = \begin{pmatrix} 2.12 \times 10^{-5} \\ 1.959 \times 10^{-5} \end{pmatrix} \cdot \frac{mol}{L}$

$\frac{f(B_T, ARS_T, OH)_1}{f(B_T, ARS_T, OH)_0} = 0.924$

$\frac{f(B_T, ARS_T, OH)_0}{B_T} = 0.391$

$B := B_T - BOH - BA = 3.417 \times 10^{-5} \cdot \frac{mol}{L}$